UNIVERSITY OF MILAN
CHEMICAL DEPARTMENT

CHEMICAL AND BIOCHEMICAL RESEARCH INSTITUTE G. RONZONI

PhD SCHOOL in INDUSTRIAL CHEMISTRY
XXX cycle

MATERIALS BASED ON BIOMACROMOLECULES AND INORGANIC COMPOUNDS:

CALCITE BASED BUILDING MATERIALS AND IRON OXIDE NANOPARTICLES

Gabriele Colombo Castelli

PhD course coordinator: prof. Maddalena Pizzotti
Supervisor: prof. Donatella Potenza
Advisors: dott. Torri Giangiacomo, dott. Annamaria Naggi, ing. Goisis Marco, prof. Luigi Cassar

Ai miei genitori

Abstract

The present project has been developed on two distinct lines of work related to the use of biomacromolecules, in particular polysaccharides, to give special purpose hybrid materials. The first is related to preparation of calcite based materials that can potentially replace cement, the second concerns the synthesis of iron oxide nanoparticles for biomedical applications.

I) Calcite-based biocomposite material with special mechanical properties

The production of building materials is essentially related to cement production. Although cement is a material characterized by the ability to quickly hydrate and to convert into a highly mechanical stress and weather agent resistant material, its production is very ancient and polluting. In fact, the raw material consists of cement minerals which are treated at very high temperatures (1450 °C) with consequent development of CO_2 which is a widely diffused greenhouse gas. Moreover, heat treatment is very expensive in terms of electricity and fossil fuel consumption.

For these reasons the development of new building materials, involving mild condition chemical processes and renewable raw materials, is highly desirable for human development.

Object of this investigation is the innovative preparation and evaluation of materials based on calcium carbonate and biopolymers as alternative to cement.

In this formulation calcium carbonate will be used without any heat treatment, avoiding the energy demanding and pollutant decarboxylation process. Our purpose is to find a formulation in which a natural polymer, interacting with calcium carbonate granules induces a mechanical reinforcement in the composite material, that will be measured by mechanical compression stresses.

The work consisted in finding the right ingredients of the formulation, which should have a consistency similar to that of mortar. A number of polysaccharides, anionic and neutral, were tested for their capacity to interact with calcite lattice. In particular carboxylated polysaccharides with high density charge such as: carboxymethylcellulose with substitution degree (DS) 2, sodium alginate, and chondroitin sulfate, were chosen. Interestingly chondroitin sulfate resulted as promising agent in improving the mechanical properties of calcium carbonate based material, in addition this hybrid material was able to raise the mechanical resistance of a concrete.

II) Biomacromolecules coated iron oxide nanoparticles: synthesis and properties

In the first year of PhD course I've worked on hybrid materials for biomedical application: nanoparticles are nowadays a new important object of studies of medicinal chemistry and different scientists collaborate in order to mix their skills: biologists, engineers , and chemists.

The goal was to synthesize nanoparticles with an appropriate size for the human tissue and with small size dispersion, with a shell made by two components biological matrix: a polysaccharide and a protein, these should ensure tissue biocompatibility and biological activity. In detail, the aim of the project is to prepare bovine serum albumin (BSA) and hyaluronic acid (HA) coated SPIONs (BSA-HA@Fe_3O_4), to characterize them, load them with drugs and chemosensitizers; the hybrid nanoparticles will be evaluated in their performance in selective drug delivery for cancer cells, and in diagnostic localization of tumors in vivo.

The adduct between nanoparticles composed by magnetite (Fe_3O_4) or maghemite (γ-Fe_2O_3) and biomacromolecules, hyaluronic acid (HA) and albumin (BSA), were obtained using dopamine (DA) to covalently bind these macromolecules to the surface of the nanoparticle iron oxide core.

The prepared product is an iron oxide nanoparticle surrounded by HA and BSA macromolecules as ligands, which act stabilizing the superstructure, anti-cancer targeting and drug delivery.

SUMMARY

PART ONE 7

CALCITE BASED BUILDING MATERIALS 7

1. INTRODUCTION 8

1.1 PORTLAND CEMENT 8

1.1.1 GENERAL ASPECTS 8

1.1.2 CEMENT PRODUCTION PROCESS 9

1.2 ENVIRONMENTAL ASPECTS 13

1.2.1 CEMENT PRODUCTION AND ENVIRONMENTAL IMPACT ON THE GLOBAL WARMING 13

1.3. BIOCOMPOSITE MATERIALS BASED ON CALCIUM CARBONATE 15

1.3.1 PURPOSE OF THE WORK 15

1.3.2 STATE OF THE ART ON THE $CaCO_3$-POLYSACCHARIDES HYBRID COMPOSITE 16

1.3.3 POSSIBLE CANDIDATES FOR $CaCO_3$ CRYSTALS BINDER AGENTS 17

Bibliography 25

2. RESULTS 28

2.1 – CRYSTALLYZATION EXPERIMENS 28

2.2 – PREPARATION OF MINI-SPECIMENS AND THEIR MECHANICAL RESISTANCE 32

2.3 TEST PIECES SCALING UP 36

2.3.1 PRELIMINARY EXPERIMENTS 36

2.3.2 –DISPERSANT PROPERTIES 40

2.3.3 EXPERIMENTS IN PRESENCE OF DISPERSANT 43

2.3.4 CALCITE – CEMENT FORMULATION 45

2.5 – ALGINATE DERIVATIZATION 52

Bibliography 56

3 – CONCLUSION AND PERSPECTIVES 57

4. MATERIALS AND METHODS 59

4.1 X-RAY DIFFRACTION ANALYSIS 59

4.2 SEM ANALYSIS 59

4.3 NMR SPECTRA RECORDING 59

4.3.1 ^{1}H NMR SPECTRA 59

4.3.2 ^{13}C NMR SPECTRA 60

4.3.3 HSQC SPECTRA 60

4.3.4 SOLID STATE ^{13}C NMR SPECTRA 61

4.4 HUMIDITY PERCENTAGE DETERMINATION 61

4.5 MOLECULAR WEIGHT DETERMINATIONS 63

4.6 CALCIUM CARBONATE CONTROLLED PRECIPITATION 64

4.7 ARTIFICIAL POLYMERS SYNTHESIS 64
4.7.1 ALGINATE DEPOLYMERIZATION 64
4.7.2 ALGINATE-ACRYLATE SYNTHESIS 65
4.7.3 ALGINATE GLYCOL-SPLIT 65
4.8 COMPOSITE MATERIALS PREPARATION 65
4.8.1 MINI SPECIMENS 66
4.8.3 SCALE-UP SPECIMENS 67
4.9 MECHANICAL TESTS 67
4.10 MINI-SPEC ANALYSIS 67
4.11 ATTENUATED TOTAL REFLECTION (ATR) ANALYSIS 68
PART TWO 69
IRON OXIDE NANOPARTICLES 69
1. INTRODUCTION 70
1.1 GENERICAL ASPECTS OF NANOPARTICLES 70
1.1. THE USE OF NANOPARTICLES OF IRON OXIDE IN BIOMEDICAL FIELD 71
1.2. AIM OF THE WORK 72
1.3. BSA and HA 73
Bibliography 75
2 – RESULTS 76
2.1. SYNTHESIS OF IRON OXIDE (MAGNETITE) NANOPARTICLES COVERED WITH HA AND BSA 76
2.1.1. SYNTHESIS OF IRON OXIDE NANOPARTICLES COATED WITH OLEATE 76
2.2. CHEMICAL CHARACTERIZATION 86
2.3. BIOLOGICAL RESULTS 89
3 CONCLUSION AND PERSPECTIVES 93
4. MATERIALS AND METHODS 94
4.1 – SYNTHESIS 94
4.1.1 – PREPARATION OF MAGNETIC COLLOID 94
4.1.2 – PREPARATION OF DA-BSA DERIVATIVE 95
4.1.3 – PREPARATION OF DA-HA DERIVATIVE 95
4.1.4 – PREPARATION OF Fe_3O_4@DA-HA/DA-BSA (ONE POT SYNTHESIS) 96
4.1.5 – PREPARATION OF Fe_3O_4@DA-HA/DA-BSA (STEP BY STEP SYNTHESIS) 96
4.2 - DLS ANALYSIS 97
4.3 - Z-POTENTIAL MEASUREMENT 97
4.4 – IN VITRO AND IN VIVO MAGNETIC RESONANCE IMAGING 97
4.5. MALDI–TOF MEASUREMENTS 98
Bibliography 99

PART ONE

CALCITE BASED BUILDING MATERIALS

1. INTRODUCTION

1.1 PORTLAND CEMENT

1.1.1 GENERAL ASPECTS

Portland cement is made by heating a mixture of limestone and clay, or other materials of similar bulk composition and sufficient reactivity, to a temperature of about 1450°C where partial fusion occurs, and nodules of clinker are produced. The clinker is mixed with a few per cent of calcium sulfate or other material and finely ground, to make cement. The calcium sulfate controls the rate of set and influences the rate of strength development. A typical clinker composition is reported in table 1.1

Table 1.1 – Cement chemical notation (CCN) and related mass composition

chemical name		CCN *	Mass %
Tricalcium silicate Ca_3SiO_5	Alite	C_3S	45–75%
Dicalcium silicate Ca_2SiO_4	Belite	C_2S	7–32%
Tricalcium aluminate Ca_3Al2O_6	Alluminate	C_3A	0–13%
Tetracalcium aluminoferrite Ca_2AlFeO_5	Ferrite	C_4AF	0–18%
$CaSO_4 \cdot 2\ H_2O$	Gypsum	$C\bar{S}H_2$	2–10%

* Chemical formulae in cement chemistry are often expressed as sums of oxides; thus, tricalcium silicate, Ca_3SiO_5 can be written as $3CaO{\cdot}SiO_2$. this does not imply that the constituent oxides have any separate existence within structure. It is usual to abbreviate the formulae of the commoner oxides to single letters, such as C for CaO or S for SiO_2, Ca_3SiO_5 thus becoming C_3S. this system is often combined with orthodox chemical notation within a chemical equation e.g. $3CaO+SiO_2 \rightarrow C_3S$.

Tricalcium silicate (Ca_3SiO_5), Alite, is the most important constituent of all normal Portland cement clinkers. It reacts relatively quickly with water, and is the most important of the constituent phases for strength development.

Dicalcium silicate(Ca_2SiO_4), Belite, constitutes 7-32 % of normal Portland cement clinkers. It reacts slowly with water, thus contributing little to the strength during the first 28 days, but have a role to the further increase in strength that occurs at lager ages. By one year, the strengths obtainable from pure alite and pure Belite are about the same under comparable conditions.

Aluminate consists 5-10% of most normal Portland cement clinkers. It is tricalcium aluminate (Ca_3Al2O_6). It Interacts rapidly with water, and can cause undesirably rapid setting unless a set-controlling agent, usually gypsum, is added.

Ferrite makes up 5-15% of normal Portland cement clinkers. The rate at which it reacts with water appears to be somewhat variable, perhaps due to differences in composition or other characteristics, but in general is high initially and low or very low at later ages. [1]

1.1.2 CEMENT PRODUCTION PROCESS

The raw materials, used to produce clinker includes naturally occurring minerals containing CaO, $CaCO_3$, SiO_2, Al_2O_3, Fe_2O_3, MgO and some materials available as waste streams from other industries. The most common combination of ingredients is limestone (for calcium) coupled with much smaller quantities of clay, shale and sand (as a source of silica, aluminum and iron). Other "alternative" raw materials such as mill scale, fly ash and slag are brought in from other industries. Plants generally rely on nearby quarries for limestone to minimize transport.

In fig. 1 the scheme of a cement manufacture plant is shown. Rock blasted from the quarry face is transported to the primary crusher where large "run of mine" rocks are broken into pieces of approximately 100mm. Generally, the other raw materials do not require crushing. The raw materials are then proportioned to the correct chemical balance and milled together to a fine powder "rawmeal". To ensure high quality of cement, the composition of the raw materials and rawmeal is very carefully controlled. Kiln exhaust gases are used in the raw mill to dry the raw materials. In some cases with wet materials, additional heat sources are required for drying. Materials are also homogenized to ensure consistency of product quality.

Raw meal is the feed material for the high temperature process in the kiln system. "Preheating" is the first part of the system and consist in a series of vertical cyclones. As the raw meal is passed down through these cyclones it comes into contact with the swirling hot kiln exhaust gases moving in the opposite direction and, as a result, heat is transferred from the gas to material. Pre-heat the material before it enters the kiln make the chemical reactions will occur more quickly and efficiently. By retaining energy from the exhaust gases, energy is saved. Depending on the raw material moisture, a kiln may have 3 to 6 stages of cyclones with increasing heat recovery with each extra stage. In Fig. 2 a scheme of the transformation process of raw meal in cement is shown.

The calciner is a combustion chamber at the bottom of the preheater above the kiln back-end. Up to 65% of the total energy needs of the kiln system can be supplied to the calciner. Calciners allow

for shorter rotary kilns and for the use of lower grade alternative fuels. Calcination is the decomposition of $CaCO_3$ to CaO, which releases CO_2 and take place at 450 °C - 900 °C. These process emissions comprise 60% of the total emission from a cement kiln. The combustion of the fuel generates the rest.

Raw meal, more accurately termed "hot meal" at this stage then enters the rotary kiln, where, above about 1300 °C, the calcium-silicate minerals are formed, mainly Ca_2SiO_4 together with intermediate calcium aluminates and calcium ferrite compounds. Fuel is fired directly into the rotary kiln and ash, as with the calciner, is absorbed into the material being processed. As the kiln rotates at about 3-5 revolutions per minute, the material slides and tumbles down through progressively hotter zones towards the flame. Coal, pet coke, natural gas and more increasingly alternative fuels such as plastic, solvents, waste oil or meat and bone meal are burned to feed the flame which can reach as high as 2000°C. This allows the materials to become partially molten as the intense heat causes the chemical (formation of Ca_3SiO_5) and physical changes that transform the raw feedstock into a material called clinker. As the clinker moves past the bottom of the kiln the temperature drops rapidly and the liquid phase solidifies, forming the other two cement minerals ($Ca_3Al_2O_6$ and Ca_2AlFeO_5). Expressed at its simplest, the series of chemical reactions converts the calcium and silicon oxides into calcium silicates, cement primary constituent. At the lower end of the kiln, the raw materials emerge as a new substance: a “red-hot particles called clinker. The clinker tumbles onto a grate cooled by forced air. Once cooled the clinker is ready to be ground into the grey powder known as Portland cement. To save energy, heat recovered from this cooling process is re circulated back to the kiln or preheater tower.

The clinker is then ground with other mineral components to cement: Gypsum is used to control the setting time of the product; slag, fly ash and gypsum can also be used to control other properties of the cement. The use of these materials reduces the total carbon footprint of the cement. In some countries, these materials are traditionally used at the concrete manufacturing plant with high clinker content cement supplied by the cement plant. Traditionally, ball mills have been used for cement milling. In recent years technologies with better energy efficiency have been developed. Compound mill systems include pre-crushing and sophisticated separator systems to reduce electricity consumption. Vertical cement mills mill the material in a roller mill with reduced electricity consumption also.

From the grinding mills, the cement is conveyed to silos for shipment. Most cement is shipped in bulk by trucks, rail or barge. A small percentage of the cement is bagged for customers who need only lesser amounts or who have special needs. [2] [3]

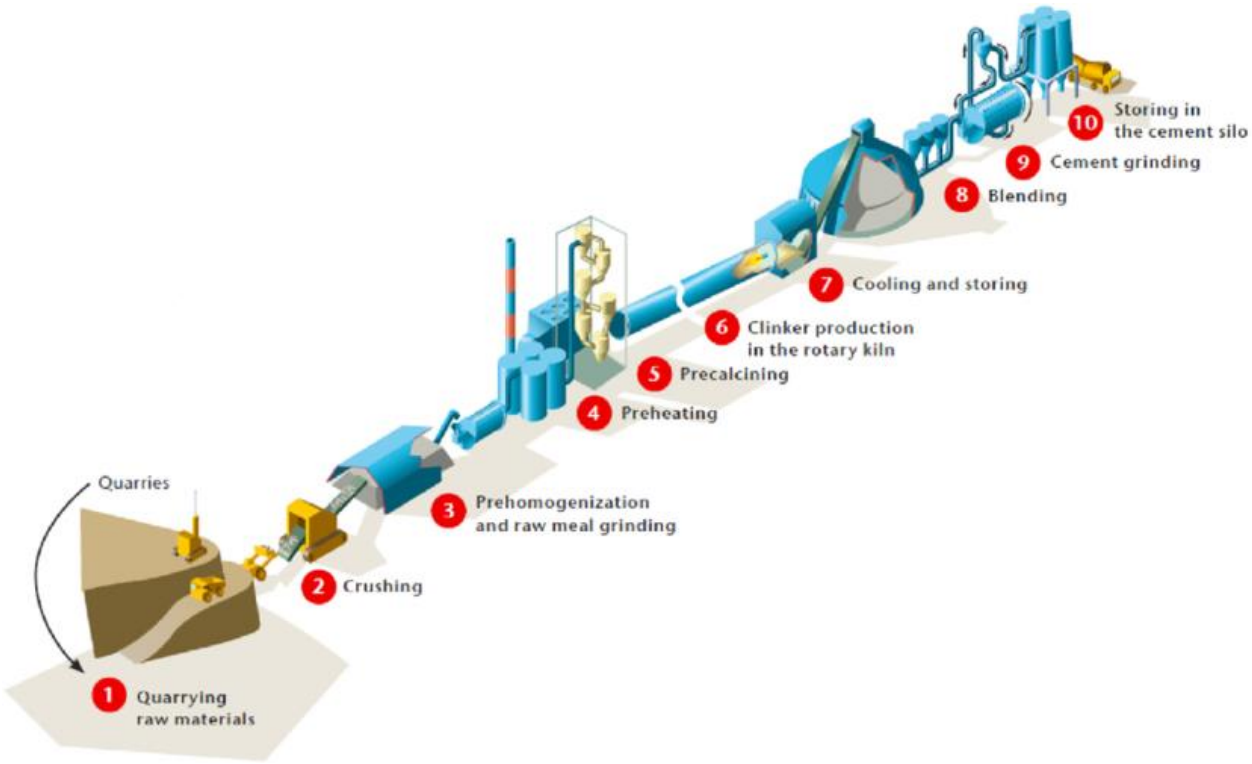

Figure1.1 – cement manufacture process at a glance

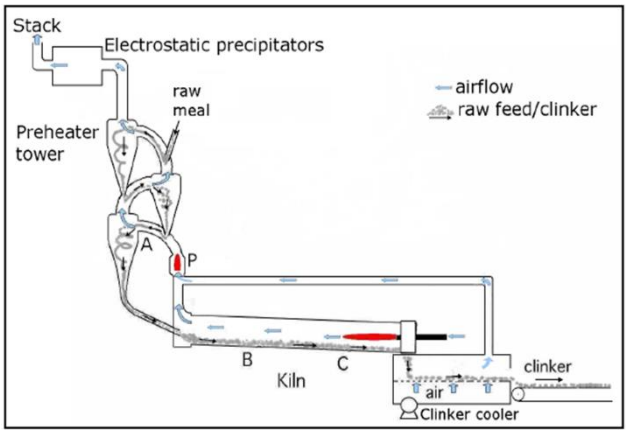

Figure 1.2 Basic principles of a precalciner cement kiln. raw meal passes down the preheater tower while hot gases rise up, heating the raw meal. At 'A,' the raw meal largely decarbonates; at 'B,' the temperature is 1000 C - 1200 C and intermediate compounds are forming and at 'C,' the burning zone, clinker nodules and the final clinker minerals ***[3b]***.

The cement resistance class depends on the grinding fineness of the particles and the percentage of tricalcium silicate compared to the bicalcic acid. The higher is the grinding quality of the cement, the faster is the development of the mechanical strength.

The higher is the tricalcium silicate content than the bicalcical and the faster is the development of the mechanical strength.

Each type of cement is potentially available in six different classes of normalized resistance (28gg).

For each class of normalized resistance, two classes of initial resistance (2 to 7 days) are defined:

• the first with ordinary initial resistance marked with the letter N;

• the second with high initial resistance marked with the letter R.

Therefore, according to UNI EN 197/1 [4] there are the following classes of cement resistance described in table 1.2:

Table 1.2 Class of cement resistance according to UNI EN 197/1 [4]

Class	initial compression resistance	Standard 28-day compression resistance
32.5N	7 days ≥ 16 MPa	≥ 32.5 ≤ 52.5 MPa
32.5R	2 days ≥ 10 MPa	≥ 32.5 ≤ 52.5 MPa
42.5N	2 days ≥ 10 MPa	≥ 42.5 ≤ 62.5 MPa
42.5R	2 days ≥ 20 MPa	≥ 42.5 ≤ 62.5 MPa
52.5N	2 days ≥ 20 MPa	≥ 52.5 MPa
52.5R	2-day ≥ 30 MPa	≥ 52.5 MPa

The resistance is also influenced by porosity. The fact that a reduction of porosity in a solid material increases its strength in general, and the strength of cement-based materials, was recognized long ago. The pore structure of cement-based materials contains air voids (coarser pores), capillary pores, and gel pores (finer pores), and the pores are randomly sized, arranged, and connected. It is a well-known fact that porosity is one of the key parameters, such as the compressive strength-modulus of elasticity relationship, which directly affect the strength and durability of cement based materials. It has also been discovered that porosity has a key role in the frost resistance of concrete. [2]

Many researchers have proposed various relationships between strength and porosity of porous material. Experimental research indicated, finer pores concrete has higher strength than the coarser one at the same total porosity. [5].

1.2 ENVIRONMENTAL ASPECTS

1.2.1 CEMENT PRODUCTION AND ENVIRONMENTAL IMPACT ON THE GLOBAL WARMING

In cement production, there is a source for environmental concern: the release of carbon dioxide. In table 1.3 are reported data of cement production relatively to 2011.

Table 1.3

The European cement industry in the EU27 (based on 2011 data)[8]

	2011	Unit
Clinker production	140	Million tonnes
Cement production	191	Million tonnes
Absolute emissions of CO_2 (excluding CO_2 from power generation)	122	Million tonnes
Volume of alternative fuels used	7.66 (25.6% of total thermal energy consumption)	Million tonnes
Volume of biomass used	2.15 (8.7% of total fuels thermal energy consumption)	Million tonnes
Use of alternative raw materials in Portland or blended cements	47.8	Million tonnes
Total thermal energy consumption (all fuel sources combined)	12.8	Million tonnes of oil equivalent (*roughly equivalent to the energy consumption of Ecuador*)
CO_2 per tonne of clinker	849	Kg CO_2/tonne clinker
Average thermal energy consumption	3,730[9]	MJ/tonne clinker
Average electrical energy consumption	114	kWh/tonne cement

[8] For the purposes of meaningful reporting, the definition of cement used in the GNR database differs slightly from that in common use. In this document, cement and cementitious products are considered equivalent.
[9] Based on grey cement

Numbers are somewhat controversial, but it is estimated that cement production accounts for about 5–6% of all carbon dioxide emissions caused by human activities. For instance, as result of Kyoto Protocol, in 2003, European Union set through the Emissions Trading Directive (ETD) specific target for the reduction of greenhouse gases. Some industrial sectors were selected, such as oil refining, pulp and paper, steel and cement. This large amount of carbon dioxide is generated by four diverse sources. 40% of this emission is in because of fossil fuel combustion, 10% is contributed due to raw material transportation as well as electricity generation and the remaining (almost 50% of total emission in cement plant) is generated by decomposition of limestone. [6]

The production of CO_2 in cement plants does not occur only in the calcination zone, inside the kiln. In fact, there are different major sources of CO_2 formation during the process as show in the scheme of figure 1.2:

1) **Calcination.** In the calcination step, the yielded CO_2 results from both fuel combustion (coal in most cases) and feedstock decomposition, and the CO_2 is more concentrated in flue gas than it is in conventional power plants. This constitutes the largest portion of the total CO_2 emissions from cement production.

2) **Combustion.** This portion of the emissions depends on the type of kilns and the type of fuel used. NSP (new suspension precalcination) kilns currently dominate cement production in China. The most widely used fuel is coal.

3) **Indirect emission.** This portion of the emissions refers to CO_2 emitted as a result of generating the power used for cement production, typically in the process of clinker grinding. CO_2 emissions from the extraction and transportation of the resultant cement are excluded in the accounting boundary.

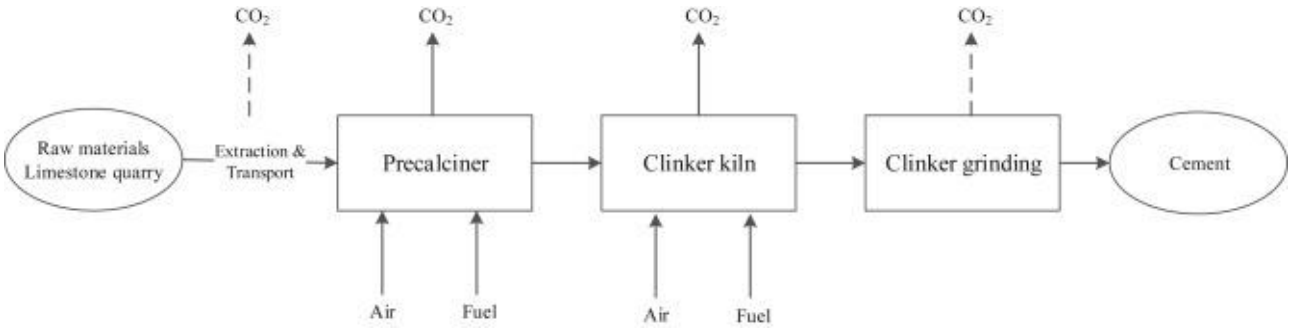

Figure 1.3 - Simplified scheme of the CO_2 emissions associated with cement production [7]

It is clear that chemical reactions, about 50% of carbon dioxide produced during cement fabrication is due to thermal decomposition of calcium carbonates. and the burning of fossil fuels are the major contributors in the process. It means that an efficient way to reduce CO_2 release is the use of lower temperatures. In practice, this is a very ambitious task, since the preparation of Ca_3SiO_5 requires massive amounts of energy. Cement manufacture is an energy intensive process. When the burning of fossil fuels and other energy sources are considered, the total balance is quite impressive: 1 ton of cement generates approximately 1 ton of carbon dioxide. Also, it consumes about 60–130 kg of fossil fuel and 110 kWh. [8]

A detailed publication of the IEA (International Energy Agency), in 2009, defined cement as the essential “glue” in concrete, a fundamental building material for society’s infrastructure around

the world. Concrete is second only to water in total volumes consumed annually by society. But IEA highlighted that the cement production process also co-produces CO_2, leading the cement industry to produce approximately 5% of current global man-made CO_2 emissions. With climate change mitigation and adaptation measures increasing, concrete demand is expected to increase even further. In developing countries, cement production is forecast to grow as modernization and growth continues. 2006 global production was 2.55 billion tons (USGS, 2008). A low growth demand scenario has been used for the roadmap with 2050 production at 3.69 billion tons. A high growth scenario, with 2050 production at 4.40 billion tons, was also modeled [9]

1.3. BIOCOMPOSITE MATERIALS BASED ON CALCIUM CARBONATE

1.3.1 PURPOSE OF THE WORK

The main aim of the present work is to set up a new like-cement building material without processing the calcium carbonate in order to do not increase the emissions of GHGs in atmosphere, limiting and contrasting the greenhouse effect.

The idea is inspired by the extraordinary performance of biological composites like bone, nacre, and the exoskeleton of brittle stars which compositions and structures have been widely studied. Such as an example, the egg shell constituted by calcium carbonate in the form of calcite crystals and a little part of organic matter: a sulphated proteoglycan, which acts as a binder between the calcite columnar particles [10] [11], or coral skeleton [12] where calcium carbonate and organic macromolecule are involved. In these biomaterials, the calcium carbonate in presence of very low content of biopolymers (< 5 wt %) produces composite materials with a resistance to fracture 3000 times higher than pure calcium carbonate.

Calcium carbonate is a widely available raw material, until now considerate as inert filler for the mortars, because it is not able to generate a hard inorganic phase as happens in concrete based material improving the compressive strength of the material [13] [14].

To overcome the poor adhesion properties of $CaCO_3$ particles and the consequent fragility of materials prepared in ordinary condition of temperature and pressure, it was considered to study the reinforcement effect that a biopolymer applies on a calcite based material, mimicking the composition of several natural biomaterials.

To develop a production process for low environmental impact building material, the group needed to explore several natural biomacromolecules as calcium carbonate binders, such as

polysaccharides, rather than polymers derived from chemical synthesis. Nature produces 170000 million tons per year of renewable carbon (biomass). People harvest about 3 per cent of this for food production and non-food applications. Less than 1 per cent of this could meet the demands of the chemical industry that currently use fossil carbon as raw material [15]. The studies first involved the identification of the natural polymer which best interact with $CaCO_3$ and then the identification of the suitable composition of formulations to have good workability of the dough and considerable mechanical properties of the obtained materials.

1.3.2 STATE OF THE ART ON THE $CaCO_3$-POLYSACCHARIDES HYBRID COMPOSITE

A literature survey showed several articles regarding the crystallization of $CaCO_3$ in the presence of natural and synthetic polymers, but has not been found any reference about the preparation of materials with high content of $CaCO_3$ on macro-scale amounts useful for building field. Some polysaccharides have already been employed in construction engineering as additives since they have a big effect on the rheology of aqueous systems acting as improving water retention agent. The most used are maltodextrins and starch ethers used in cement concrete or putty as thickening and plasticizer or retard agent for mortar [16]. Another application is their use, especially cellulose, as inert components for the preparation of insulating panels. But they have been never used as gluing agent for calcium carbonate made concrete, so this project can be considered as a pioneering research. Suggestions can be taken from literature that, although not exposes works on building biomaterials, it reports some examples of composite biomaterials constituted by polysaccharides or organic polymers containing $CaCO_3$as minor component.

Gebauer synthesized, by precipitation of calcium carbonate in a nanocellulose dispersion, hybrid material of nanocellulose and $CaCO_3$ particles as promising candidates for biodegradable multifunctional materials [17]. The mixing of the two compounds resulted in an optically transparent and relatively hard material of which the 30% of inorganic part. In conclusion, the authors claim that a resilient cellulose film packaging can be produced with potential flame retardant qualities. Takashi Kato and Atsushi Arakaki developed a method to prepare a transparent, flexible, and mechanically strong film composed by calcium carbonate and polyacrylic acid matrix doped with nanocellulose. The authors explain that the oxidized cellulose nanofibril

surfaces bind through carboxylate groups to calcium ions in the nano-segregated calcium carbonate/polyacrylic matrix.

The mixing of the two compounds resulted in an optically transparent and relatively hard material. It contained the 30% too of inorganic part. In conclusion, the authors claim that a resilient cellulose film can be produced. [18][19].

Other examples of $CaCO_3$ biocomposites deals with films or nanoparticles materials, but show examples of electrostatic interactions between polysaccharides functional groups and calcium carbonate powder obtained through the simple mixing of the organic with small amount of inorganic components (0, 0.02, 0.04, 0.06, 0.1 and 0.5%) [20].

Few other studies have been carried out on synthetic materials containing of calcium carbonate, for biomedical applications. A product considered as a possible a bone prosthesis [21] was prepared by mixing of calcium carbonate with caprolactone before polymerization. the dry scaffold was characterized and showed a compressive strength of 50 MPa

Unlike what is reported in the literature our intent is to produce a composite material maximizing the content of $CaCO_3$ as raw material, and to minimize the polymeric part constituted by a natural polymer.

1.3.3 POSSIBLE CANDIDATES FOR $CaCO_3$ CRYSTALS BINDER AGENTS

Several articles report precipitation of calcium carbonate from soluble salts in presence of soluble polysaccharides as crystal growing agent [22a,b,c]. Biomacromolecules can play an important role in influencing the crystallinity, the shape, and the dimensions of crystal aggregates during the precipitation step. The negative charge of anionic polymers can interact with the surface of $CaCO_3$ through electrostatic forces, in particular with the plane of the crystals with calcium atoms exposed [23].

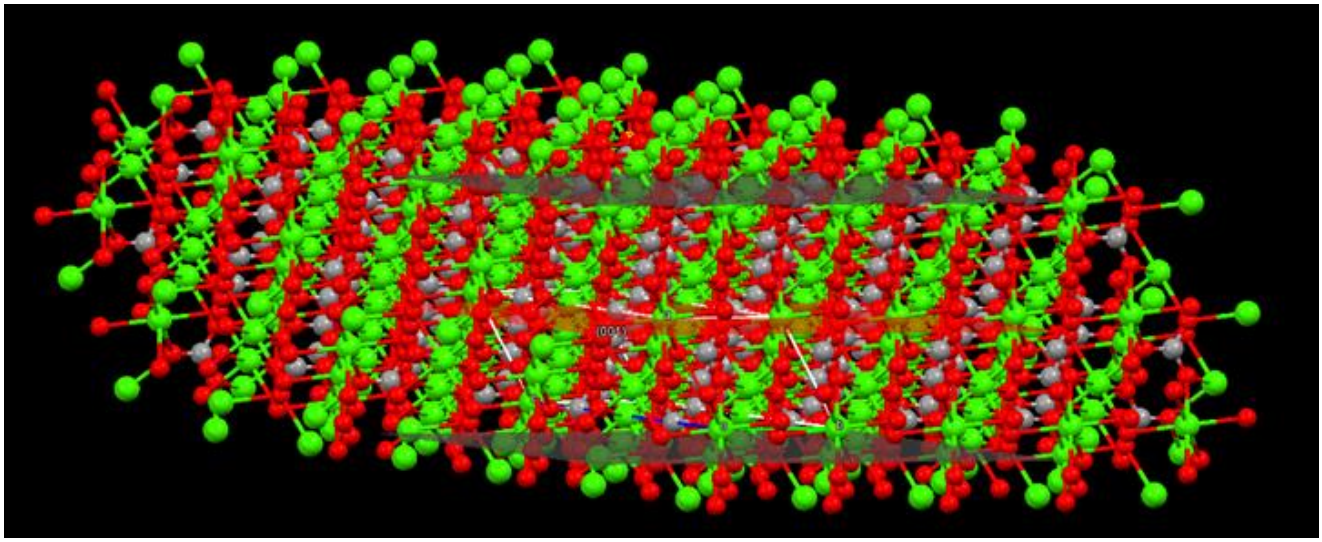

Figure 1.4 – plane [001] shows calcium atom (green) exposed in calcite packaging. The other colors: red (oxygen atoms); grey (carbon atoms). Image obtained with "Mercury" program.

Several biopolymers, listed below, have been identified as possible binders for calcium carbonate matrix. The selection criteria were: hydrophilicity, the presence of anionic groups, as carboxylates, phosphates, and/or sulfates, with potential ability to interact with calcium carbonate particles and gelling polymers. They differ in charge density, molecular weight, and back bone chemical structure.

- **Alginate**

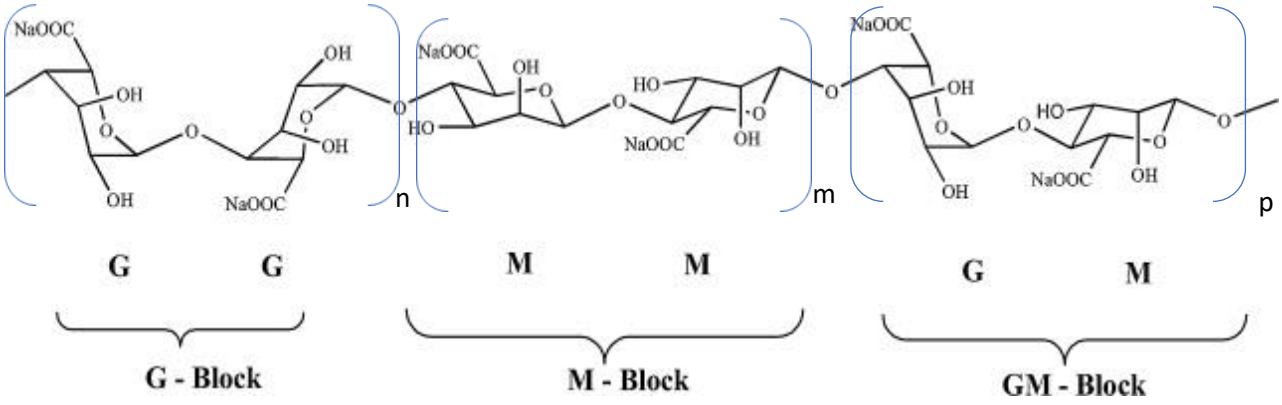

Figure 1.5 – Schematic representation of sodium alginate structure [29]

Alginates are a family of linear polysaccharides consisting of 1-4 linked βmannuronic acid (M) and its C-5 epimer α-L guluronic acid (G). It is a block copolymer composed of homopolymeric regions of M and G, interspersed with regions of alternating structure of MG-blocks. Commercial alginates

are produced mainly from algae, such as brown algae, and from some bacteria, such as Pseudomonas (not commercial). The copolymer sequence and molecular weight vary with the source, the seasonal and growth conditions.

There is a so large amount of alginate present in nature that its industrial production – approximately 30000 metric tons annually – is estimated to comprise less than 10%. Therefore, there is a significant additional potential to design sustainable material based on alginates.

This polysaccharide, that hasn't a nutritional value, is widely used as thickening agent and moisture retainer in food industry and cosmetic area, it is also employ as auxiliary for tissue printing, in pharmaceutical formulations and there are currently researches about its medical potential advantages for diabetes treatment.

The solubility of alginates in water is governed by pH, ionic strength and the presence of gelling ions (divalent cations). Alginate solutions may behave in two different way when the solution pH is lower than 3.5 value. An abrupt lowering of pH causes the precipitation of alginic acid molecules, while a slow acidification may result in formation of a gel. [*24*] At high ionic strength the solubility is also affected. Salt concentration of less than 0.1 M is sufficient to slow the kinetic of dissolution process and reduces solubility. If alginates have to be used at high salt concentrations, the polymer should first be hydrated in pure water before the addition of salt under mechanical stirring. Alginate chelates quickly with bivalent ions to form a hydrogel. Gel formation is driven by the interaction between G-blocks which associate to form tightly held junctions in presence of these metal ions (Fig. 1.6) [25].

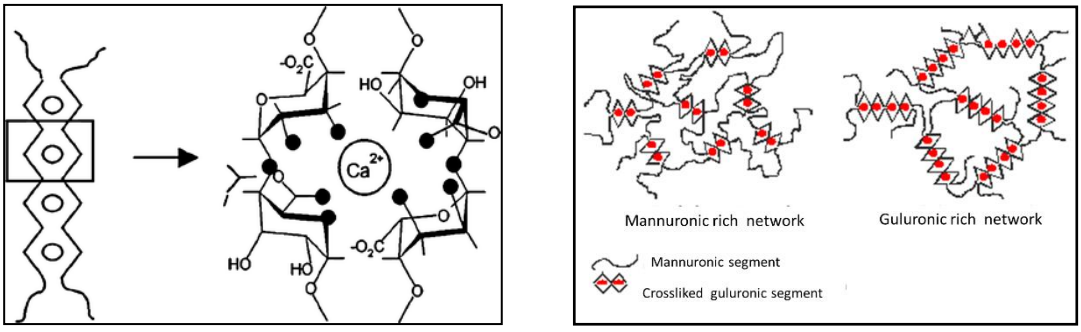

Figure 1.6 - The "egg-box" model for calcium alginate gel and the interaction between calcium cations and oxygen atoms on the guluronate monomers [26]

- **Chondroitin sulfate**

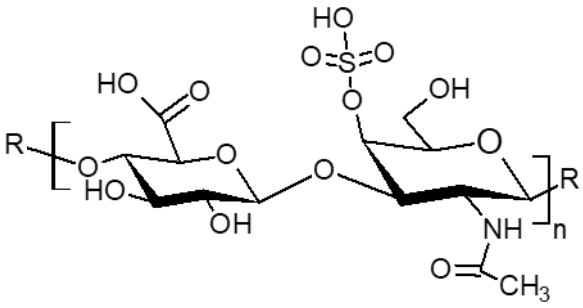

Figure 1.7 – Schematic representation of chondroitin sulfate structure

Chondroitin 4, 6 sulfates, and dermatan sulfate comprise a group of glycosaminoglycans of wide occurrence in human and animal tissues containing a repeated disaccharide unit constituted by a uronic acid and a sulfated N acetylgalactosamine. Chondroitin 4- (figure 1.7) and 6-sulfate, also known as chondroitin sulfate A (ChS A) and C (ChS C), contain β-D-glucuronic acid residues and differ for the site of sulfation of galactosamine residues. Dermatan sulfate, also known as chondroitin sulfate B (ChS B) is sulfated at position 4 of the galactosamine residues but contains residues of α-L-iduronic acid as major uronic acid component. Chondroitin, which are widely distributed as glycosaminoglycan sidechains of proteoglycans in cartilage, in the extracellular matrix and at cell surfaces, are implicated in the signaling functions of various heparin-binding growth factors and chemokines [27].

The commercial sources of such products are: pig skin or intestinal mucosa for ChS B, cartilage of bovine or pig for ChS A and of shark, and squid for ChS C. The main field of application is the treatment of arthritis as they are used as anti-inflammatory agents. Some medical researchers are working on their use as anti-viral and anti-cancer molecules [28].

- **Dextran sulfate**

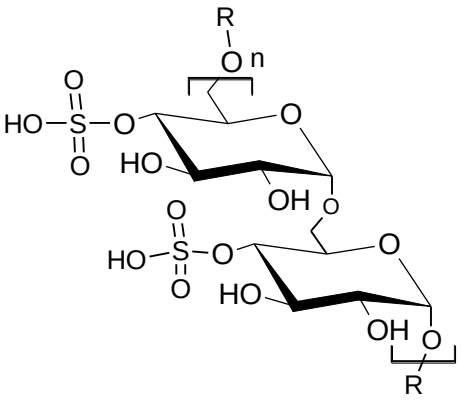

Figure 1.8 – Schematic representation of dextran sulfate structure

Dextran is synthesized from sucrose by lactic acid bacteria such *Leuconostoc mesenteroides,* and consists of (1→6)-a-D-glucan with branches of (1→3)-a-glucopiranoside residues. The degree of branching is approximately 5% Dextran sulfate is its anionic derivative obtained by chemical sulfation, with chlorosulphonic acid or other sulfating agents. It is freely soluble in water. It has anticoagulant activity (15% respect to heparin) but it could be a toxic because may produce anaphylactic reactions [29].

- **Carboxymethylcellulose**

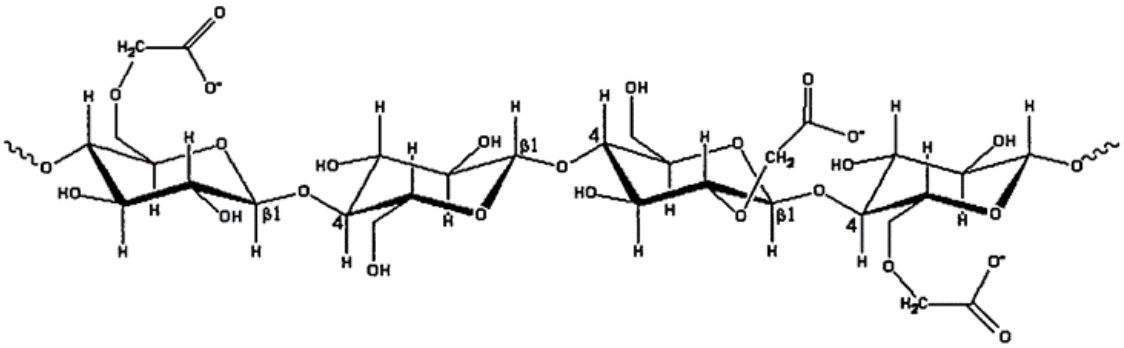

Figure 1.9 – Schematic representation of sodium carboxymethylcellulose

Carboxymethyl cellulose (CMC) is a water-soluble, polyanionic compound derived from cellulose, that can exist either as free acid or its sodium salt or mixtures thereof. It is prepared by a reaction with mono chloroacetic acid in alkali conditions [30] [31]. The introduction of carboxymethyl

groups along the cellulose chains, makes possible the hydration of the polysaccharide giving rise to very viscous solutions. The reaction to produce CMC is a controllable process thus it is possible to obtain the desirable property such as viscosity, thixotropy and pseudoplasticity through the appropriate molecular weight, substitution degree and uniformity of chemical substitution. Commercially, CMC is available with a substitution degree (DS) ranging between 0.4 to 2.

Besides controlling the rheology, CMC is known for its excellent water retaining capacity. CMC has large uses and applications in several fields: food, textile, adhesive, paper industry and for drugs and cosmetics productions. [32]

- **Dermatan sulfate**

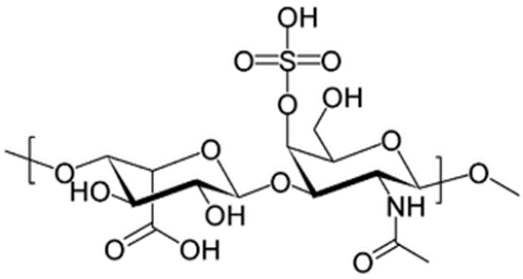

Fig 1.10 – Schematic representation of dermatan sulfate structure

Dermatan sulfate is a glycosaminoglycan of the skin and it is present in many mammalian tissues. It is composed of disaccharide repeating units consisting of N-acetyl-Dgalactosamine and L-iduronic acid. These alternating disaccharide units can be variably O-sulfated at the C-4 and C-6 positions in GalNAc, and the C-2 position in IdoA. Dermatan sulfate binds to a variety of proteoglycans and modulates various biological processes such as coagulation, angiogenesis, tumor migration and growth factor expression.[33]

- **Hyaluronate**

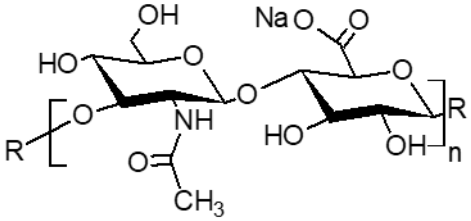

Figure 1.11 – Schematic representation of sodium hyaluronate structure

Hyaluronic acid is a linear polysaccharide consisting of a repeating disaccharide: β-1,4 D-glucuronic acid and β-1,3-N-acetyl-D-glucosamine. It is ubiquitous in the human body, essential for many cellular functions. It is distributed in the extracellular matrix besides collagen, fibronectin and heparansulfate proteoglycans. Hyaluronic acid solutions have typical polyelectrolytic behavior of charged macromolecules and the specific high viscosity of its solutions acts as shock adsorbing fluid in cartilage and as an ocular lubricant and in function of this properties it is used in clinical medicine for over thirty years for joint care and in ophthalmology [34; 35].

- **Locus Beam Gum**

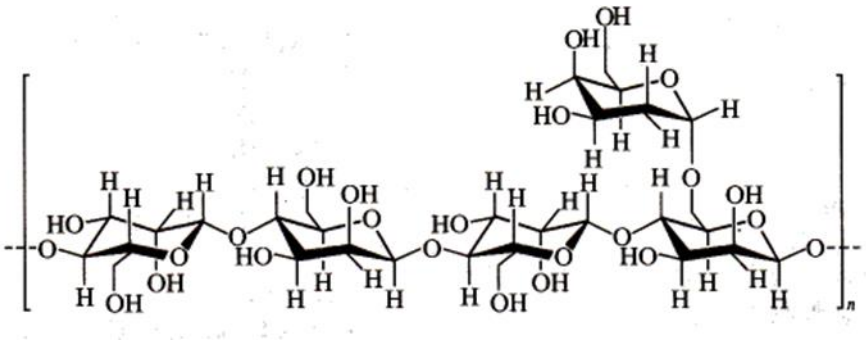

Fig 1.12 - Schematic representation of Locus Beam Gum (LBG) structure

Locust bean gum is composed of a straight backbone chain of D-mannopyranose units with a side-branching unit of D-galactopyranose having an average of one D-galactopyranose unit branch on every fourth D-mannopyranose unit. This polysaccharide is sweet—with a flavor similar to chocolate—and it is used to sweeten foods and as a chocolate substitute [36]

- **Xanthan**

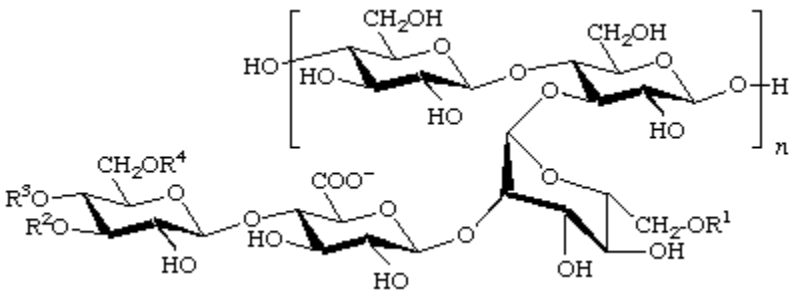

R1=H or Ac;
R2=R3=R4=H or R2=Ac;

R5=R4=H or R2=H;
R5=R4=CH_3COO^-

Fig. 1.13 – Schematic representation of Xanthan

Xanthan gum is an acidic polymer made up of pentasaccharide subunits, forming a cellulose backbone with trisaccharide side-chains composed of mannose (β1→4) glucuronic-acid (β1→2) mannose attached to alternate glucose residues in the backbone by a1→3 linkages. This polysaccharide is widely used as a rheology modifier agent in both food and non-food industries. As example it is suitable as a stabilizer for a wide variety of suspensions, emulsions, and foams [37].

- **Phosphated starch**

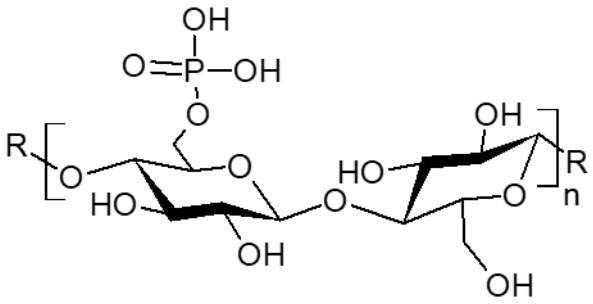

Fig. 1.14 - Schematic representation of Phosphated Starch

Different types of starch are phosphorylated to different degrees of substitution using monosodium and disodium hydrogen orthophosphate at 160 °C under vacuum. Solubility and swelling power greatly increase when phosphorylation is carried out to a low degree of substitution, while the solubility and swelling power decreased gradually by increasing the degree of substitution. [38]

Bibliography

[1] Cement chemistry, H.F.W. Taylor, Thomas Telford Pubblishing, 2004

[2a] http://www.eblockcement.com/index-2_facts.html; [2b] http://www.understanding-cement.com/

[3] La chimica e l'industria: critical reviews, Francesca Ridi, (2010), 109-117

[4] European norm EN 197-1

[5] Zhao, Haitao, et al. "Influence of pore structure on compressive strength of cement mortar." The Scientific World Journal 2014 (2014).

[6] Benhelal, Emad, Gholamreza Zahedi, and Haslenda Hashim. "A novel design for green and economical cement manufacturing." Journal of Cleaner Production 22.1 (2012): 60-66.

[7] Zhou, Wenji, et al. "Capturing CO_2 from cement plants: A priority for reducing CO_2 emissions in China." Energy 106 (2016): 464-474.

[8] Rodrigues, F.A. and Joekes, I. Cement and Industry: Sustainability, Challenges and Perspectives. Environmental Chemistry Letters, 9, (2011) 151-166.

[9] WBCSD, IEA *Cement Technology Roadmap 2009 Carbon emissions reductions up to 2050, World Business Council for Sustainable Development and International Energy Agency (IEA).< http://wbcsdcement. org/pdf/technology/WBCSD-IEA_Cement% 20Roadmap. pdf*, 2009.

[10] Rodríguez-Navarro, Alejandro B., et al. "Amorphous calcium carbonate controls avian eggshell mineralization: a new paradigm for understanding rapid eggshell calcification." Journal of structural biology 190.3 (2015): 291-303.

[11] Panheleux, M., et al. "Organic matrix composition and ultrastructure of eggshell: a comparative study." British poultry science 40.2 (1999): 240-252

[12] Goldberg, Walter M. "Acid polysaccharides in the skeletal matrix and calicoblastic epithelium of the stony coral Mycetophyllia reesi." Tissue and Cell 33.4 (2001): 376-387

[13] Cao, Mingli, Ling Xu, and Cong Zhang. "Rheology, fiber distribution and mechanical properties of calcium carbonate ($CaCO_3$) whisker reinforced cement mortar." Composites Part A: Applied Science and Manufacturing 90 (2016): 662-669.

[14] Cao, M.L. and J.Q. Wei. "Whisker-reinforced Cement". Journal of Wuhan University of technology-materials science edition, 26(5): 1004-1009

[15] Eggersdorfer, M., J. Meyer, and P. Eckes. "Use of renewable resources for non-food materials." FEMS microbiology letters 103.2-4 (1992): 355-365.

[16] Handbook of bioplastic and biocomposites. Engineering applications, Wiley (2011) 320-333

[17] Gebauer, Denis, et al. "A transparent hybrid of nanocrystalline cellulose and amorphous calcium carbonate nanoparticles." Nanoscale 3.9 (2011): 3563-3566.

[18] Saito, Tsuguyuki, et al. "Bioinspired stiff and flexible composites of nanocellulose-reinforced amorphous $CaCO_3$." Materials Horizons 1.3 (2014): 321-325.

[19] Arakaki, Atsushi, et al. "Biomineralization-inspired synthesis of functional organic/inorganic hybrid materials: organic molecular control of self-organization of hybrids." Organic & biomolecular chemistry 13.4 (2015): 974-989.

[20] Shi, Jun, et al. "Biomimetic fabrication of alginate/$CaCO_3$ hybrid beads for dual-responsive drug delivery under compressed CO_2." Journal of Materials Chemistry 21.40 (2011): 16028-16034.

[21] Olah, L.A.S.Z.L.O., and L.A.J.O.S. Borbas. "Properties of calcium carbonate-containing composite scaffolds." Acta of Bioengineering and Biomechanics 10.1 (2008): 61.

[22a] Arias, José L., et al. "Sulfated polymers in biological mineralization: a plausible source for bio-inspired engineering." Journal of Materials Chemistry 14.14 (2004): 2154-2160.; [22b] Matahwa, H., V. Ramiah, and R. D. Sanderson. "Calcium carbonate crystallization in the presence of modified polysaccharides and linear polymeric additives." Journal of Crystal Growth 310.21 (2008): 4561-4569.; [22c] Yang, Lin, et al. "Interfacial molecular recognition between polysaccharides and calcium carbonate during crystallization." Journal of inorganic biochemistry 97.4 (2003): 377-383.

[23] Xu, An-Wu, et al. "Polymer-Mediated Mineralization and Self-Similar Mesoscale-Organized Calcium Carbonate with Unusual Superstructures." Advanced Materials 20.7 (2008): 1333-1338.

[24] A. Haug, B. Larsen, The solubility of alginate at low pH, Acta Chem Scand 17:1653 (1963)

[25] Pawar, Siddhesh N., and Kevin J. Edgar. "Alginate derivatization: a review of chemistry, properties and applications." Biomaterials 33.11 (2012): 3279-3305.

[26] Fu, Shao, et al. "Relevance of rheological properties of sodium alginate in solution to calcium alginate gel properties." Aaps Pharmscitech 12.2 (2011): 453-460.

[27] Recent advances in the structural biology of chondroitin sulfate and dermatan sulfate K Sugahara T Mikami T Uyama S Mizuguchi K Nomura H Kitagawa Current Opinion in Structural Biology 13, 5, 2003, 612-620

[28] Schiraldi, Chiara, Donatella Cimini, and Mario De Rosa. "Production of chondroitin sulfate and chondroitin." Applied microbiology and biotechnology 87.4 (2010): 1209-1220.

[29] Tazi, Loubna M., and Shiranthi Jayawickreme. "Determination of residual dextran sulfate in protein products by SEC–HPLC." Journal of Chromatography B 1011 (2016): 89-93.

[30] https://www.cpkelco.com/products/cellulose-gum

[31] http://celluloseether.com/manufacturing-process-of-carboxymethylcellulose

[32] C. B. Hollabaugh, Leland H. Burt, Anna Peterson Walsh, Carboxymethylcellulose. Uses and Applications, Ind. Eng. Chem., 1945, 37 (10), pp 943–947

[39] Kandasamy, Jeyakumar, et al. "Modular automated solid phase synthesis of dermatan sulfate oligosaccharides." Chemical Communications 50.15 (2014): 1875-1877.

[40] Trowbridge, Janet M., and Richard L. Gallo. "Dermatan sulfate: new functions from an old glycosaminoglycan." Glycobiology 12.9 (2002): 117R-125R.

[41] Goa, Karen L., and Paul Benfield. "Hyaluronic acid." Drugs 47.3 (1994): 536-566.

[42] Utilization of natural polysaccharide gums in the food industry, Research Center. General Foods Corporation. Tarrytotun. New York (1963)

[43] Becker, A., et al. "Xanthan gum biosynthesis and application: a biochemical/genetic perspective." Applied microbiology and biotechnology 50.2 (1998): 145-152.

[44] Sitohy, Mahmoud Z., et al. "Physicochemical properties of different types of starch phosphate monoesters." Starch-Starke 52.4 (2000): 101-105.

2. RESULTS

The experimental work was divided in two parts:

- screening of various polysaccharides in order to find the best interaction with the calcium carbonate through calcium carbonate crystallization experiment and preliminary small scale formulation.
- optimizing the formulation to obtain a homogeneous and workable paste, and scale up for the production of sample suitable to the mechanical properties measurements.

2.1 – CRYSTALLYZATION EXPERIMENS

An optimal polymer acting as binder for calcium carbonate micro-particles should interact with electrostatic charged surfaces exposed by the lattice structure. For these reasons the selected polymers should have anionic groups. Polysaccharides with carboxyl groups could be thought particularly interesting at this level of the investigation, due to the strong affinity of the carboxyl group toward the Ca^{+2} ions. A first screening of the polymers to use as calcium carbonate binder was done through characterization of the $CaCO_3$ crystals generated by mixing solutions of Na_2CO_3 (0,05M) and $CaCl_2$ (0,05M) with a soluble polysaccharide, in order to evaluate its interaction with the growing faces of $CaCO_3$ crystal seeds. The following polysaccharides have been used at the concentration of 0.025M (calculated on repetitive unit base): carboxymethylcellulose DS2, dermatan sulfate, dextran sulfate, sodium alginate totally or partially (30%) salified, sodium hyaluronate, and chondroitin 4-sulfate. Samples were obtained adding, at room temperature, a stoichiometric amount of Na_2CO_3 (0.05M) to a solution of polysaccharide and $CaCl_2$. After two hours the precipitates were recovered by centrifugation or filtration, dried in open air and analyzed by IR spectroscopy, scanning electronic microscopy (SEM). The results were compared with the $CaCO_3$ obtained by the precipitation without the presence of the biomacromolecule. All samples presented a IR spectrum (figure 2.1a) characterized by the calcite bands at 1400 cm^{-1} (v_3 asymmetric CO_3 stretching), 870 cm^{-1} (v_2 out-of plane CO_3 deformation) and 711.3 cm^{-1} (v_4 in-plane CO_3 deformation) except for the precipitate obtained with Hyaluronate (Figure 2.1b) that presents in addition to the calcite bands, also a small band at 745.8 cm^{-1} characteristic of vaterite crystal form [*1*]. The crystalline structures were confirmed by X ray diffraction of powders.

In figure 2.2 the SEM images of the obtained precipitated are shown. The results indicate that polysaccharides greatly affect their morphology. Crystals produced in presence of sodium alginate (E), dermatansulfate (B) and carboxymethylcellulose (C) differ significantly from the control (A),

obtained without the polymer, that shows rhombohedral structure. Differently, samples prepared in presence of dextran sulfate (D) and chondroitin sulfate (G), at this magnification level, present shape comparable better with the morphology of the control (A).

Figure 2.1 IR spectra of $CaCO_3$ precipitates from solutions containing a) alginate b) hyaluronate.

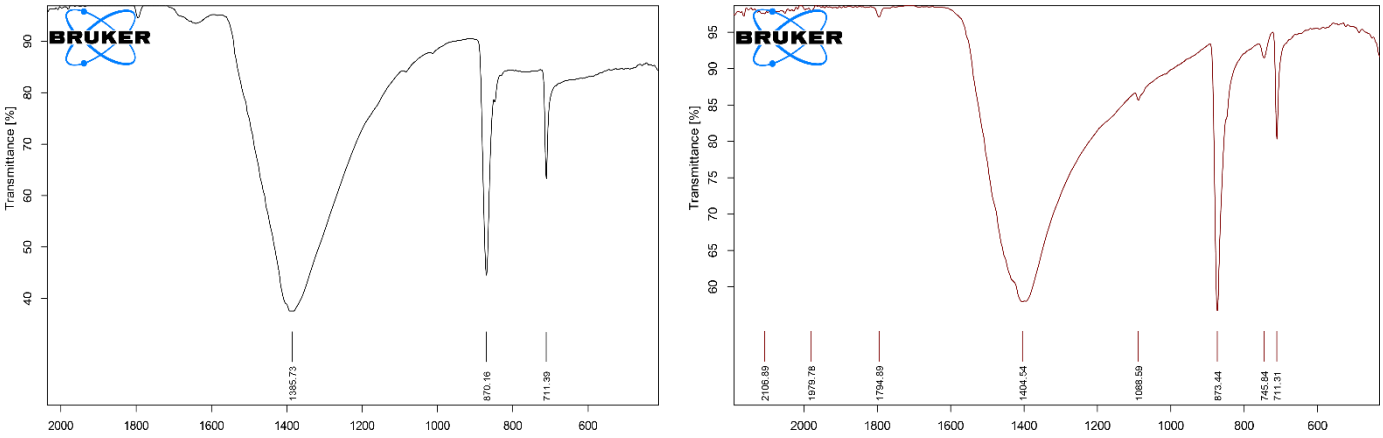

The analysis of the SEM images in Fig.2.2 underline how the polymer affects also the size of the calcium carbonate crystals: in fact the average diameter size of the precipitated crystrals of the control experiment (sample A) is around to 5 µm, whereas the dimensions of the products obtained in presence of the alginate as control growing agent (E) are much smaller. Also the low dimension of the calcium carbonate crystalline particles of the product (B) underlines how an other hightly carboxylated polysaccharide (carboxymethylcellulose DS 2) can inhibit the crystal growing process. A possible explaination involves the polymer that interfers with the growing calcium carbonate crystals due to the electrostatic interaction between the anionic charges of the carboxylated polymer and the partial positive charges of the calcium atoms exposed on the surface of the inorganic crystal structure. The experiment demostrates that both the sodium alginate and the carboxymethylcellulose can hightly influence the shape and the dimensions of the calcium carbonate crystals; thus it could be supposed that the most carboxylated biopolymers could have a better interaction with the calcium carbonate particle surfaces respect than the other anionic tested carbohydrates.

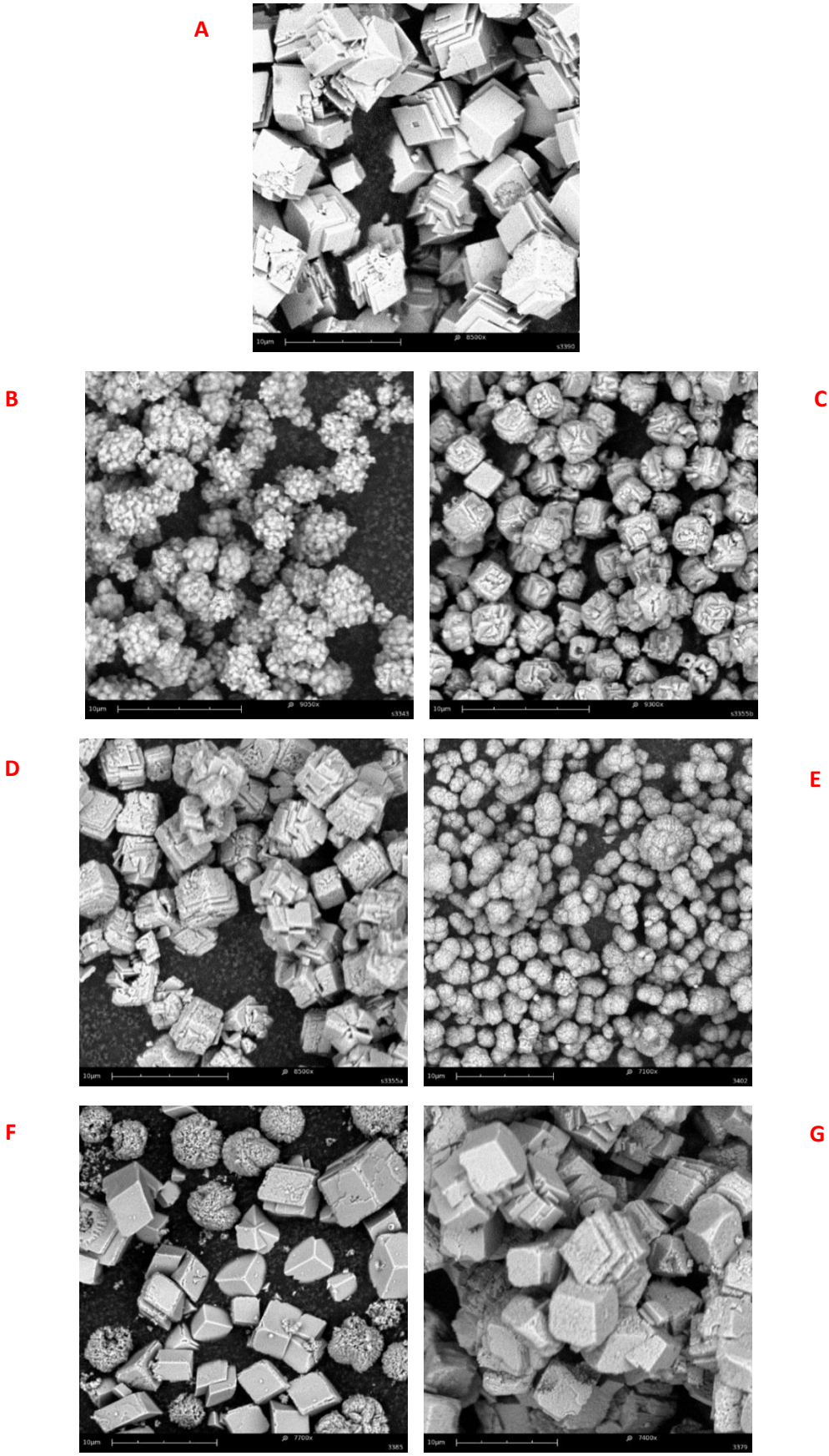

Fig. 2.2 – SEM images of precipitated crystalline calcium carbonate; control sample precipitated in absence of polysaccharide (A); in presence of carboxymethylcellulose DS2 (B); dermatan sulfate (C); dextran sulfate (D); sodium alginate (E); sodium hyaluronate (F) ; chondroitin 4-sulfate (G). Bar scales: 10µm

A different sample was obtained using alginate in a solution with lower pH (pH 4.5), following a similar procedure. A dispersion of alginic acid (0.05 M) in water was prepared, then solution of $CaCl_2$ and Na_2CO_3 were added. The calcium carbonate precipitated was embedded in the not soluble polymeric matrix. The sample was filtered and dried at the air at room temperature. The final product was a discoid compact material. The SEM images (Figures 2.3) show clearly two phases: the dark phase corresponds to the polymer, while the white part represents the inorganic spherulitic particles. This last sample is caracterized by a polymer content of about 30% by weight as determined by TGA experiment. The insoluble polymer acts as a binder between the particles of the material, resulting in a consolidant agent. SEM shows that the shape of the crystals doesn't change. The material resistance shows good mechanical resistance at empirical tests, and further investigations are required.

The TGA of the hybrid material (fig 2.4.B) presents the thermal decomposition of the biopolymer between 200°C and 300°C, and the decomposition of the calcite between 600°C and 750°C. The thermal decomposition curve of the alginic acid present in the material is only slightly different from the curve of the pure alginic acid (fig. 2.4.A), because the peak is asymmetrical, tailored versus higher temperatures, possibly correlated to the decomposition of a fraction of the organic part which interacts with calcium carbonate. This underlines the organic-inorganic interaction, not evident neither through solid state NMR studies (data not shown). From the SEM images it can be noted the contrast between the colors of the dark polymeric part vs the white inorganic spherulitic particles. The shape of the $CaCO_3$ crystals is similar to that obtained with sodium alginate (Fig. 2.2 E). The insoluble polymer act as a glue between the particles of the material, resulting in a consolidant agent.

X-ray (not reported) and microscopy analysis of hybrid material prepared with alginic acid reveals a poor crystallinity and that the $CaCO_3$ part has calcite structure, moreover it is not negligible the presence of NaCl, by-product of the preparation.

A 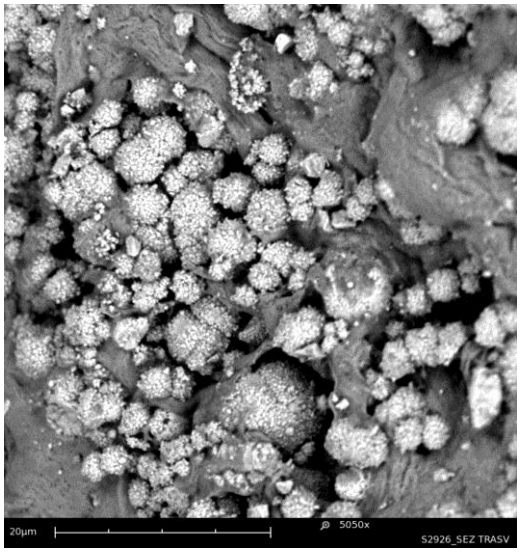

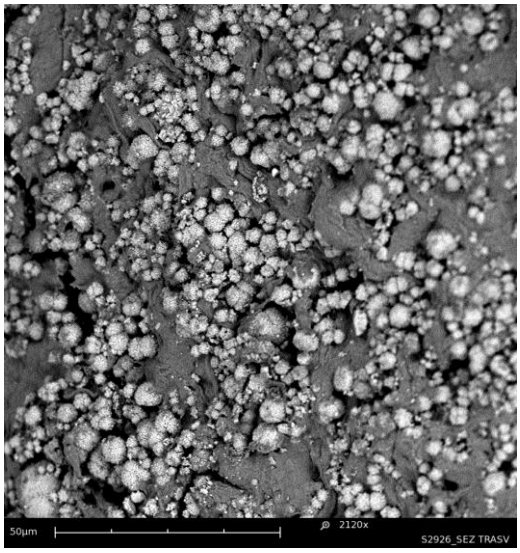

B

Figures 2.3 A and B – hybrid material made up by calcium carbonate particles precipitated in presence of alginic acid. 5050x and 2120x SEM enlargements of the sample cross section

A 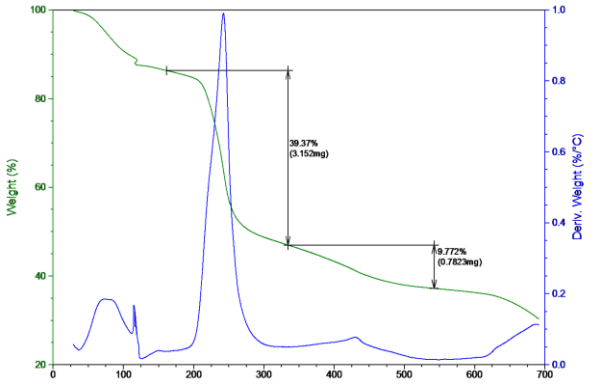

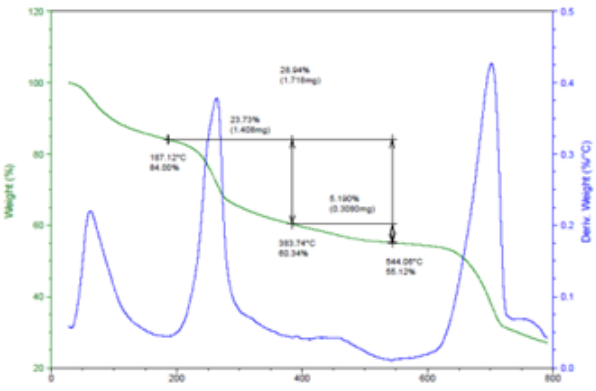

B

Figures 2.4 A and B – TGA of alginic acid (A) and alginic acid/calcium carbonate material (B).

2.2 – PREPARATION OF MINI-SPECIMENS AND THEIR MECHANICAL RESISTANCE

The experimental work has been addressed to observe the properties of materials prepared by the mixture of $CaCO_3$, H_2O and polysaccharides. $CaCO_3$ used for the experiments was a commercial sample of calcite for construction. It has a particle size higher than 100 mesh for more than 62% (measurement performed through particle sieves), a density of 0,168 g/ml (measured through a 1L cylinder), and a water content percentage, measured through NMR studies (fig.2.7), of 1,7%. XRD patterns (fig. 2.6.B) and IR spectrum (figure 2.5) confirm the calcite nature of the powder and the

absence of significant impurities. The scanning electron microscopy (SEM) showed irregular shape and not homogeneous dimensions of calcium carbonate particles ranging from small aggregates, of less than 1 µm, to other of more than 20 µm lengths (figure 2.2.A).

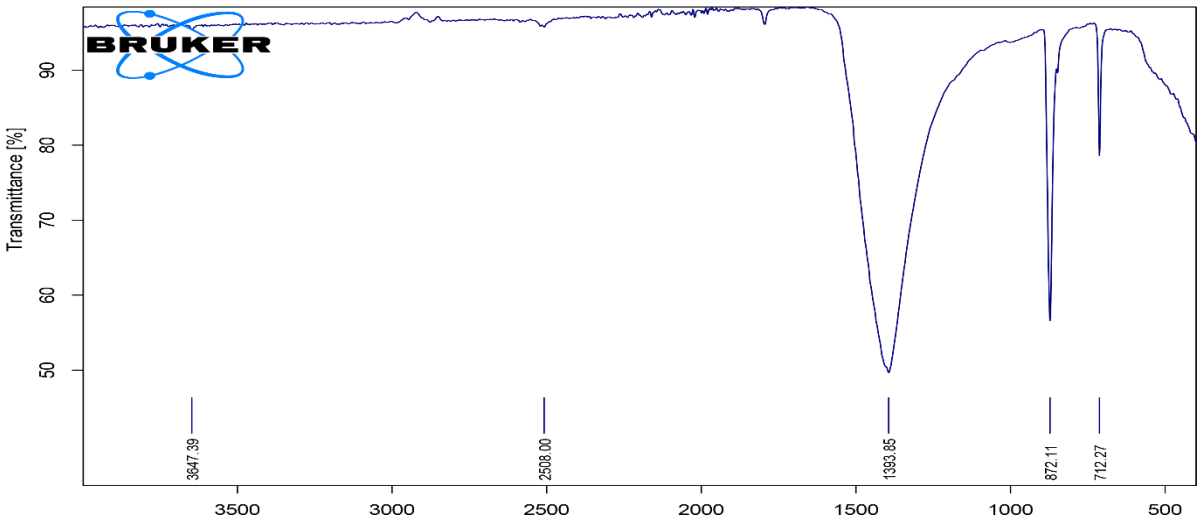

Fig. 2.5 - FT-IR analysis of the raw material

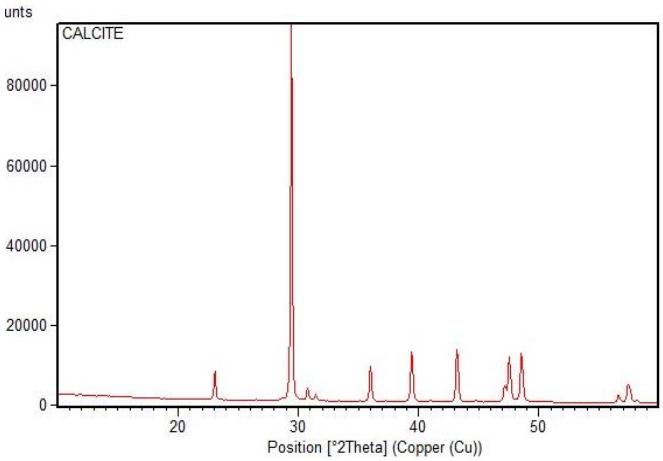

Fig 2.6 - calcium carbonate (raw material). A) SEM images B) XRD analysis

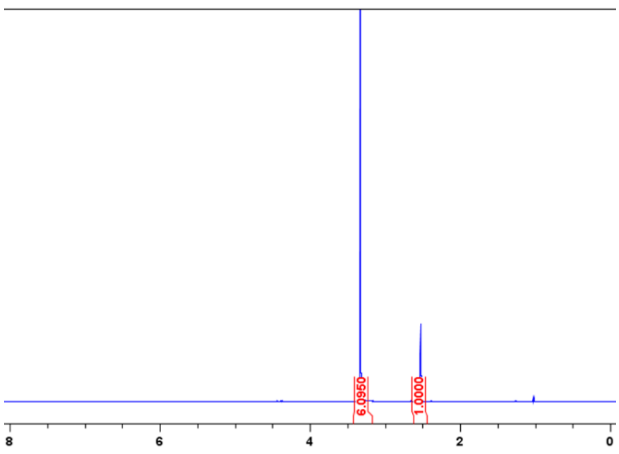

Fig 2.7 - The residual water was extracted from calcium carbonate and the value of the integral of the water extracted from the 100 mg sample was interpolated with the calibration curve having equation: y =3,6712x (*see "material and methods" paragraph*)

Preliminary tests on $CaCO_3$/polymer based materials were done using a selection of soluble polysaccharides. They can be divided into two groups of compounds:

- anionic polymers: chondroitin sulfate A and B both in salt and acid form, alginic acid and totally or partially (30%) alginate sodium salt, two carboxymethylcellulose with different carboxylation degree: CMC DS 2, and CMC DS 0.33, phosphate starch and dextran sulfate. All this compound can interact with the positive charge on the surface of particles of $CaCO_3$. Some examples of this kind of interaction were already reported by the literature [2a,b,c],
- viscous and gel forming polysaccharides as xanthan and locus beam gum, or their heated mixture, cross-linked carboxymethylcellulose. They were used in order to assess the behavior of $CaCO_3$ particles dispersed in a medium which reduces the molecular mobility and to evaluate the possibility of including the inorganic particles in a polysaccharide cage.

$CaCO_3$ was introduced into the polysaccharide solutions and, after stirring, it was poured into a mould. The amount of polymer introduced (Table 2.1) depends from its solubility and from the viscosity of the mixture with the calcium carbonate: the workability of the formulations was qualitatively standardized for all preparations. The viscosity must be such that it does not prevent the mixing of the paste with the mechanical stirrer equipped with a steel propeller; moreover the viscosity of the dough should, however, allows its casting into the mould. Several discoid specimens were produced using petri dishes as molds, of 5 cm in diameter and 1 cm wide. They resulted approximately resistant to the mechanical compression, the rupture tests were carried out manually. The empirical values of mechanical resistance were described by a score from 1 to 4 "+" reported in the last column of the table 2.1, which also shows the amount of water used in the formulation (usually about 50% of the calcite weight). Polymers with higher charge density give better results than the other polysaccharides. The DS2 CMC interacts well with the calcium carbonate and develops a paste that once dried assumes discrete mechanical properties. The specimens made up by calcite and sodium alginate showed the best mechanical properties at the empirical test. Interestingly the mechanical resistance of this specimen is found to improve when the polymer molecular weight increases, or its percentage in the mixture increases.

Table 2.1 Preparation of test-pieces with $CaCO_3$ and different polysaccharides

Polysaccharides	Charge density /monomer (CD)	Polysacch./CaCO$_3$ % (w/w)	Polysacch./CaCO$_3$ (mol/mol)	H_2O/ Ca CO_3 (w/w)	Time of drying days	IR results	Empirical evaluation of resistance
Chondroitin Na salt	1.2	2% 6%	0,004 0,013	52% 51%	2 2	calcite calcite	++ +++
Chondroitin H+ form	1.2	6%	0,013	51%	2	Calcite	++
Alginic acid (70%)	1	2%	0,006	52%	2	Calcite	+
Alginic Acid	1	2%	0,007	52%	2	Calcite	+
Sodium alginate medium viscosity	1	10% 2%	0,025 0,005	200% 50%	5 2	Calcite Calcite	++++ +++
Xantan	0.2	1%	0,001	50%	2	Calcite	+
LBG	0	1%	0,001	50%	2	Calcite	+
Xantan + LBG (T°C=60°)	0.1	1%	0,001	50%	2	Calcite	+
Phosphated starch	0.2	10%	0,015	43%	2	Calcite	++
cross-linked CMC	0.7	10%	0,025	48%	2	Calcite	++
CMC DS 0.33	0.33	10%	0,025	48%	2	Calcite	+
CMC DS 2	2.0	10% 2%	0,025 0,005	48% 48%	2 2	Calcite Calcite	++++ +++
Dermatan sulfate	1.2	6%	0,013	51%	2	Calcite	++
Dextran sulfate	1.5	6%	0,013	51%	2	Calcite	++

For further studies the high carboxylated biopolymers, as carboxymethyl cellulose D.S.2, chondroitin sulfate and sodium alginate were chosen. Moreover, it was used sodium polyacrylate, a polymer with high carboxylated groups density, to assess the strong interaction between these kind of charged functional groups and the calcium carbonate surface particles.

Specimens characterizations

The chemical and physical characterization, such as: the crystallographic form, the content of organic material and the morphology of some of these preliminary samples, were analyzed through SEM and TGA (Table 2.2). The crystallographic form (calcite) was maintained and the appearance of crystalline particles was smaller than the powder particles of calcium carbonate raw

material. The reason is that, once dispersed in solution, calcium carbonate particles disaggregate, then they are solvated by the polymeric chains, which interact with carboxylated groups with the inorganic surface. The shape of the disaggregated particles tends to become regular, almost rhombohedral. The amount of the organic part measured is less than the theoretical, for the reason that a part of polymer could be bound to the calcium carbonate particle surfaces and its decomposition temperature range is different from the free polymer decomposition temperature range. This observation has already been done for the co-precipitated calcium carbonate/alginic acid materials (paragraph 2.1).

Table 2.2 Evaluation of crystallographic form, content of organic material and morphology of selected samples

Theoretical Polymer%	Polymer	Ratio $CaCO_3/H_2O$ (g/ml)	$H_2O/CaCO_3$ % mix	TGA % estimation of organic content	XRPD	SEM
6,7	Chondroitin	0.9	125	3.95	calcite	rhombohedral
10	Polyacrylate	1.3	76	4.10	calcite	rhombohedral
16.7	Polyacrylate	1.8	57	3.28	calcite	rhombohedral
20	Polyacrylate	1.5	69	6.60	calcite	rhombohedral
10	Polyacrylate	2.4	42	n.d.	calcite	rhombohedral
10	Alginate	0.5	194	n.d.	calcite	rhombohedral
10	Alginate	0.8	128	n.d.	calcite	rhombohedral
10	CMC DS 2	0.8	125	n.d.	calcite	rhombohedral

2.3 TEST PIECES SCALING UP

2.3.1 PRELIMINARY EXPERIMENTS

In order to measure the mechanical strength of the test pieces it is necessary to prepare regular samples with smooth, parallel surfaces, and dimensions larger than 1 cm. The characteristics of a first screening of $CaCO_3$/polysaccharide materials samples of parallelepipeds shape with 4 cm x 2 cm x 3 cm dimensions are reported in Tab 2.3 a, b. They were prepared with 36 g of $CaCO_3$ mixed with alginate at low and medium molecular weight, carboxymethyl cellulose with a substitution degree of 2 (DS2 CMC) and 0.33 (CMC DS 0:33), chondroitin sulfate and a polyacrylate, considering different amounts respect to $CaCO_3$ from 1 to 10 %. Also in these experiments the amount of water depends from the polysaccharide solubility and viscosity

Both the mechanical resistance and the shape of these samples were evaluated by empirical observations using a score from "–" to four "+". The best mechanical properties were observed using medium molecular weight (200,000 Da) sodium alginate. The shape of these latter, however, were irregular. The test pieces presented fissures and cavities due to the volume reduction after water evaporation. Using a depolymerized alginate with lower molecular weight (25000 Da) (see 2.5 paragraph), it was possible to reduce the viscosity of the mixture, and the amount of H_2O giving as final results some specimens with a better shape. Tab. 2.3b shows that using alginate to reinforce calcium carbonate, a correlation between the polymer molecular weight and the mixture viscosity is seen. More interestingly, for polymer with molecular weight of 200000 Da at concentration polymer/$CaCO_3$ 10%. a significant reinforcement of the dried sample, can be observed. In conclusion, fixing the polymer molecular weight, the mechanical resistance properties increases as the polymer concentration increases.

Table 2.3a Summary of $CaCO_3$ /CMC parallelepipeds test pieces 4 cm x 2 cm x 3 cm

polysaccharide	CMC MW (Dalton)	polymer/$CaCO_3$ (% w/w)	Polymer solution (mg/ml)	$CaCO_3/H_2O$ (g/ml)	Paste viscosity	Empirical evaluation	
						Resistance	Shape
CMC DS 0.33	200000	10	100	1	high	+	+ +
CMC DS 0.33	200000	8	75	0,9	high	+	+ +
CMC DS 0.33	200000	1	20	1.8	medium	+	+ +
CMC DS 0.33	200000	1	25	1.2	medium	+	+ +
CMC DS 2	200000	10	80	0.8	high	+ +	-
CMC DS 2	200000	10	65	0.6	medium	+ +	-
CMC DS 2	200000	5	80	1.6	high	+ +	-

Table 2.3b Summary of $CaCO_3$ /Alginate parallelepipeds test pieces 4 cm x 2 cm x 3 cm

polysaccharide	Alginate MW (Dalton)	polymer/$CaCO_3$ (% w/w)	Polymer solution (mg/ml)	Ratio $CaCO_3/H_2O$ (g/ml)	Paste viscosity	Empirical evaluation	
						Resistance	Shape
alginate	200000	10	51	0.5	medium	+ + +	-
alginate	200000	2	36	1.7	high	+ +	+
alginate	80000	10	180	1.8	very high*	+ +	-
alginate	80000	10	100	1	high	+ +	-
alginate	80000	5	100	2	high	+ +	-
alginate	80000	10	78	0.8	medium	+ +	-
alginate	25000	5	150	3	low	+	+ + +

This first scale-up suggests that sodium alginate and CMC DS2 are potentially interesting additives for building $CaCO_3$/polymer hybrid materials, because the generated pastes show viscosity low enough to fill regular shape moulds, and give dried material which mechanical properties are reinforced compared to pure calcium carbonate

A deeply investigation on alginate with 80000 Da Mw was performed as it was considered as the most suitable organic binder for the calcium carbonate, because of its performance showed in table 2.1. Sodium alginate was characterized by ^{13}C-NMR spectra (Figure 2.8). In table 2.4 the measured chemical shifts of sodium alginate, in agreement with literature [5], are reported. The alginate structural characterization gives a composition ratio of the two monosaccharides mannuronate : guluronate of about 2:1

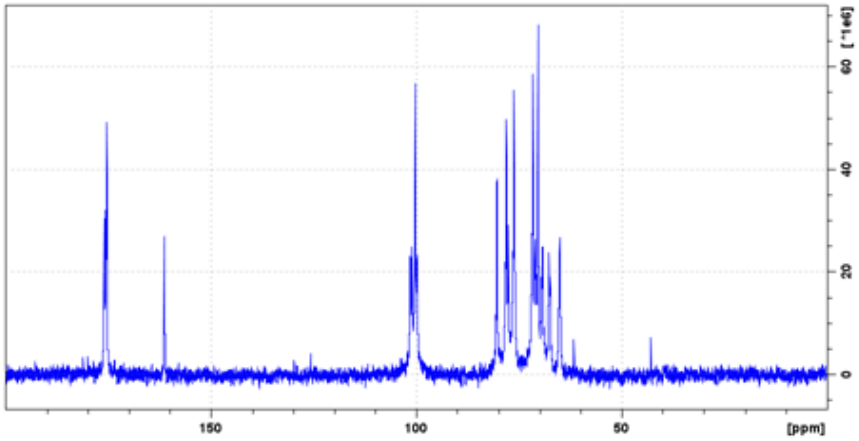

Figure 2.8 – ^{13}C spectra of sodium alginate

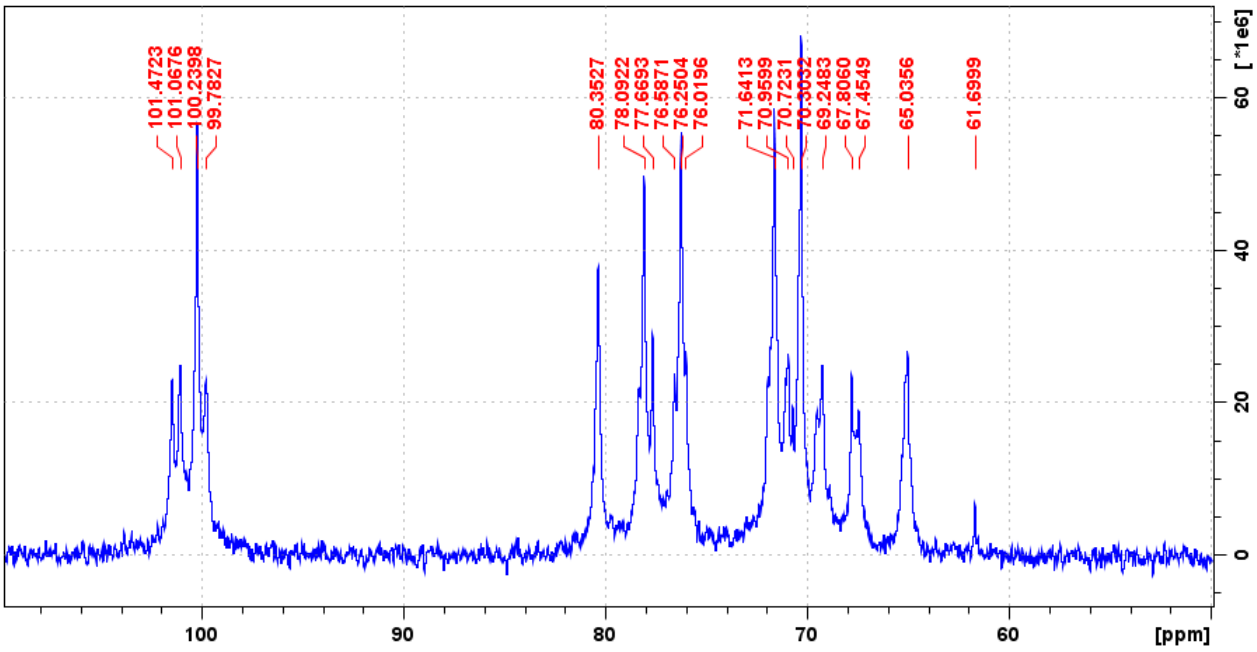

Figure 2.9 – ^{13}C NMR spectra. Expansion 50 -110 ppm

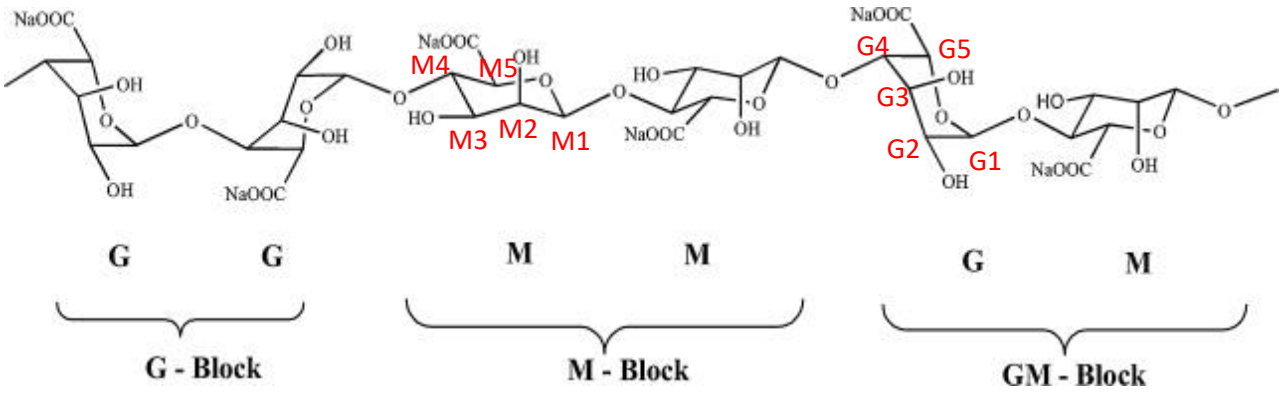

Figure 2.9 – G (guluronic) and M (mannuronic) monosaccharides of the alginic sodium salt [4]

Carbon	^{13}C (ppm)
G1	101
M1	100
G2	65
M2	70
G3	69
M3	71
G4	80
M4	78
G5	67
M5	76

Table – 2.4 Chemical shift for sodium alginate are assigned as reported by the literature [5]

For mechanical strength measurements it is necessary to obtain block having parallel faces and a sides length of 4 cm. Thus, a further scale up was done using cubic metal mould. With a view to industrial application, to contain the cost, a low amount (1%) of sodium alginate and carboxymethyl cellulose D.S. 2, was initially considered. Considering that formulation should have a viscosity low enough to be mechanically stirred and to fill homogeneously the mould, the $CaCO_3/H_2O$ ratio was initially set at 40%. Calcite was introduced into the polysaccharide solution and, after stirring, it was poured into the mould, then was dried at the open air. The obtained test pieces presented fissures and cavities due to the volume reduction after water evaporation.

As macro defects significantly decrease the mechanical resistance of the material, a possible solution could be to reduce the water amount in the formulation, without increasing the viscosity of the $CaCO_3$/polymer/water mixture, a necessary condition for the workability of the paste. To meet this objective, we identified three lines of work:

• to use a dispersant able to improve the workability (reduce the viscosity of the mixture) in presence of less amount of water

• to introduce in the mixture a component able to absorb/consume excess water

• to reduce the viscosity of the mixture by chemical modification of the polysaccharide.

In the following paragraph it is explained how these three strategies were developed.

2.3.2 –DISPERSANT PROPERTIES

Two dispersants currently used in cements and cement pastes were tested, their commercial name are SPS and 425-P. The first has a much lower solubility compared to the latter, and it also shows a worse performance than 425-P to disperse calcite powder. Various tests were carried out with different weight ratio among calcite, water and dispersant from 18: 2: 0.12, up to 18: 6: 0.12. Two procedures have been used depending to the homogeneity/viscosity of the mixture after the addition of dispersant:

a) For a not homogeneous mixture, sodium alginate was added in solution
b) For a homogeneous mixture, sodium alginate was added in powder:

Experiments are summarized in tables 2.5a and 2.5b respectively.

Table 2.5a Effect of dispersant 425-P on the appearance of the mixture using alginate (A) solution

430-P Mg	$CaCO_3$ /H_2O g/ml	appearance of $CaCO_3$ +430-P in H_2O	alginate solution g/ml	appearance of alginate solution	weight ratios $CaCO_3$/430-P/Alg/ H_2O	Appearance of mixture
60	**18 / 2**	**Lumpy**	**1,8 / 8**	**Partially dissolved**	**1 / 3x10^{-3} / 0.1 / 0.55**	**Mixture irregular and thick**
-	18 / 2	Lumpy	1,8 / 8	Partially dissolved	1 / 3x10^{-3} / 0/ 0.55	Mixture irregular and thick
60	**18 / 3**	**Paste**	**1,8 / 7**	**Partially dissolved**	**1 / 3x10^{-3} / 0.1 / 0.55**	**Mixture irregular and thick**
-	18 /3	Lumpy	1,8 / 7	Partially dissolved	1 / 3x10^{-3} / 0/ 0.55	Mixture irregular and thick
120	**18 / 3**	**Paste**	**0,9 / 7**	**viscous solution**	**1 /6x10^{-3} / 0.05 / 0.55**	**Mixture uniform and thick**
-	18 / 3	Lumpy	0,9 / 7	viscous solution	1 / 6x10^{-3} / 0 / 0.55	Mixture uniform and thick

Table 2.5b Effect of dispersant 425-P on the appearance of the mixture using alginate (A) powder

425-P Mg	$CaCO_3/H_2O$ g/ml	appearance of mixture of $CaCO_3$ +430-P in H_2O	Alginate: Powder g	weight ratios $CaCO_3$/430-P/Alg/H_2O	appearance of the mixture
120	**18 / 4**	**workable paste**	**0,9**	**1 /6x10^{-3} / 0.05 / 0.2**	**Mixture uniform and thick**
	18 / 4	lumpy	Not added	1 / 6x10^{-3} / 0 / 0.2	Mixture irregular and lumpy
120	**18 / 8**	**paste**	**0,9**	**1 / 6x10^{-3} / 0.05 / 0.4**	**Mixture uniform and thick**
	18 / 8	paste	0,9	1 / 6x10^{-3} / 0 / 0.4	Mixture uniform and thick
240	**18 / 8**	**fluid paste**	**0,9**	**1 / 1x10^{-2} / 0.05 / 0.2**	**Mixture uniform and fluid**
	18 / 8	semi fluid paste	0,9	1 / 1x10^{-2} / 0/ 0.2	Mixture uniform and thick

With a calcite: water : dispersant weight ratio of 18: 3: 0.12 the mixture becomes workable, although showing an high viscosity. Meanwhile, in the absence of dispersant, with the same calcite : water ratio, the mixture can't be worked. To obtain mixture with a low enough viscosity water must be added until a ratio of 18 : 8.

425-P dispersant was characterized by NMR. The ^{13}C NMR spectrum reveals a structure consisting of a polyacrylate esterified with PEG chains with a degree of 88%.

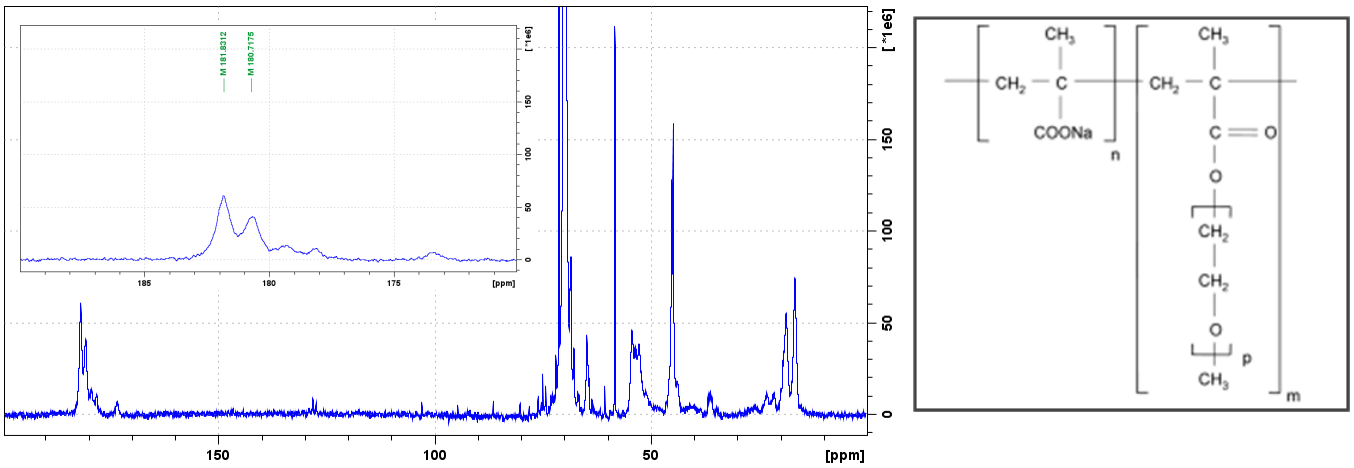

Figure 2.10 – ^{13}C NMR spectrum of 425-P in the insert expansion of carboxyl signals

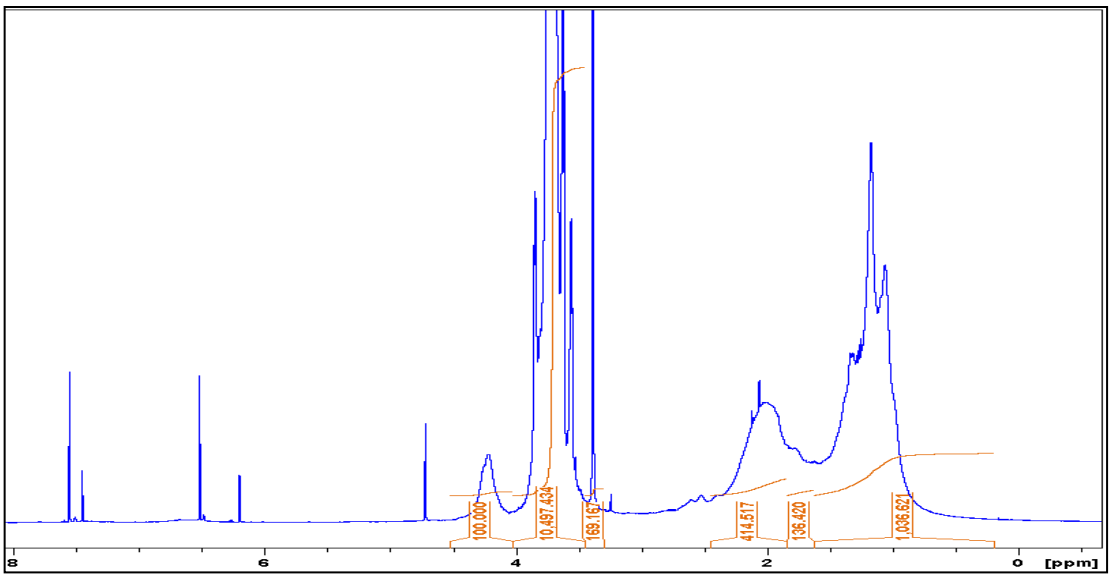

Figure 2.11 – ^{1}H NMR spectrum of 425-P

Two signals at low-fields of the ^{13}C NMR spectrum (at about 181 ppm) show the presence of two types of carboxyl groups: one is esterified with the polyethylene glycol, while the other in acidic free form. The degree of esterification calculated from the integrals of signals (4.2 and 3.4 ppm) of the PEG structure (-CH_2 linked to carboxyl and -CH_3) was 87%.

The carboxyl group can interact with the surface of the calcium carbonate particles, while PEG chains act as steric hindrance to prevent the aggregation of the particles as schematized in the figure 2.12.

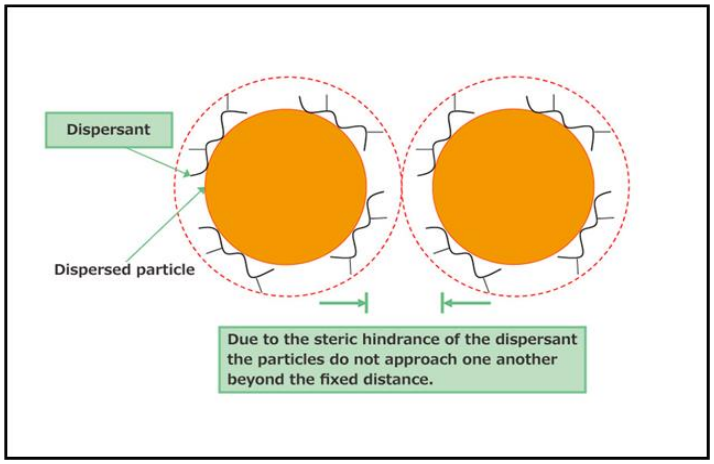

Figure 2.12 - Scheme of action of dispersant 425-p with $CaCO_3$ particles. It adsorbs to the surface of $CaCO_3$ particles through COO^- groups, while PEG chain forms a steric repulsive layer around the particles.

The average molecular weight of 425-P determined by HPSEC-TDA is 24000 Dalton. The product is characterized by a large polydispersion being the peak eluted between 12 ml to 19 ml. In figure 2.13 the Right Angle Laser (RALLS) and Refractive Index (RI) profiles are reported. The signals of the two detectors are not superimposed highlighting a non-homogeneous distribution of the molecular weight. In fact, the first part of peak, species with higher molecular weight are present in very low concentration (low response of IR detector and high response of Light scattering detector) suggesting the presence of some aggregates, instead in the second part the smaller species are eluted and these are present in higher concentration. By elaboration of chromatograms it is possible to obtain the molecular weight distribution and the weigh fraction of the two different species and the results, reported in table, confirmed the observations previously reported.

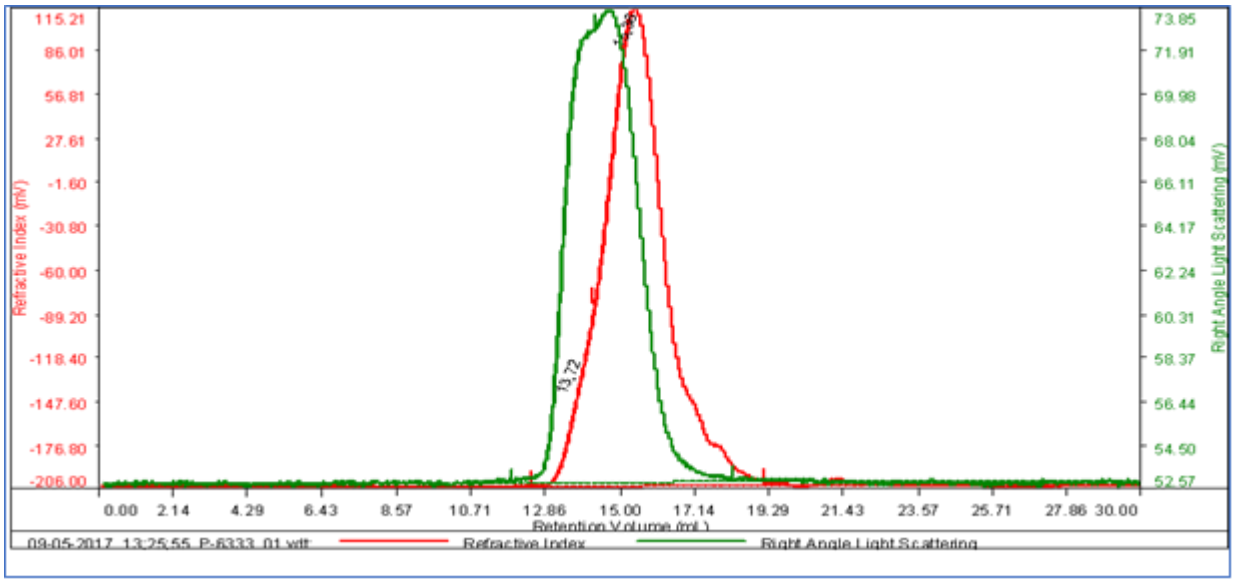

Figure 2.13 – HPSEC-TDA profiles of 425-P dispersant. Green light scattering, red refractive index

2.3.3 EXPERIMENTS IN PRESENCE OF DISPERSANT

In the preliminary tests of the dispersant the viscosity of the mixture: $CaCO_3$/polysaccharide/H_2O was significantly reduced making the sample preparation easier, and in some cases possible; for that reason, further test pieces were prepared with a % of dispersant of 0.67 or 0.35 respect to $CaCO_3$. In table 2.7 the ratio among the components of the mixture and an empirical evaluation of shape and resistance of the test pieces are shown. A score of "+" and "–" was used. Shape was positively evaluated for the absence of cavity, cracks, and deformation, resistance was evaluated taking as reference the strength needed to break the test piece.

Also in presence of dispersant, good mechanical resistance was obtained for polyacrylate (0.1%) and 22% of H_2O, and for high carboxylated polysaccharides, as low viscosity alginate (0.05%) and H_2O ranging between 33 and 44%, CMC DS 2 (0.05%) and 33% H_2O.

Using a low viscosity alginate and CMC it was possible to reduce the % of H_2O in comparison to the previous experiments obtaining, as results, test pieces with a better shape. However, for the majority of samples, cavities, cracks and deformations, that do not allow to perform the standard mechanical tests, were observed. To overcome this drawback, which is associated to the shrinkage of the material as a result of drying, considering that the amount of water can't be reduced further, a possible solution is to add in the test pieces formulation ($CaCO_3$/polymer/H_2O/dispersant) a component that can absorb the excess water, for example linking it by chemical reaction.

Table 2.7: Summary of $CaCO_3$ with CMC, ChS, A, and polyacrylate parallelepipeds test pieces 4 cm x 2 cm x 3 cm prepared in presence of dispersant.

code	ml H_2O; w/w % (H_2O/ $CaCO_3$)	w/w % dispersant 430P/$CaCO_3$	polysaccharide	w/w % Polysacch./$CaCO_3$	Shape	Resistance
S3008	4 (22%)	0.67	polyacrylate	10	+	++
S3005	5 (28%)	0.67	polyacrylate	10	-	++
S3056	8 (44%)	0.67	alginate l.w.	5	+	+++
S3057	8 (44%)	-	alginate l.w.	5	+	+++
S3037	9 (33%)	0.35	alginate l.w.	3.3	+	+++
S3067B	9 (33%)	0.35	CMC DS 2	3.3	+	+++
S3067	8 (44%)	0.67	CMC DS 2	5	-	+++
S3060	8 (44%)	-	chondroitin	10	-	+
S3068	9 (33%)	0.35	chondroitin	4.4	-	+

Score: 1) shape +++ no formation of bubbles or crack;- formation of many bubbles or cracks

2.3.4 CALCITE – CEMENT FORMULATION

Choosing the substance to include in the test formulation $CaCO_3$/polymer/H_2O/dispersant, able to absorb/consume the excess of water, two options were considered: CaO and cement.

CaO reacted too fast with water preventing the formation of the slurry, while preliminary tests with cement at the contrary, showed a good results. Therefore, the next experiments will be focused on the optimization of the formulation including Portland cement (CEM 52.5) in variable amount, to obtain test materials with good mechanical properties.

When anhydrous cement is mixed with water, a number of exothermic chemical reactions take place both simultaneously and successively, commonly denoted with the term hydration. The mechanism of cement hydration can be described as a topochemical process.

When water reaches anhydrous grains it reacts rapidly on the surface, in an exothermic process. For tricalcium silicate, it takes about 15 min. As consequence, an external core is formed; the presence of hydrate cement particles will retard internal hydration of cement grains. This is sometimes referred as the dormant period, and it takes about 2 h. After this period, by diffusion, water penetrates into the particles, promoting the set of cement. Finally, after many months the hydration will be almost complete. [3]

Tricalcium silicate (C_3S) is the most abundant and important cement mineral in Portland cements, contributing to the most of the early strength development.

The hydration of C_3S can be written as:

$$C_3S + (1.3 + x)H \rightarrow C1.7SH_x + 1.3CH$$

where 1.7C-S-H_x is the calcium silicate hydrate (C-S-H) gel phase and CH is calcium hydroxide, which has the mineral name portlandite. The variable x represents the amount of water associated with the C-S-H gel, which varies from about 1.4 to 4 depending on the relative humidity inside the paste. For example (C_3S) phase reacts with water molecules to produce C-S-H crystal as shown in figure 2.14 For every kilogram of cement between 0.2 and 0.3 kg of water is required to complete the hydration reactions. The water-to-cement ratio is the ratio between the weights of water and cement in a concrete mix. For proper hydration, this ratio (commonly called the w/c ratio) should be almost 0.20, assuming no contribution to hydration from external water sources. Differently to obtain a pourable mixture, water–cement ratios between 0.45 to 0.60 should be used.

$C_3S + (1.3 + x)H \rightarrow C1.7SHx + 1.3CH$ *(simple formula)*

$2(CaO)_3(SiO_2)+7H_2O \rightarrow (CaO)_3(SiO_2)_2{\cdot}4(H_2O)+3Ca(OH)_2$ *(extended formula)*

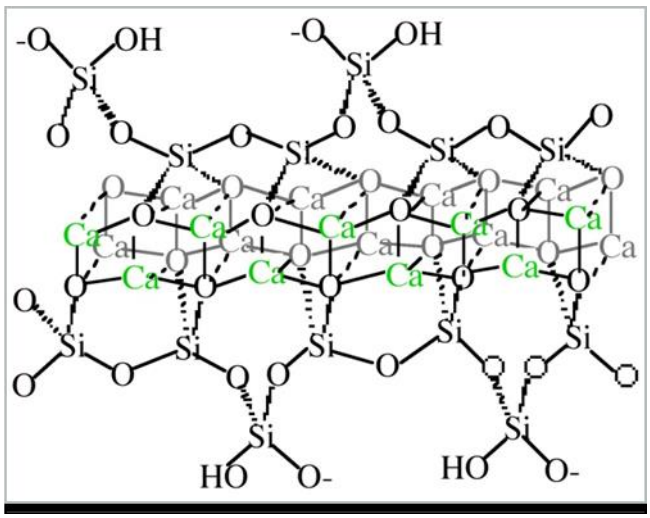

Figure 2.14 – C-S-H crystalline structure

To verify the hypothesis that cement, can subtract the excess of water during the drying phase of the materials containing the previously optimized mixture ($CaCO_3$/polymer/H_2O/dispersant), a new experimental design was done. A variable amounts of cement was introduced maintaining a constant amount (0.7% w/w) of alginate (80 KDa) and dispersant, the updated formulation are showed in table 2.4.1. Proportions among the components, and in particular the amount of water, have been set to obtain in the final samples a comparable porosity generated by evaporation of the same amount of water (35 g) considering as cement hydration water 2 g for 10 g of cement. Prismatic specimens of the size 4 x 4 x 4 cm have been produced mixing, under manual stirring, the $CaCO_3$ powder to the solution of dispersant, at which the solution of alginate was further added. The mixture was then worked with a mechanical stirrer, at 300 rpm for 10 minutes. Maturation was carried out at room temperature. After 3-4 days the samples were removed from the moulds, while the hardening process was followed for 28 days in a lab dryer in the presence of silica gel. A set of reference samples without alginate was also prepared maintaining the same ratio between the other components; their properties are summarized in table 2.8.

Almost all the test pieces were obtained with a good shape (regular parallelepipeds) without visible crackings or appreciable distortions of the surfaces. The samples were evaluated for loss of water during the curing time (Fig. 2.15), and for the mechanical resistance (table 2.9).

The weights of the specimens were monitored for the loss of water during the curing time: in this period the water molecules that do not enter the crystalline cement lattice can evaporate. Most of

the water was lost in the first 48 hours, the time between the filling of the molds and their removing. After that time the decrease in weight was slower. The lost weight percentages range between 21% and 5%. It was found that samples formulated without cement lost much more water and faster, while those with the highest cement percentage were characterized by the lower water evaporation. All samples, including the 100% $CaCO_3$, show a weight decrease lower than the expected 35% considering the hypothesis that water needed for cement hydration could be about 20% of its weight.

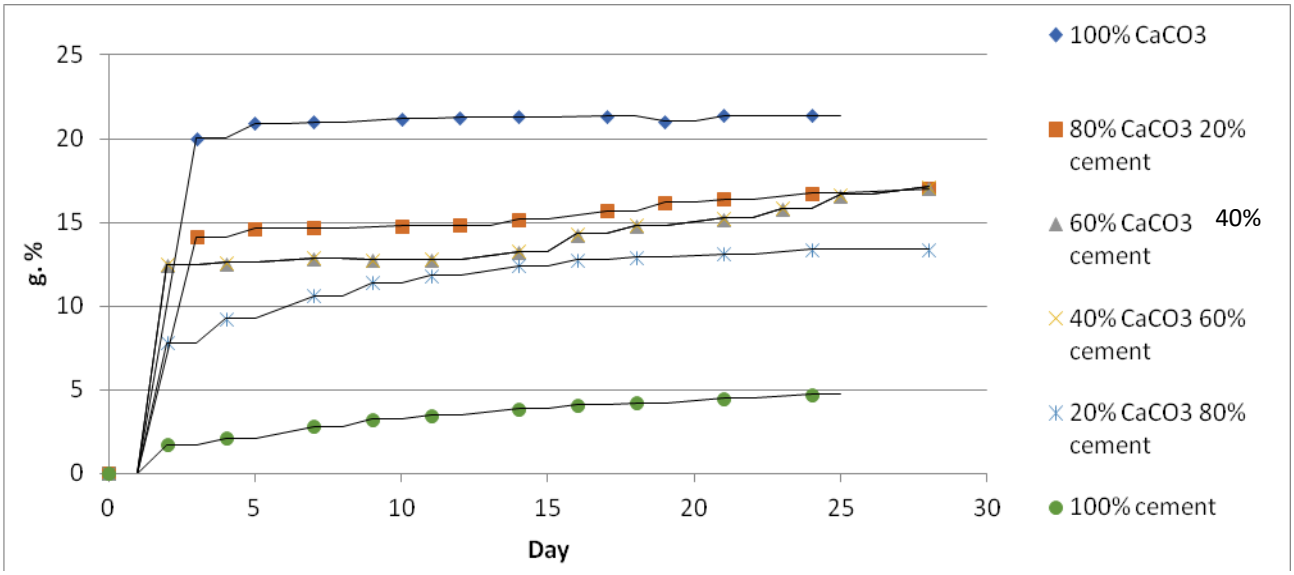

Figure 2.15 – Loss of water in $CaCO_3$ / alginate test pieces with different content of cement

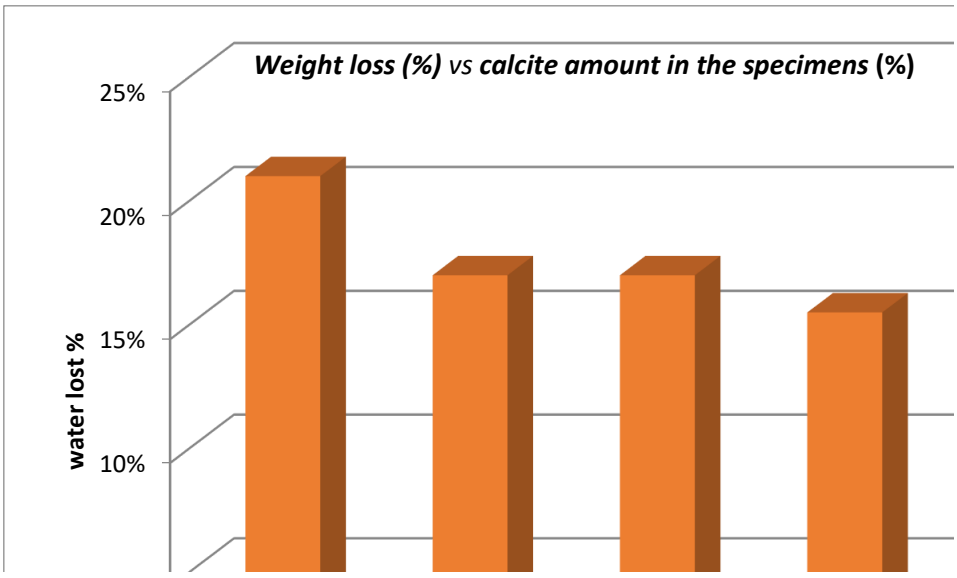

Figure 2.16 - Percentage of weight loss of every specimen after a month.

The strength of samples at 28th day in presence of alginate increases as cement percentage increases, the values are comparable with the corresponding parameters of light concrete. In the conditions described above the samples without cement was not tested because the test pieces presented significant surface irregularities.

At the time of the testing, prismatic specimen is placed in a compression testing machine where a load is applied at the constant rate of stress within the range of 0.2 to 0.4 MPa. Under pure uniaxial compression loading, the failure cracks generated are approximately parallel to the direction of the applied load.

Table 2.8 – Test pieces prepared with different ratio $CaCO_3$ /cement

	$CaCO_3$ (g)	Cement (g)	H_2O (g) for mixing + cement hydration	H_2O polysac. (g)	H_2O total (g)	H_2O(g) lost after 28 days	resistance MPa	density g/cm³
A	100	0	20	15	**35**	28,9	**n.d**	**1.4**
B	80	20	24	15	**39**	23,4	**12.1**	**1.5**
C	60	40	28	15	**43**	22,6	**16.5**	**1.5**
D	40	60	32	15	**47**	21,3	**20.6**	**1.5**
E	20	80	36	15	**51**	**15.9**	**37.0**	**1.6**
F	0	100	40	15	**55**	**10.0**	**34.6**	**1.6**

Table 2.9 - Test pieces prepared with different ratio $CaCO_3$ cement without alginate

	$CaCO_3$ (g)	Cement (g)	H_2O (g) for mixing + cement hydration (g)	H_2O added (g)	H_2O total (g)	H_2O lost after 28 days	strength MPa	Final density
A	100	0	20	15	**35**	27.1	**n.d**	**1.4**
B	80	20	24	15	**39**	20.6	**38,7**	**1.5**
C	60	40	28	15	**43**	15.9	**33,5**	**1.5**
D	40	60	32	15	**47**	16.1	**30,2**	**1.5**
E	20	80	36	15	**51**	15.9	**37.0**	**1.6**
F	0	100	40	15	**55**	10.0	**48,2**	**1.6**

Reference samples have density and weight loss by drying very similar to that of the corresponding samples including alginate in their formulation. The samples with alginate show a direct correlation between the cement amount and the compression resistance, but all the data are less than resistance values of the corresponding reference samples obtained without alginate. A possible reason of this result could be related to the alginate gelling property in presence of bivalent cations in solution. The formation of the alginate hydrogel is supported by an increase of the paste viscosity during the preparation, when polysaccharide and cement are both present. In fact it is known that cement contains soluble salts of bivalent cations. As a practical result the workability of the mixture decreases: pouring the paste and filling the moulds became difficult. The alginate hydrogel does not affect the water evaporation rate of the materials, despite it is supposed to strongly interact with water, but, during the beginning of the maturation period, retaining water in the hydrogen bond network, impairs the hydration process of the cement, generating a mechanically weaker material.

A significant difference was observed between the dried sample materials obtained from a mixture: $CaCO_3$/alginate/H_2O/disperdent/cement, and the corresponding in which alginate is not present; the former shows a uniform distribution of the mixture, while the latter surprisingly show, particle stratification. For this reason, the formation of the hydrogel, have the useful action to maintain the stability of the mixture (suspension) allowing calcite and cement particles to not aggregate, whereas in the reference specimens the particle separation was observed during the first 6 hours.

To exploit this propriety, a one set of test-pieces were prepared using a small amount of alginate as suspending / thickener and a different charged polysaccharide as binder. The composition of the inorganic part of the material used was 80% $CaCO_3$ and 20% cement. Sodium alginate was used in a very low amount. The amount of water was maintained less than 30% of the weight of mineral powders (the sum of the weight of cement and calcite), to avoid the decrease of mechanical strength of the final material.

The amount of charged polymers (binder) where chosen to obtain the same rheological characteristics for all the mixtures. In parallel samples reference were prepared, whose formulation, did not include the polymer binder.

The ratios were the following:

- calcite (240g) + cement (60g) = 300g (mineral powder)
- water = maximum 90 ml

- 425-P = 1 g (dispersant)
- sodium alginate = 0.3 g (suspending agent)
- binder polymer of the mineral fraction = 3.0 g (if not viscous) or 2.1 g (if very viscous)

In the first step the binder polymer was dissolved in water, then the previously mixed mineral powder was added to the dispersant, and the formulation was mixed with a mechanical stirrer. Then the sodium alginate solution was added. The mixture was continuously stirred, once homogeneous, the mixture was poured into the metal moulds. Test pieces were prepared in triplicate and their mechanical resistance was tested.

The tested polysaccharides were: dextran sulfate, chondroitin and dermatan sulfate, alginate derivatives (RO, Ox, depolymerized, and grafted with acrylate see paragraph 2.5). For the sake of comparison, synthetic polymers such as polyacrylates with different molecular weights, 15,000 Dalton and 7,000 Dalton were additionally tested as binders. In table 2.10 the list of tested polysaccharides and the amount of H_2O used is reported. This last parameter varies depending on solubility of the polymer and on viscosity of its solution. Also, this last test confirmed an inverse relationship between the amount of water in the slurry and the strength of the dried samples at the end. Compressive strength values higher than 30 MPa, were obtained with chondroitin sulfated and dextransulfate, both characterized by high density of electrostatic charge and high molecular weight polymers. Is interesting to observe how test pieces prepared with Chondroitin sulfate exhibit values of compressive strength higher than the corresponding references prepared with the same ingredients without ChS (45.2 vs 36.8), and, although sample contains only the 20% of cement, this value is in the range of Portland cement of class 32.5N and 32.5R (see paragraph 1.2).

It is to note that this good compressive strength was obtained even if chondroitin test pieces present some defect in the shape.

The good performance of chondroitin and dextransulfate could be explained by their high solubility. This allows reducing the amount of water (22% by weight with respect to the weight of mineral powder) in the formulation maintaining the workability of the dough. Moreover, the high charge density of the polymer, due to the presence of sulfated groups, can strengthen the interactions with the positive charge on the surface of calcite particles.

Table 2.10a - Compressive resistance (MPa) of test pieces prepared with different charged polysaccharides as binder.

% H2O	**Test samples** Compression resistance results (MPa)		
22	45,2 Chondroitin	32,7 Dextran sulfate	
24	25,3 Dermatan sulfate		
25	1,6 Alginate 200000 Da oxidized*		
26	7,3 Polyacriyate 7000 Da		
28	20,9 Polyacrylate 15000 Da		
30	19 Alginate 40000 Da**	1,1 Alginate 200000 Da RO	1,8 Acrylate grafted alginate

Note: *Alginate 200000 Da oxidized: alginate totally oxidized to di-aldehyde via sodium periodate, not reduced, stored under dark and cold conditions to limit the degradation reactions. Used just synthesized to prepare the specimen's formulation. **Alginate 40000 Dalton: depolymerized alginate 80000 Dalton as described before (see next paragraph).

Table 2.10b – Compressive strenght of reference specimens

% H2O	**Reference samples** Compression resistance results (Mpa)
22	36,8
25	32
28	25,3
30	22,8

Histogram 2.1 – Compressive resistance (MPa) of test pieces prepared with different polysaccharides as binder and compressive resistance of control specimens (in red)

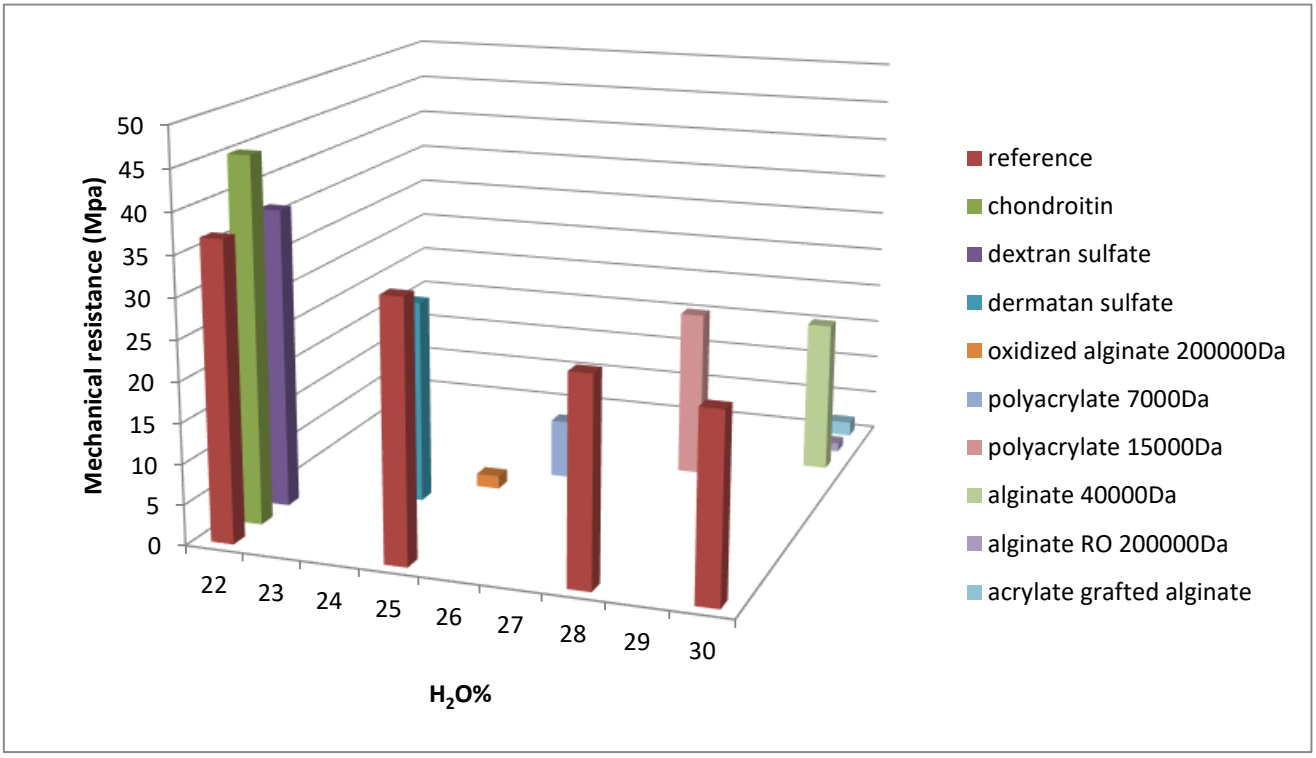

2.5 – ALGINATE DERIVATIZATION

Several modifications to the structure of alginate could be performed to reduce the viscosity of its solution, the simpler correspond to a depolymerization under basic conditions, that allow to reduce the average length of the polymer chain. This reaction takes place at 80°C through a beta-elimination mechanism, reported in fig. 2.17.

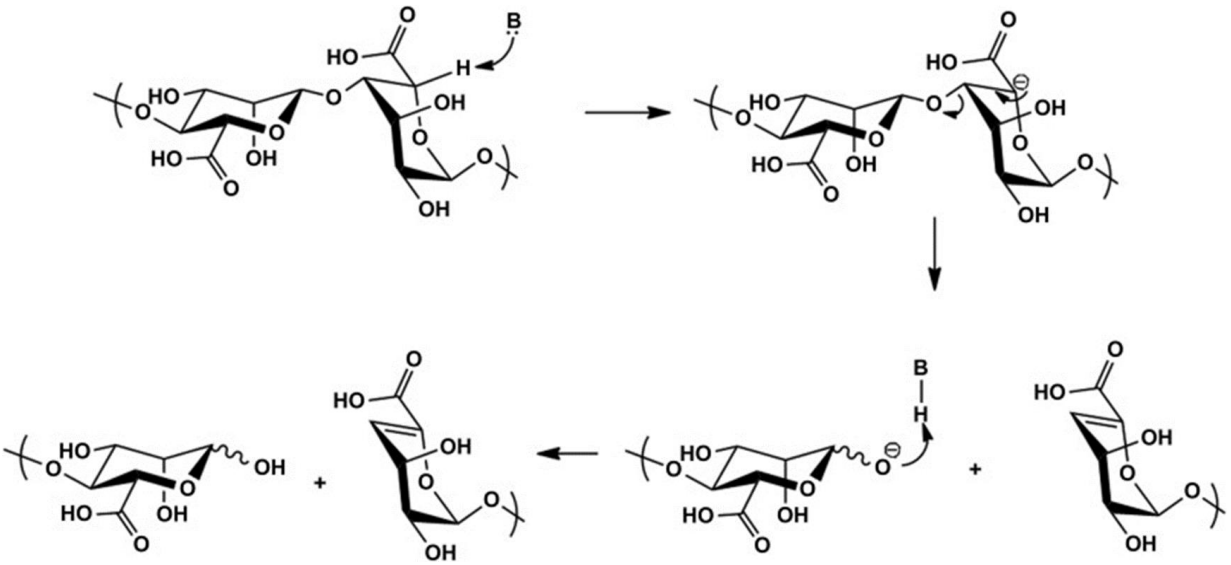

Figure 2.17 – alginate depolymerization via β-elimination mechanism [5]

The depolymerization ratio is influenced by the temperature and by the reaction time: after 3 hours at 80°C degree the average M_W changes from 80000 Dalton to 40000 Dalton, as confirmed by HPSEC-TDA analysis, showed below (fig 2.18).

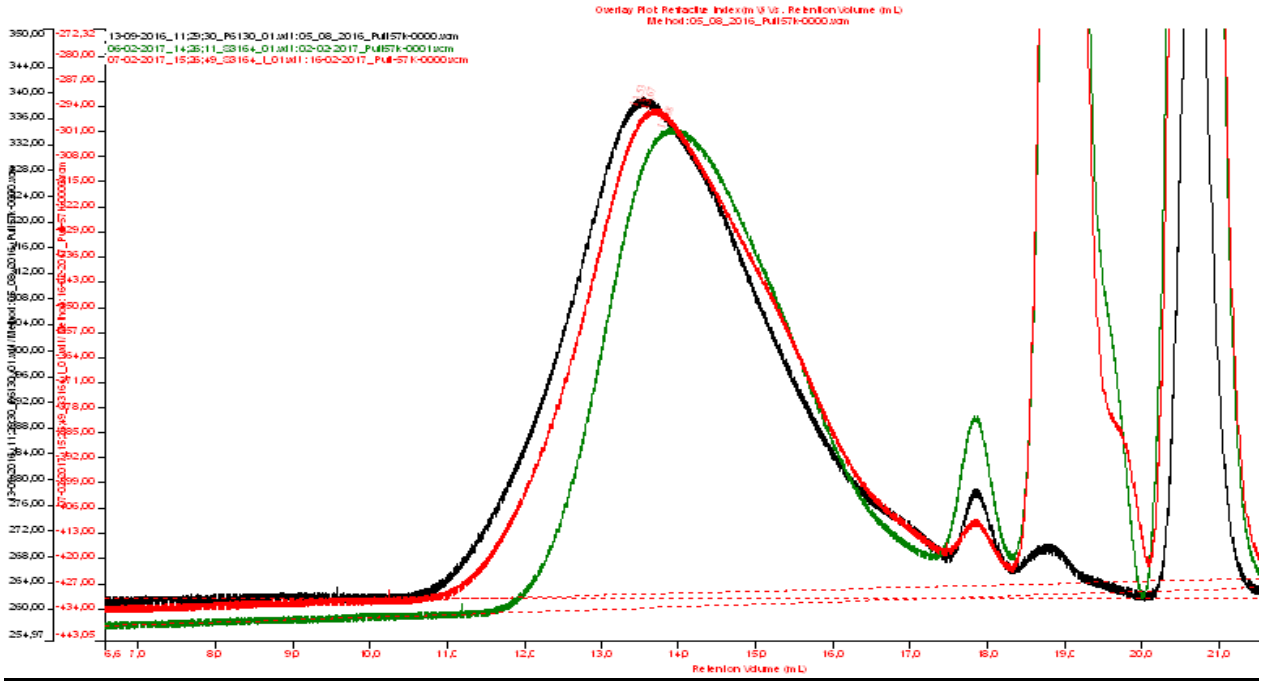

Figure 2.18 – HPSEC-TDA refractive index profiles of the starting alginate (black curve), after 45 min of reaction (red curve), and after 3 hours of reaction (green curve).

Another modification of sodium alginate was carried out by oxidation of C2 and C3 carbons, with sodium periodate, to open the ring structure, and followed by a reduction of the aldehyde group to a primary alcohol in order to stabilize the molecule once introduced into aqueous solution. Alginic acid sodium salt (80000 Dalton) was solubilized in 500 ml H_2O and then sodium periodate was added to the solution. To avoid the degradation of the product the reaction need to be performed in dark conditions. Between the oxidation and reduction reaction, a dialysis purification was performed, and a second dialysis was carried out to purify the finished product, and then it was dried under vacuum. The product was characterized by NMR and HPSEC-TDA techniques. The NMR analysis showed the expected structure modification of the polysaccharide the oxidation was complete, and the aldehyde produced was then reduced to primary alcohol. TDA analysis on the final product of the ring opening process, showed also that a depolymerization was occurred, and the final average molecular weight of this polymer was approximately half of the initial value.

In order to prevent this depolymerization, a more gentle reduction reaction (with a slight stochiometric excess of hydride) was also conducted. In the same step, the reaction time was halved. Also in this case the molecular weight of the product was too low in comparison to the starting product, this is not completely unexpected because some literature's articles report that, alginate may depolymerize during the C2 and C3 oxidation step [6].

These experiences suggest that this chemical modification applied on alginate polymer require a more careful control of the condition, possibly using only a partial oxidation, monitoring the temperature and lowering the time reaction. Next reactions will be conducted on a higher molecular weight starting material to obtain the final product with an average molecular weight not less than 40,000 Dalton.

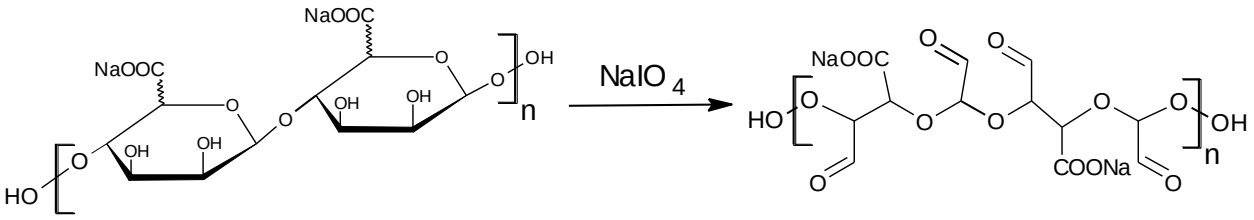

Figure 2.19 – Scheme of alginate oxidation with sodium periodate

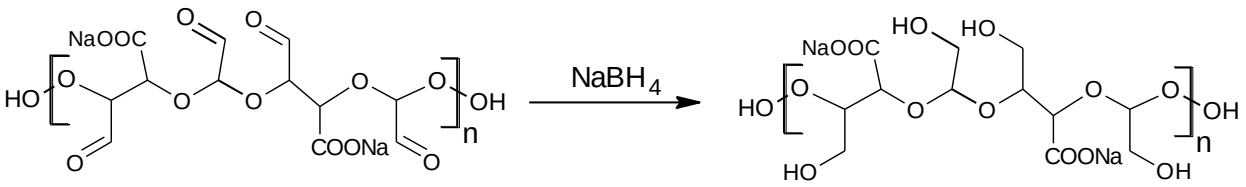

Figure 2.20 – Scheme of reduction of aldehyde groups with sodium hydride to obtain alginate "RO" (Oxidated and Reduced)

A semi-natural polymer was synthesized by grafting sodium polyacrylate on an alginate backbone, with the aim to obtain a polymer giving solution with significantly lower viscosity The grafted polymer alginate-polyacrylate was synthesized according to the literature, introducing some modifications [7]. Alginate (80000 Da) was derivatized with acrylic acid in NaOH in presence of ammonium persulfate at 80°C. As supposed previously the viscosity of the new polymer was found lower in comparison to alginate which chain length correspond to the backbone chain length of the grafted polymer.

The ^{1}H-NMR analysis show the resonances typical of the grafted polymer: the signals of acrylic moiety at high fields whereas the polysaccharide signals between 3.5 and 6.5 ppm. From the ratio between the integral of carbohydrate and acrylate signals a molar substitution (MS) of 2 was found (fig. 2.21).

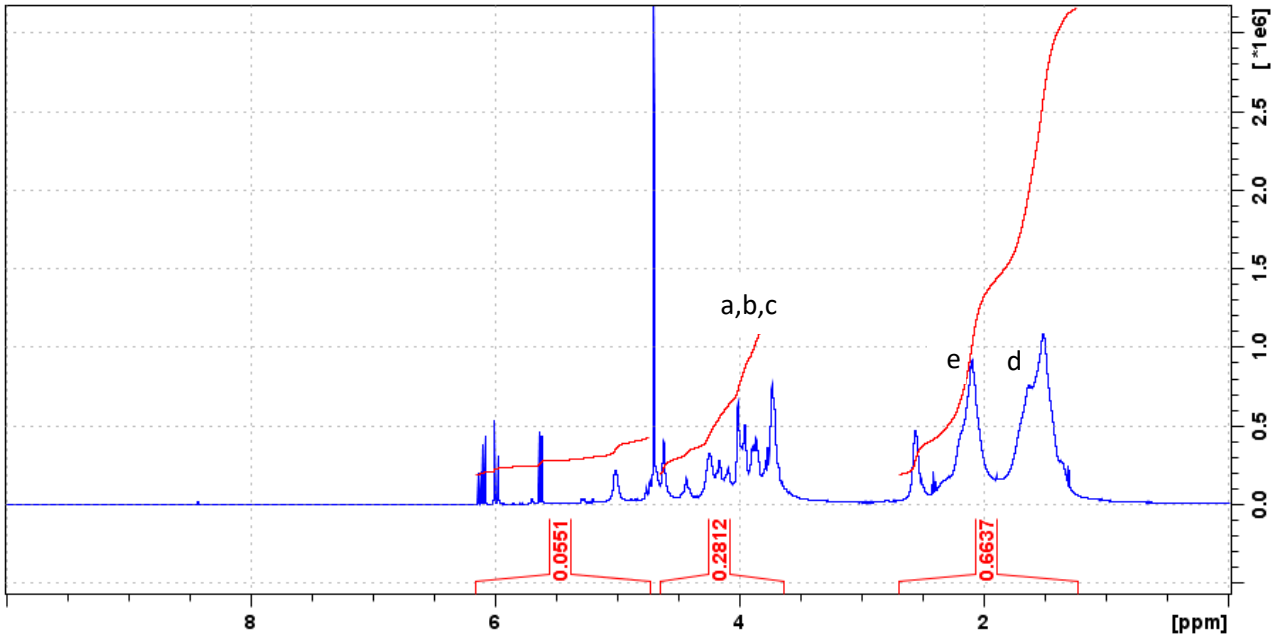

Figure 2.21 – ^{1}H- NMR spectra of polyacrylate-grafted alginate polymer

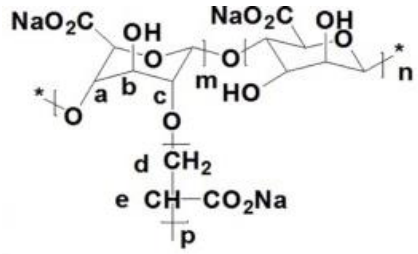

Figure 2.22– polyacrylate grafted alginate

Bibliography

[1] N.V. Vagenasa A. Gatsouli C.G. Kontoyannis Talanta 59, 4, 10 2003, 831-836

[2a] Arias, José L., et al. "Sulfated polymers in biological mineralization: a plausible source for bio-inspired engineering." Journal of Materials Chemistry 14.14 (2004): 2154-2160.; [2b] Matahwa, H., V. Ramiah, and R. D. Sanderson. "Calcium carbonate crystallization in the presence of modified polysaccharides and linear polymeric additives." Journal of Crystal Growth 310.21 (2008): 4561-4569.; [2c] Yang, Lin, et al. "Interfacial molecular recognition between polysaccharides and calcium carbonate during crystallization." Journal of inorganic biochemistry 97.4 (2003): 377-383

[3] Somayaji, Shan (2001). Civil Engineering Materials. Upper Saddle River: Prentice Hall. p. 129. ISBN 0-13-083906-X.

[4] Daemi, Hamed, Mehdi Barikani, and Mohammad Barmar. "Compatible compositions based on aqueous polyurethane dispersions and sodium alginate." Carbohydrate polymers 92.1 (2013): 490-496.

[5] Pawar, Siddhesh N., and Kevin J. Edgar. "Alginate derivatization: a review of chemistry, properties and applications." Biomaterials 33.11 (2012): 3279-3305.

[6] Gomez, C. G., M. Rinaudo, and M. A. Villar. "Oxidation of sodium alginate and characterization of the oxidized derivatives." Carbohydrate Polymers 67.3 (2007): 296-304.;

[7] Bardajee, Ghasem Rezanejade, and Zari Hooshyar. "Optical properties of water soluble CdSe quantum dots modified by a novel biopolymer based on sodium alginate." Spectrochimica Acta Part A: Molecular and Biomolecular Spectroscopy 114 (2013): 622-626.

3 – CONCLUSION AND PERSPECTIVES

The purpose of the work was to identify a natural polymer, that it would be useful to act as a binder for mineral powder, made up of calcite. Different types of polysaccharides have been tested, the most performing were anionic ones, such as sodium carboxymethylcellulose, sodium alginate and chondroitin 4 sulfate. However, the first two polymers generate a high viscous paste, when mixed with calcium carbonate and water, that require a huge amount of water to be workable, in fact further evaporation produces pores and fractures in the drying material, giving as a final result, a decrease of their mechanical resistance properties. For these reasons strategies that reduce the amount of water added were investigated.

Briefly the paste obtained mixing $CaCO_3$/polymer/water should be formulated with a low amount of water, and should have the following properties: homogeneity, workability and pourability, to facilitate its production process and its applications.

The physical chemistry of the formulations was studied, evaluating appropriate dispersants, and the organic chemistry of the polymers, altering the structure to eliminate its viscosity.

The results obtained were different: the alginate, and the depolymerized alginate, in 1% amount, were both effective to strengthen calcite but not to obtain high values of mechanical resistance. Then the material was allowed with a certain amount of cement (CEM I), in order to absorb some water and to increase the mechanical resistance value. The specimens made up of 20% cement and 80% calcite yielded different results than expectations: sodium alginate precipitates by the ions released from the cement, in the form of hydrogel, a gelatinous composition which absorbs the water of the formulation, lowering its workability. As a precipitate it can't interact with the surface of the calcite particles and does not act as a binder. The polysaccharide with the best performance results the chondroitin and to a lesser extent dextransulfate, because these are not a viscous compounds, and do not precipitate in the presence of cations.

Chondroitin could be an interesting macromolecule to use in the concrete research, but it is not an economic resource, as it is alginate or its derivatives. For this reason, future work will still focused on sodium alginate. The intention is to produce structural modification maintaining the carboxyl groups. As example it can be carried out partial glycol split reaction: only a partial oxidation of C2 and C3 groups may limit the depolymerization rate and, at the same time, it could sufficiently decrease the polymer viscosity. In this way, a lower amounts of sodium periodate and reducing agent could also be used, which would also result in a lower process cost. Other strategy could be the introduction of substituents to increase charge density like sulfate groups.

Further analysis should be carried out to investigate more deeply the nature of the interaction between the anionic charges of polysaccharide and the surface of calcium carbonate. From bibliographic references it is assumed that the partial positive charge generated by the calcium atom on the surface of the carbonate crystal can attract the anionic charge of the natural polymer, and the interaction is also demonstrated by

the present work: inorganic particles gain strength of cohesion due to the presence of the polymer between them. Solid-state NMR experiments do not show the interaction between the anionic groups and the surface of the calcium carbonate because the spectrum of the hybrid material doesn't show change if compared to the starting materials analysis.
Further characterizations will be carried out by means of TD NMR investigations, to study the hydration of calcium carbonate, cement, and hybrid material, in order to quantify the amount of free water that may be trapped in the system. The goal is to understand as much as possible the most resistant material until now produced.

The primary aim of the work is a key point that has been satisfied: it is the investigation of a still unexplored research field, in fact until nowadays no chemist has tried to produce a building material based on calcium carbonate particles and a bonding polymer. In the present work it is demonstrated that it is not impossible to obtain a material with highly resistant mechanical properties through the use of suitable natural polymers and calcite, until now considered only a filler for the cement industry. It must be considered that in any case a small amount of cement powder is required to reinforce the structure of the material, and that the natural polymer must not precipitate when in contact with its solubilized cations.
The results open the way to a new, vast research area, where it is important to focus deeply on the best biomacromolecular binder, the best calcite dispersant, and the optimal formulation procedure, starting from the bases of my work.

4. MATERIALS AND METHODS

4.1 X-RAY DIFFRACTION ANALYSIS

Materials:

The X-ray powder diffraction patterns were obtained using a Philips X'PertPro diffractometer.

Method:

- Sample preparation:

  from 5 to 10 mg of each sample were used

- Recording conditions:

  The diffraction patterns were collected using a voltage of 40 kV and a current of 40 mA. A diffraction region between 20° and 60° of 2θ was scanned. The measurements were carried out directly on the microscope slide on which particles were deposited.

4.2 SEM ANALYSIS

Materials:

- the SEM analysis were conducted in a scansion electronic microscope using a Phenom microscope.

Method:

- Sample preparation:

5 mg of each sample were deposited on the stub and the powder was analyzed at various enlargement (from 1000x to 10000x)

4.3 NMR SPECTRA RECORDING

4.3.1 ^{1}H NMR SPECTRA

Materials:

- D_2O 99.9%
- NMR tube (diameter: 6 mm)
- Spectrometer Bruker Avance 500 equipped with high sensitivity 5 mm TCI cryoprobe

Method:

- Sample preparation:

from 20 to 30 of each sample were dissolved in 0,6 ml of D_2O 99.9% water.

- Average recording conditions:

monodimensional ^1H spectra were obtained with presaturation of residual HDO, from 32 to 128 scans and a recycle delay of 10s. the ^1H spectra were recorded at 303°K with 32 K of data points. Spectra were elaborated with the software TOPSPIN 2.1. Chemical shift values were measured in accordance with calculated SR at various temperature (-5.53).

4.3.2 ^{13}C NMR SPECTRA

Materials:

- D_2O 99.9%
- NMR tube (diameter: 10 mm)
- Spectrometer Bruker Avance 400

Method:

- Sample preparation:

from 170 to 200 mg of each sample were dissolved in 2,5 ml D_2O 99.9%.

- Average recording conditions:

monodimensional ^{13}C spectra were measured with proton decoupling during acquisition time at 40°C. recycle delay was 4s and the number of scans 40000.

4.3.3 HSQC SPECTRA

Materials:

- D_2O 99.9%
- NMR tube (diameter: 10 mm)
- Spectrometer Bruker Avance 500 equipped with high sensitivity 5 mm TCI cryoprobe

Method:

- Sample preparation:

from 170 to 200 mg of each sample were dissolved in 2,5 ml D_2O 99.9%.

- Average recording conditions:

two dimensional heterocorrelated spectra were measured with carbon decoupling during acquisition with 320 increments of 24 scans for each. The polarization transfer delay was set with a $^1J_{C\text{-}H}$ coupling values of 150 Hz

4.3.4 SOLID STATE ^{13}C NMR SPECTRA

Materials:

- NMR zirconium rotor, 4mm in diameter and 21mm high
- Spectrometer Bruker Avance 300

Method:

- The ^{13}C cross polarization magic angle spinning (CPMAS) spectra were recorded with Bruker Avance 300 spectrometer operating at 75.47MHz. The following conditions were applied: repetition time 8s, ^{1}H 90 pulse length 4 us, 1.2ms contact time, 2048 or 4096 number scans, Acquisition time 35ms and spin rate 10 KHz. The compounds were placed in the zirconium rotor. The chemical shifts were recorded relative to tetramethylsilane via benzene as a secondary reference.

4.4 HUMIDITY PERCENTAGE DETERMINATION

Materials:

- high purity (> 99.9%) deuterated DMSO purchaised from Sigma Aldrich
- NMR 500Hz
- Mini spin centrifuge

Method:

- Sample preparation:

100 mg of calcium carbonate powder (raw material) was collected and centrifugated in an eppendorf with 0,6 ml deuterated DMSO for 4 minutes at 12500 rpm. Then an aliquot of 0.5 ml of surfactant was introduced in a NMR tube and analysed in order to evaluate the amount of extracted water through the interpolation with a calibration curve. Not deuterated DMSO peak was used as reference (Area value = 1.0000) for H_2O area value determination.

- Calibration curve preparation:

0,5%, 1%, 2%, and 3% H_2O aliquots in deuterated DMSO were added, and these four samples were analyzed through ^{1}H-NMR experiments. Not deuterated DMSO peak was used as reference (Area value = 1.0000) for H_2O area value determination. Data were used to design a graph "H_2O area values" vs "H_2O mg added" and the interpolation curve passing from the origin (0,0).

- Analysis of residual water in 100 mg calcium carbonate powder extracted with deuterated DMSO was performed with quantitative ^{1}H-NMR experiments. Value of integral was interpolated by a calibration curve to obtain the mg_{H2O} amount in 100 mg $CaCO_3$. Experiments were prepared with four different amounts of water in four respective deuterated DMSO solution in order to obtain a calibration linear curve: the validity of the methods is measured by the significative R^2 (0,957).

- The NMR spectra and the calibration curve are showed below

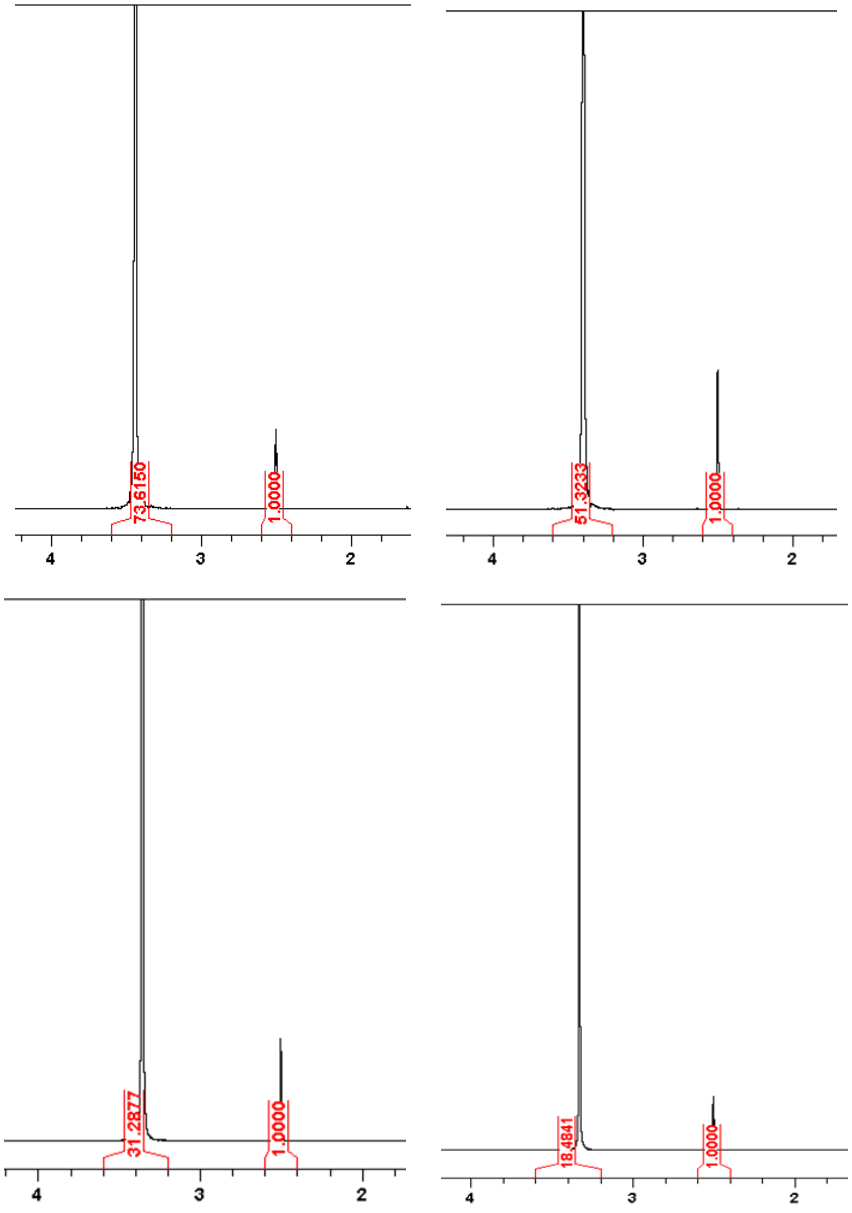

Fig 2.1 – ^{1}H-NMR integrated spectra for the calibration curve preparation

mg of water	H_2O peak Area
3,4	18,5
6,9	31,3
13,9	51,3
20,9	73,6

Table 2.1

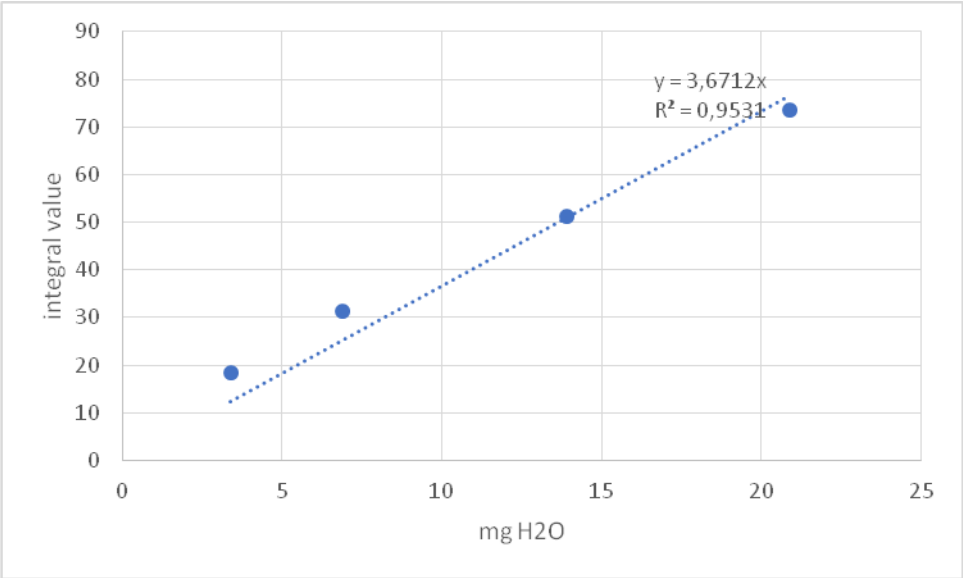

Figure 2.2 – calibration curve obtained by the results showed in 2.1 table

- the ^{1}H-NMR integral value of the water extracted from the 100 mg sample of composite material will be interpolated with the curve having equation: y =3,6712x

4.5 MOLECULAR WEIGHT DETERMINATIONS

Materials:

- Molecular weight determinations were performed using a HP-SEC-TDA on a Viscotek instrument equipped with a VE1121 pump, Rheodyne valve, and triple detector array 302 equipped with refraction index (RI), viscometer, and light-scattering (90° and 7°) systems.

Method:

- Sample preparation:

10 mg of each sample were dissolved in 5 or 10 ml $NaNO_3$ 0.1M

- Average recording conditions:
    - Mobile phase: $NaNO_3$ 0.1M + NaN_3 0.05
    - Columns: TSK gel; 2x GMPWXL (7.8 x 30 cm pore size 13 um -Tosoh Bioscience)
    - Temperature: 40°C
    - Injection volume:100ul
    - Flow: 0.6 ml/min

Data were elaborated with Omnisec 4.6.2 Software (Viscotek)

4.6 CALCIUM CARBONATE CONTROLLED PRECIPITATION

General data:

- Compounds were purchaised by Sigma Aldrich and used without further purification. Deionized water was produced by *Pharma 80 system* deionizator (Culligan) and used at value of 0.05 uS conducibility

Procedure:

- Polysaccharide (0.3 g) was dissolved in a flask containing 50 ml H_2O, then $CaCl_2$ (0.275 g) was added and dissolved.

  A Na_2CO_3 solution of equal volume (0,265g in 50 ml H_2O) was added to the already prepared solution. The precipitation reaction was stirred at 350 rpm for 3 hour, at 30°C.

  The product was filtered on 0.22 um filter and, once dryed, analyzed throught SEM, IR, and XRD.

4.7 ARTIFICIAL POLYMERS SYNTHESIS

General data:

- commercial products were purchaided by Sigma Aldrich, analysed by HPSEC-TDA instrument and characterized by NMR experiments; used without further purification.

4.7.1 ALGINATE DEPOLYMERIZATION

Procedure:

- commercially medium viscosity alginate sodium salt (4 g) were dissolved in a NaOH solution (0.8 L; pH=10.5), and heated at 80°C for different times, from 30 minutes to 3 hours, in order to obtain different molecular weight depolymerized products. 0,1 M NaCl was used as ionic force to prevent polysaccharide inter-chains and intra-chains aggregations.

After the pH neutralization, products were purified by dialysis using deionized water as extra dialysis and a dialysis tube with average size pores of 3500 Dalton.

4.7.2 ALGINATE-ACRYLATE SYNTHESIS

Procedure:

- a slightly medicated procedure reported by [1] was used in order to obtain an alg-PAA product with high percental of PAA.

  Sodium alginate medium viscosity (2 g) were dissolved in 150 ml H_2O and heated to 60°C under N_2 atmosphere. after half an hour 0.36 g ammonium persulfate were slowly added to the solution. Then it was mixed for 30 minutes.

  5.75 g acrylic acid was neutralized using NaOH 1M and added to the solution. The solution was heated to 80°C and stirred for 3.5 hours.

  After cooling the product is dialyzed against distilled water in 3500 Dalton pores tubes for three days and then dried under vacuum.

4.7.3 ALGINATE GLYCOL-SPLIT

Procedure:

- the reaction procedure is divided in two steps.

  During the first step sodium alginate low or medium viscosity (4 g) was dissolved in 500 ml deionized water. A solution of $NaIO_4$ (3.0 g in 300 ml) was added to the alginate solution, and the total glycol split was carried out at environmental temperature, under vigorous stirring and in the dark conditions for different times.

  The product was dialyzed against deionized water using a 3500 Da medium pore tube, for 3 days.

  In the second step the intermediate was reacted with a large excess of sodium borohydride (5 g) at low temperature (5-10°C) in order to reduce the aldehydic groups and to obtain the final product. Then is was purified through dialysis.

4.8 COMPOSITE MATERIALS PREPARATION

Procedure:

- The first step consisted in a pretreatment of calcium carbonate with a dispersant.

  The calcium carbonate was modified with a dispersant which was adsorbed on its surfaces

Calcium carbonate pretreated with the dispersant and dried was then embedded in a solution of polysaccharides, through stirring for 10 minutes at 300 rpm, in accord with these ratios:

polysaccharide/calcium carbonate (w/w): 1%

water/polysaccharide (w/w): from 25 to 50% (depending to the viscosity of the polysaccharide)

dispersant/calcium carbonate: 0.33%

With the scale up of the specimens formulations also the cement powder was used, in order to obtain higher mechanical resistance and to study the evaporation rate of the samples; this procedure is described below:

- Dispersant 425-P was solved, then the premixed powders of cement and calcium carbonate were added to the dispersant solution, and, after all, a solution of sodium alginate – the suspending agent - was introduced; finally the paste was stirred until complete homogenization, and poured into the molds. The ratios between the dough ingredients are listed in table 2.8 and 2.9.

When different polysaccarides and polysaccharides derivates into the specimens were tested as possible binder agents (table 2.10a) for the mechanical resistance increase, the procedure was the following described:

- Binder agent was solved, then the premixed powders of cement, dispersant, and calcium carbonate were added to the solution, and, after all, a solution of sodium alginate – the suspending agent - was introduced; finally the paste was stirred until complete homogenization, and poured into the molds.

4.8.1 MINI SPECIMENS

Dimensions:

- Shape: cilindrical
- Diameter: 5 cm
- Thickness: 0.5 cm

Procedure:

- The fresh formulations already described were poured into a plastic petri dishes and then left to dry

4.8.3 SCALE-UP SPECIMENS

Dimensions:

- Shape: prismatic
- Size: 4 x 4 x 4 cm

Procedure:

- The fresh formulations already described were poured into a metallic mould and then left to dry

4.9 MECHANICAL TESTS

Materials:

- Mechanical resistances of 4 cm x 4 cm x 4 cm prismatic samples are tested through a press equipped with a deformation force measurer.

Method:

- The most common age at testing is 28 days. At the time of the testing prismatic specimen is placed in a compession testing machine where a load is applied at the constant rate of stress within the range of 0.2 to 0.4 MPa. Under pure uniaxial compression loading, the failure cracks generated are approximately parallel to the direction of applied load. The compression testing system rather develops a complex system of stresses due to end restrains by steel platens.

4.10 MINI-SPEC ANALYSIS

Materials:

- Time domain NMR experiments were carried out on a Bruker Minispec mq20 spectrometer.

Method:

- Experiments were performed operating at around 0.5 T static magnetic field, with a proton resonance of 19.65 MHz, a p/2 pulse length between 2.05 and 2.20 ms, a phase switching time of around 2.1 ms and a receiver dead time t set at 14 ms. Samples were prepared by inserting in 10 mm outer diameter tubes a quantity of rubber chunks sufficient to fill the region of maximum

magnet homogeneity (about 8 mm height), where the sample was then carefully centered. Estimation of the rigid fraction was obtained by acquiring MSE refocused Free Induction Decay (FID)44 and applying a proper back correction for the inherent inefficiency of the sequence.

4.11 ATTENUATED TOTAL REFLECTION (ATR) ANALYSIS

Materials:

- The solid phase ATR spectra of the powders were generated using an ALPHA spectrometer (Bruker, Bremen, Germany). Data were analyzed using OPUS software, version 7.0 (Bruker, Bremen, Germany).

PART TWO

IRON OXIDE NANOPARTICLES

1. INTRODUCTION

1.1 GENERICAL ASPECTS OF NANOPARTICLES

Each chemical compound with at least one characteristic dimension between 1 and 100 nm can be defined as "nanomaterial". The importance of nanomaterials for science and technology has increased considerably in the last three decades. This has allowed to reach more efficient synthetic pathways towards the production and functionalization of different kind of nanoparticles (NPs): the variety of nanomaterials production involves a widely range of raw inorganic materials as noble metals (also useful as catalysts), semiconductors, TiO_2, InP, and magnetic compounds (important for the nanomedicine development). Synthesis and functionalization optimization studies about nanoparticles are producing remarkable advances for their real applications; moreover, the development in molecular detection and imaging in biomedical field have permitted to test new target therapies, and to make progress in the prevention or control of diseases [1].

Fig. 1.1 highlights the number of articles published in international journals from 1980 until today. The studies on nanostructures have been carried out since the 1980s, but this field of research has spread only over the five years period 2006-2010, with 26380 published articles. Over the last two years, the number of publications has increased exponentially, more than 46000 studies have been performed, witnessing the great interest of many researchers in the field of nanomaterials.

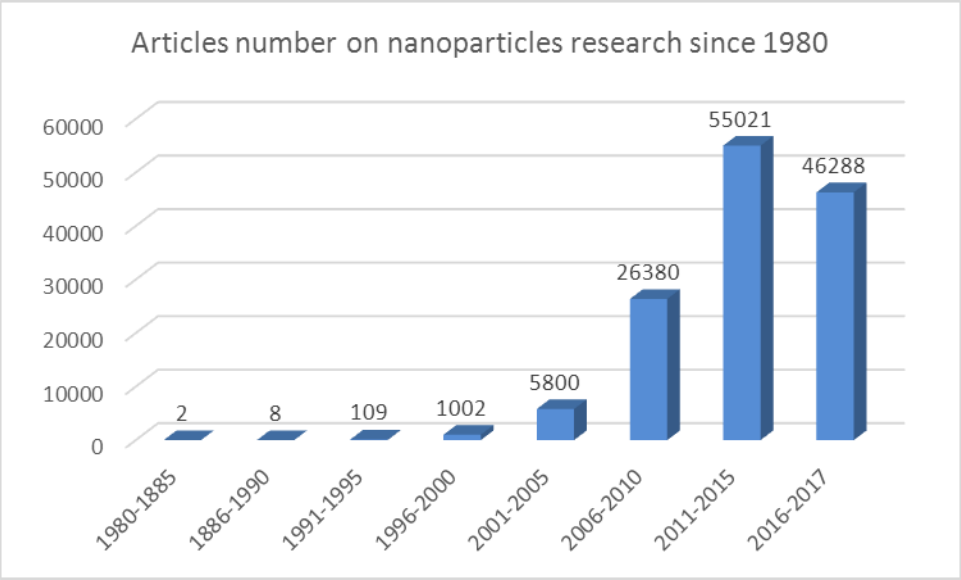

Figure 1.1 – Trend of the nanomaterial articles publications during the last 47 years

1.1. THE USE OF NANOPARTICLES OF IRON OXIDE IN BIOMEDICAL FIELD

Magnetic nanoparticles can be coated with biological molecules to modulate their interaction with a biological entity of interest, such as tissues or receptors, and can be manipulated by an external magnetic field gradient. In this way the nanoparticles can deliver a 'package', such as an anticancer drug, to a targeted region of the body, such as a tumor. The major disadvantage of most chemotherapies is that they are relatively non-specific. The therapeutic drugs which are administered intravenously have a widely uncontrolled distribution in the human tissues, resulting deleterious because of their side effects when drug attacks healthy cells also. The objectives of the nanoparticles studies are two: to limit the amount of systemic distribution of the cytotoxic drug, and to reduce the drug's dosage. In magnetically targeted therapy, the cytotoxic drug interacts with the biocompatible magnetic nanoparticle which act as a carrier. Once these compounds are injected into the bloodstream, an external magnetic field could be used to target them at the specific human cancer tissue. Once the nanoparticles are concentrated at the cancer cells, they should release the drug via enzymatic activity.

Superparamagnetic iron oxide nanoparticles (SPIONs) - composed of iron oxides: magnetite (Fe_3O_4), maghemite (Fe_2O_3), or other ferrites - have magnetic properties inside a magnetic field. These compounds are useful as contrast agents for magnetic resonance imaging, due to their large effect on T1 and T2 relaxation times. In details, Magnetic Resonance Imaging (MRI) contrast relies on the different excitation of the protons present in a biological tissue. Every radiofrequency pulsed signal permits to obtain the excitation of the protons present in the cellular systems and the FID is registered respecting the longitudinal relaxation time (T1, spin-lattice), and transversal (T2, spin-spin) [2].

An example of the using of nanoparticles as contrast agents is the following: after intravenous injection, nanoparticles are taken up by macrophages: phagocytosis occurs in the liver and spleen, and the longest half-lives of these compounds is estimated to be up to 36 h.

Healthy liver tissue is rich in macrophages, which phagocytose SPIONs produce a dark signal due to the T1 and T2 relaxations, whereas no modification of contrast signals is seen in malignant liver tumors due to the absence of macrophages [3].

The size distribution of SPIONs are important parameters: particles should be smaller than 100 nm to escape from the reticuloendothelial system, and to pass through the capillary system. Moreover, also particles larger than 10 nm can be poorly adsorbed by human cells at physiological

conditions. [4]. Therefore the synthesis conditions should be optimized to control the size of nanoparticles.

1.2. AIM OF THE WORK

The main goal of the present project is to prepare bovine serum albumin (BSA) and hyaluronic acid (HA) coated SPIONs, to characterize them, load them with drugs and chemosensitizers. The NP performances in selective delivery of drugs into cancer cells will be evaluated, together with their ability to localize in tumors in vivo. The two compoments of the NP shell should contribute with a specific function. BSA was chosen in order to improve the stability of the SPIONs acting as external sterically stabilizing shell, and also to bind many chemotherapeutic drugs; whereas HA can specifically bind to CD44 receptors overexpressed by various cancer cells. Moreover, HA can act as a hydrophilic shell of the nanoparticle allowing a longer circulation in the bloodstream, which may increase the probability of reaching the target tumor.

The novelty of our approach is to combine two types of coating for these SPIONs: both BSA and HA. The project aims to optimize the synthesis of coated nanoparticles, already produced by the research group. The preliminary preparation procedures were modified to obtain products characterized by lower, diameter less than 10 nm, and more homogeneous size. To link the protein and the carbohydrate polymer to the inorganic core of the nanoparticles Dopamine (DA) was chose as linker. DA is a water-soluble and biocompatible compound, and can act as a chemical bridge between BSA, or HA and the NP, via amide bonds with their carboxylic groups, and catechol group, to bind the iron oxide core. A schematic representation of the nanoparticle structure is showed in figure 1.2.

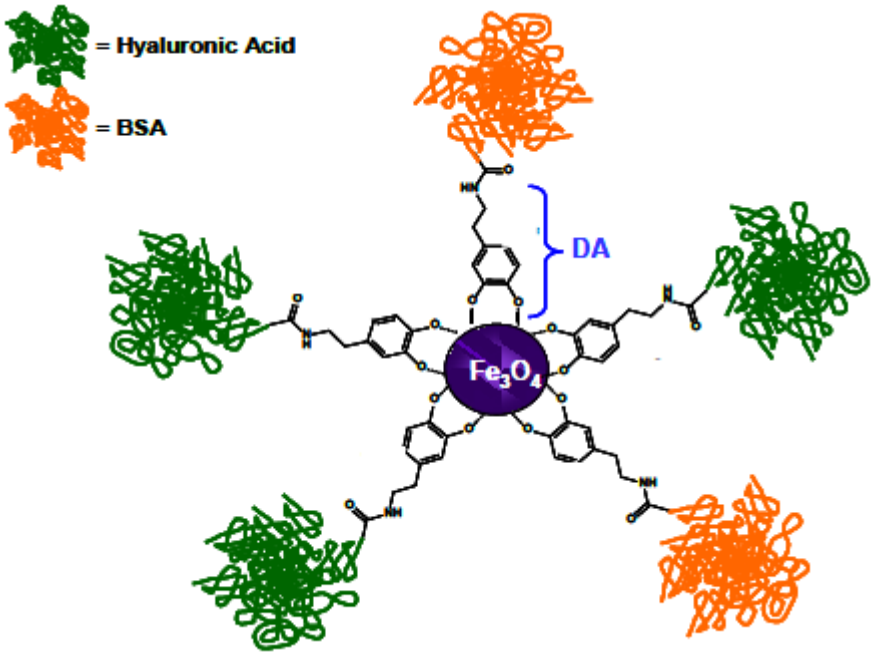

Figure 1.2 – Schematic structure of the desired nanoparticle

Biological evaluation of the samples will be carried out by a research group based at Israeli Technion Institute, especially through MRI studies.

1.3. BSA and HA

BSA protein has been one of the most extensively studied proteins because of its sequence and structural homology with human serum albumin (HSA). It is considered one of the most promising biocompatible MNPs coating for biomedical applications. BSA is an abundant serum protein with a MW of ~66 kDa. The primary physiological function of BSA is to transport lipids and metabolites present in blood plasma; hence, it is a suitable carrier for hydrophobic drugs. Being highly similar to human serum albumin (HSA), BSA is considered biocompatible, and has been used to form NPs for drug delivery.

Due to the high protein binding of various drugs, it could be used for effective incorporation of these compounds. It has an extraordinary ligand binding capacity, providing a depot for a wide variety of compounds with favorable, noncovalent reversible binding characteristics for transport in the body and release at the cell surface [5].

HA is a natural linear anionic polysaccharide (glycosaminoglycan) with averge molecular weight between 5 to 104 kDa. The chemical structure consists of a disaccharide repeating unit: [(β1→4)-GlcA-(β1→3)-GlcNAc-]$_n$, as shown in fig 1.3. It occurs in the extracellular matrix and synovial fluids of the vertebrates [6]. Due to its excellent characteristics of biocompatibility and biodegradability, HA has been widely investigated for biomedical applications. Since HA can specifically bind to the CD-44 receptor over-expressed by some cancer cells, many researchers are focusing their studies on the pharmaceutical applications of HA for the development of anti-cancer drugs. Most HA-drug conjugates have been synthesized for cancer chemotherapy as macromolecular pro-drugs. HA has also been linked to the core of some nanoparticles prepared for the drug delivery. These products with HA were loaded with anticancer agents such as paclitaxel, doxorubicin, butyric acid, mitomycin C and siRNA, exhibiting enhanced targeting ability to the tumor and resulting in high therapeutic efficacy [7].

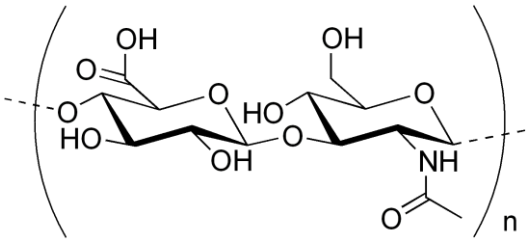

Figure 1.3 – hyaluronic acid chemical structure

Bibliography

[1] Conde, João, et al. "Revisiting 30 years of biofunctionalization and surface chemistry of inorganic nanoparticles for nanomedicine." *Frontiers in chemistry* 2 (2014).

[2] Pankhurst, Quentin A., et al. "Applications of magnetic nanoparticles in biomedicine." *Journal of physics D: Applied physics* 36, 13 (2003): R167.

[3] Corot, Claire, and David Warlin. "Superparamagnetic iron oxide nanoparticles for MRI: contrast media pharmaceutical company R&D perspective." *Wiley Interdisciplinary Reviews: Nanomedicine and Nanobiotechnology* 5, 5 (2013): 411-422.

[4] Mahmoudi, Morteza, et al. "Superparamagnetic iron oxide nanoparticles (SPIONs): development, surface modification and applications in chemotherapy." *Advanced drug delivery reviews* 63.1 (2011): 24-46.

[5] Aires, Antonio, et al. "BSA-coated magnetic nanoparticles for improved therapeutic properties." *Journal of Materials Chemistry B*3, 30 (2015): 6239-6247.

[6] Mende, Marco, Martin Nieger, and Stefan Bräse. "Chemical Synthesis of Modified Hyaluronic Acid Disaccharides." *Chemistry-A European Journal* (2017).

[7] Choi, Ki Young, et al. "Self-assembled hyaluronic acid nanoparticles for active tumor targeting." *Biomaterials* 31.1 (2010): 106-114.

2 – RESULTS

2.1. SYNTHESIS OF IRON OXIDE (MAGNETITE) NANOPARTICLES COVERED WITH HA AND BSA

Synthesis of iron oxide nanoparticles could be divided in three or four steps:

a) synthesis nanoparticles coated with oleic acid (OA),
b) synthesis of bovine serum albumin (BSA) and hyaluronic acid (HA) derivatives
c) substitution of OA coating of the nanoparticles with BSA and HA derivatives contemporaneously

or :

a) synthesis nanoparticles coated with (OA),
b) synthesis of BSA and HA derivatives
c) substitution of OA coating of the nanoparticles with HA derivative
d) adding of the BSA derivative in the shell of the nanoparticles

2.1.1. SYNTHESIS OF IRON OXIDE NANOPARTICLES COATED WITH OLEATE

(a)

Magnetite structure, formally $Fe(II)Fe(III)_2O_4$, or better Fe_2O_3, has a cubic shape, and it is delimited by an oxygen cubic close packing with cations in the interstitial tetrahedral and octahedral sites. This kind of structure presents one Fe^{3+} ion which occupies a tetrahedral site, whereas each of the two other ions, Fe^{3+} and Fe^{2+}, occupy octahedral sites. This kind of structure is typical of many AB_2O_4 compounds, where A is a trivalent cation and B a bivalent one (fig 2.1) [1] [2].

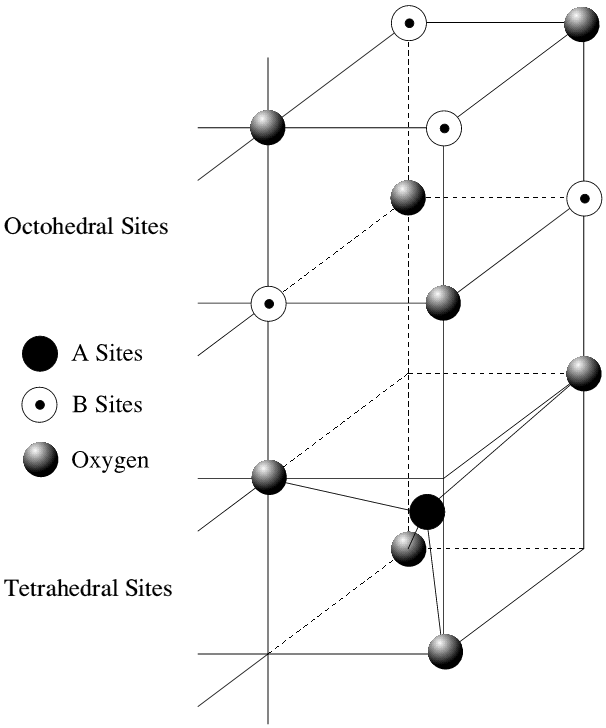

Figure 2.1- crystal structure of magnetite

A protective coating is important in order to avoid the collision of the nanoparticles and to prevent the aggregation, maintaining the nanoparticle in suspension in water solution, where the chemical derivatization could be performed. Different approaches have been tested to obtain the iron oxide NP coated with oleic acid (OA) having the desired dimensions (Table 1). Fe_3O_4 nanoparticles covered with oleic acid were prepared according to the "thermal synthesis" method and reported in the literature [3, 4], in which magnetite was coated with oleic acid heating the mixture at 80°C. In this process two approach were evaluated:

The first approach apply the method reported by Korpany [3], in which $FeCl_3 \cdot 6H_2O$ and $FeCl_2 \cdot 4H_2O$ and sodium oleate were used. The second route, follow the procedure reported by the Liu and Xianqiao [4], in which the co-precipitation of a Fe(II) and Fe(III) salts from aqueous solution is perform with an alkaline agent followed by addition of oleic acid under stirring and heating. Both the methods produced nanoparticles of interest, because they showed small size diameter (2-3 nm) of the core, and the diameter of the coated magnetic nanoparticles is between 10 to 100 nm. For the nanoparticle synthesis another procedure, named 'thermal decomposition', was tested, in which big colloids of Fe_3O_4 are produced and then disaggregated by the heat[5]. The obtained NP did not show the desired core size and coated nanoparticles.

In all cases, the magnetic nanoparticles were separated from the solution by a magnet and washed with water. The two thermal synthesis have produced analogous samples but the second approach modification was chosen because it allows a simpler way to further link HA and BSA Products were characterized by FT-IR spectroscopy dynamic light scattering (DLS) and TEM microscopy (Fig. 2.2 and 2.3).

Table 1

Method employed	**Literature reference**	**Diameter dimension**
Thermal synthesis A	*Materials chem. and Phys. (2013) 138, 29 [3]* *Adv. Mater. (2008) 20, 4154*	10-100 nm
Thermal synthesis B	*J. magn. and magn. mater. 306 (2006) 248 [4]*	10-100 nm
Thermal decomposition	*J. magn. and magn. mater. 321, 19 (2009) 3093 [5]*	Too bigger

The IR spectrum of the product is below presented. It shows the oleic acid stretching bands in the range 800-3000 cm^{-1} and the Fe-O stretching band in the range 500-600 cm^{-1}.

DLS analysis shows the distribution of particle size evaluated by size between 10 and 100 nm, while the TEM imagine highlight the homogeneity of the preparation.

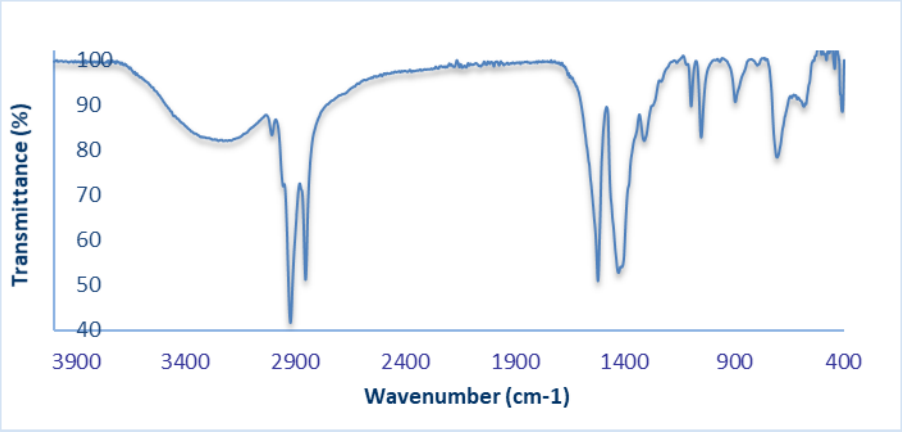

Figure 2.2 – ATR spectra of Fe_3O_4@OA – the spectra show the oleic acid stretching bands in the range 800-3000 cm^{-1} and the Fe-O stretching band in the range 500-600 cm^{-1}

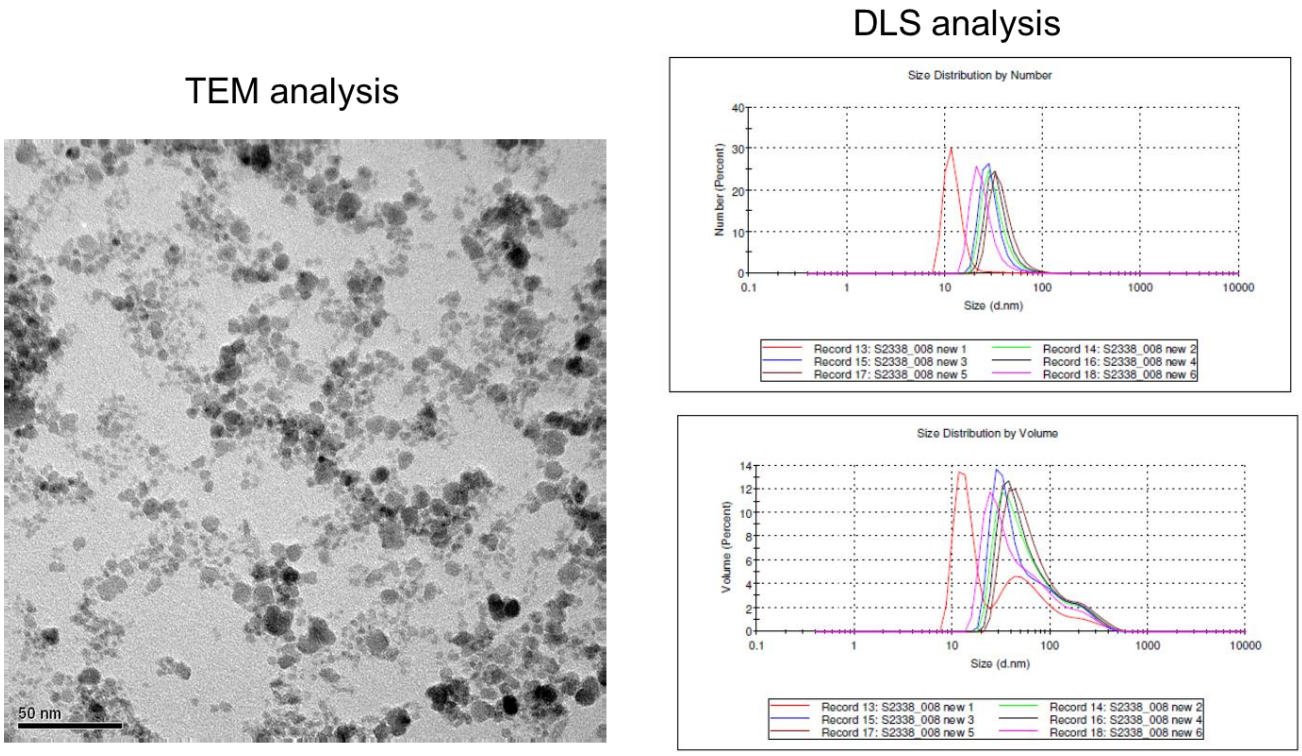

Figure 2.3 – morphological and dimensional aspects of Fe_3O_4@OA

2.1.2. SYNTHESIS OF HA-DOPAMINE AND BSA-DOPAMINE (b)

In order to link BSA and HA to the magnetite both biomacromolecules were derivatized with dopamine (DA), which structure is shown in fig 2.2

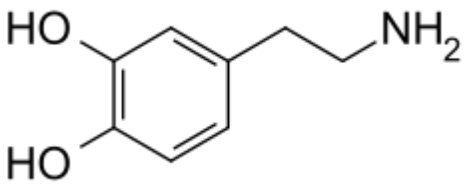

Figure 2.4 – Dopamine molecule consists of a catechol structure (a benzene ring with two hydroxyl side groups) with one amine group attached via an ethyl chain. As such, dopamine is the simplest possible catecholamine.

For conjugation reaction were exploit the carboxylic groups present in both the macromolecules. and the amino group of dopamine to form an amidic linkage. Carboxyl groups were activate with

EDCI (1-ethyl-3-3(3'-dimethil aminopropyl) carbodiimide, and combined with dopamine hydrochloride.

In the case of BSA, the reaction lasted 20 hours and was conducted in an obscured flask at 4°C. In table 2 the stoichiometry of reagents is shown. The PBS (phosphate buffer) solution changed color during the first ten minutes: from transparent it turned to brown. Products was purified by dialysis using membrane with an average pore size of 3500 Dalton.

Table 2 - Stoichiometric reagent used for preparation of BSA dopamine adduct

	BSA	**DA-HCl**	**EDCI**
Molar ratio	1	708	1,1
Weight ratio	1	2	1

The linker between the protein and dopamine was highlight by IR. In the ATR spectra of Fe_3O_4@DA-BSA - around 1700 cm^{-1} is present the band of the C = O bond of the amide group. Moreover, there are the two characteristic bands of the oleate alkyl chain are present at 2900 cm^{1}. This is due to the presence of oleic acid as impurity which makes difficult the purification of the product. The best and easier way to avoid this contamination is to centrifuge the product for long time at a high rotation speed.

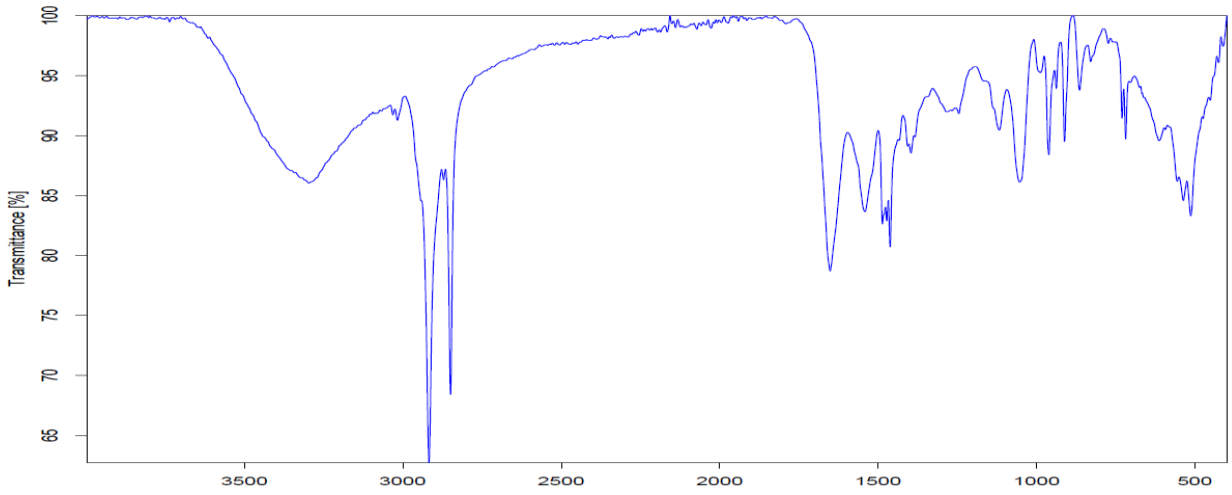

Figure 2.5 – ATR spectra of Fe_3O_4@DA-BSA

The BSA degree of substitution was evaluated by MALDI–TOF analysis (Figure 2.6). The difference between the masses of BSA and its DA derivative is 4000 g/mol. This indicate that 26 mol of dopamine are linked to the protein (4000g/mol : 152 g/mol).

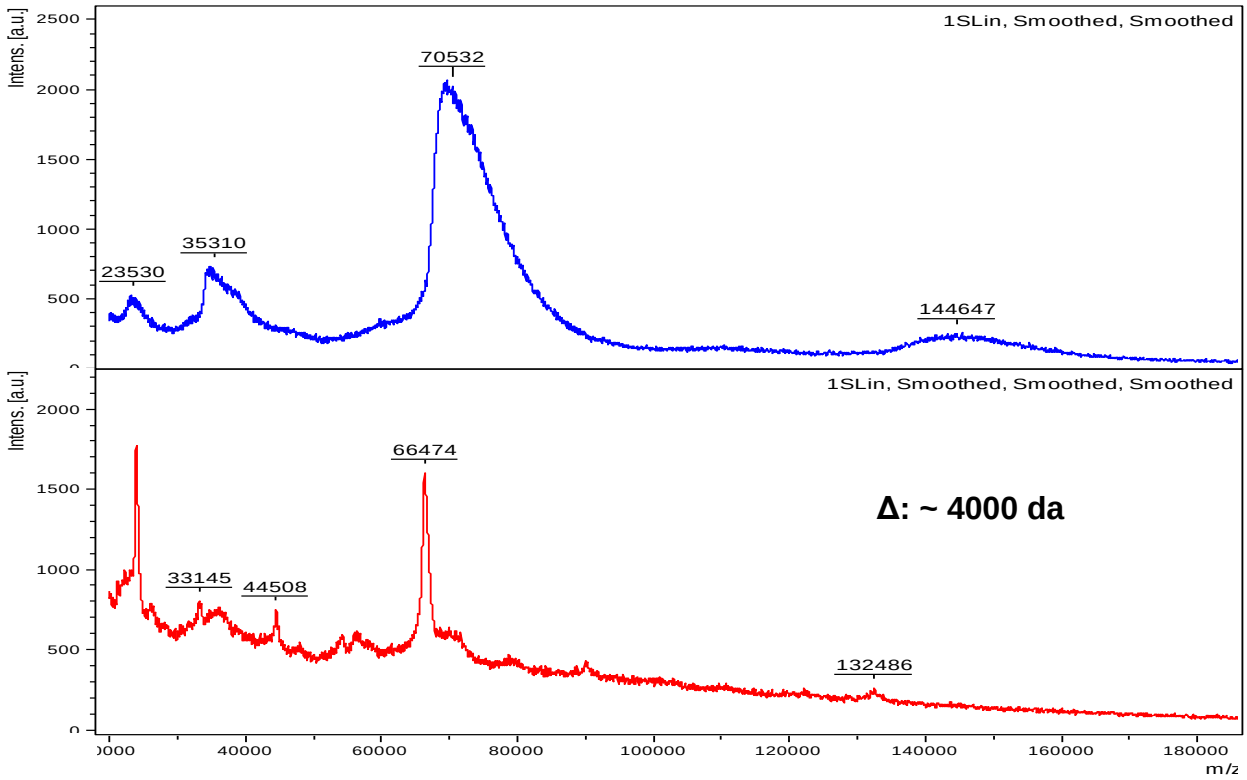

Figure 2.6 – Matrix assisted laser desorpion /ionization MALDI TOF spectra of BSA protein and BSA-dopamine derivative.

HA-dopamine conjugates (HA-DA) were prepared using conventional EDCI chemistry in pH 5.5 solution to avoid irreversible oxidation of dopamine *[6]*. In table 3 the stoichiometry of reagents is shown. Two HA samples having 7000 and 30000 Dalton molecular weight respectively were used.

Table 3 - Stoichiometric reagents used for preparation of HA dopamine

	HA	DA-HCl	EDCI
Molar ratio	1	1	0,45
Weight ratio	2.15	1	2,57

The obtained products were analysed by ^{1}H-NMR technique that confirmed the formation of the HA-DA adduct with 15% of substitution degree (fig. 2.7) . The main signals of Hyaluronic acid are unmodified, while new minor signals, attributable to DA appear in the aromatic region (6.5 -7

ppm), in agreement with the planed low substitution degree. By the weighted ratio between the integrals of hyaluronic and aromatic signals (see paragraph 4.1.3) the presence of 1.5 DA for each 10 disaccharidic residues of the polysaccharide were found.

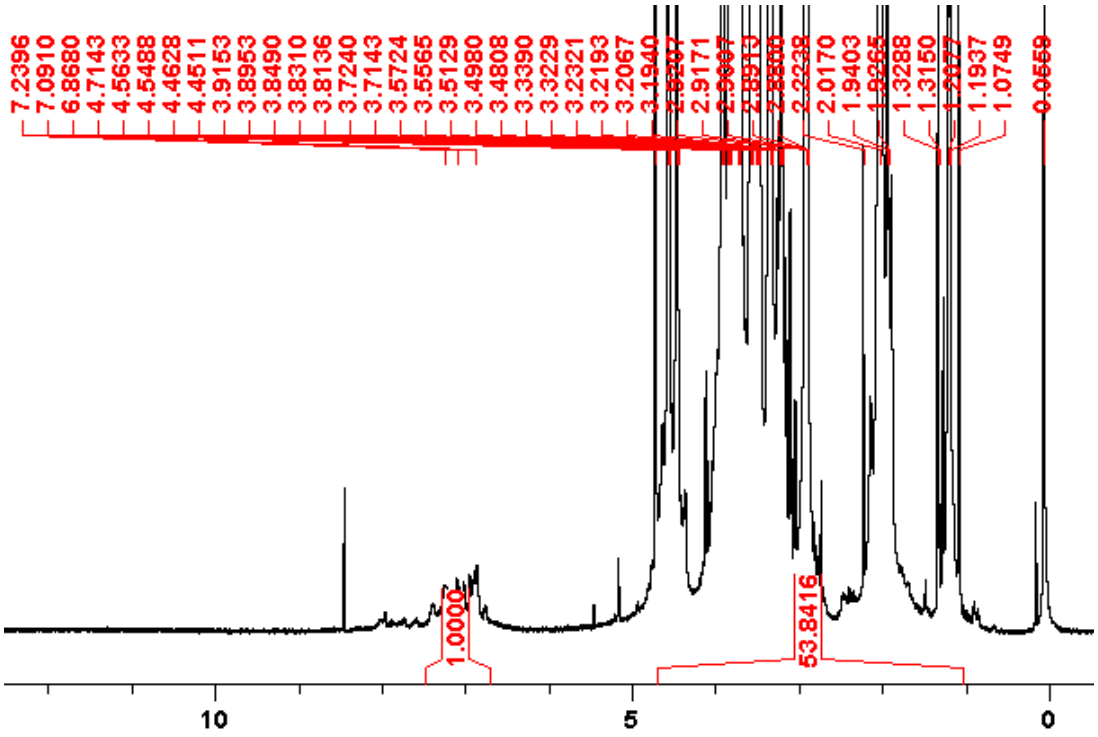

Figure 2.7 – ^{1}H-NMR – HA-DA.

Figures 2.6 and 2.7 show that the carboxyl groups of both bovine serum albumin and hyaluronic acid reacted with dopamine, establishing the amide bond. The substitution degree of both the biomacromolecules with the catecholamine, is deliberately low because it is important to modify as little as possible the structure of the macromolecules as not to alter their own tertiary structure.

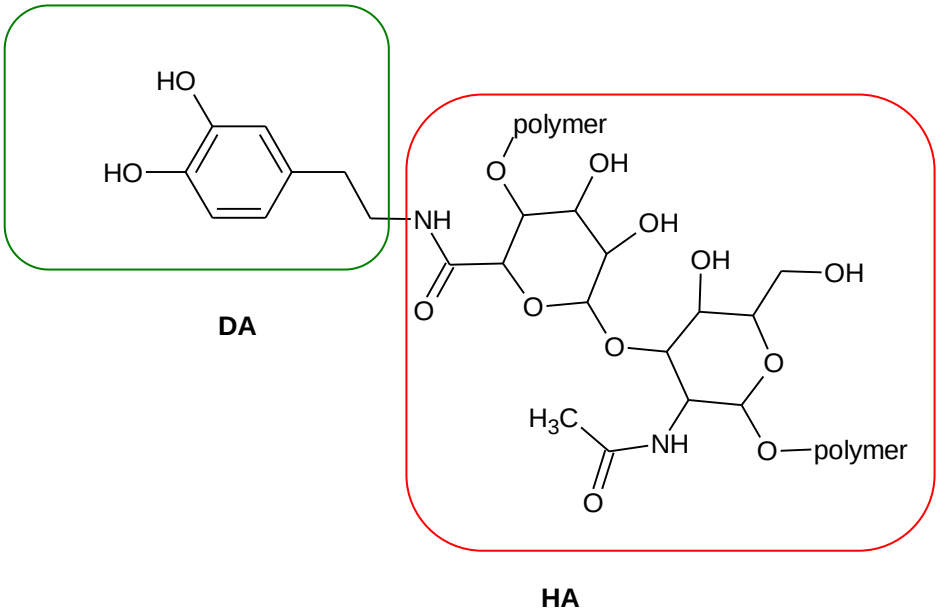

Fig. 2.8 – scheme of derivatized hyaluronic acid with dopamine

2.1.3 - SYNTHESIS OF Fe_3O_4·DA-BSA/HA NANOPARTICLES (c) [3][6]

This reaction is a simple exchange between oleic acid that covers the nanoparticles and the chelating agent. The reaction, facilitated because of the entropic effect, was performed in one step. Fe_3O_4@OA nanoparticles were dispersed in chloroform and then, an aqueous solution, containing CTAB (hexadecyltrimethylammonium bromide) as phase transfer agent, was added under vigorous stirring. This allow to suspend Fe_3O_4@OA nanoparticles in the aqueous buffered solution (PBS). Chloroform was carefully evaporated under reduced pressure.

The Fe_3O_4@OA solution was added dropwise, under vigorous stirring, to DA-HA and DA-BSA mixture PBS solution, to obtain the ligand exchange reaction forming the Fe_3O_4@DA-HA/DA-BSA product. In table 3 the stoichiometry of reagents is shown.

Table 4 - Stoichiometric reagents used to prepare Fe_3O_4@DA-HA/DA-BSA coated nanoparticles

	Fe_3O_4@OA	DA-BSA	DA-HA
Molar ratio		1,6	1
Weight ratio	1	2,2	1,3

The precipitate salt of CTAB and oleate were discarded through centrifugation. After centrifugation the supernatant containing Fe_3O_4@DA-HA/DA-BSA appeared brown in colour and was transparent. This product was stored at 4°C in a dark glass container in order to precipitate the small amount of CTAB later removed by further centrifugation.

The organic coatings of different preparations differed slightly because the hyaluronic acids used have different weights: one product is composed by 7000 Da hyaluronic acid, whereas the other product is composed by 30000 Dalton hyaluronic acid.

Various batches were prepared to meet the amounts of product needed for biological tests *in vitro* and *in vivo* on mice.
The organic coatings were slightly different; the nanoparticles are diversified because the hyaluronic acids used have different weights: one product is composed by 7000 Da hyaluronic acid, whereas the other product is composed by 30000 Dalton hyaluronic acid

Table 5 - Stoichiometric reagents used to prepare different Fe_3O_4@DA-HA/DA-BSA coated nanoparticles

	Fe_3O_4@OA	DA-BSA	DA-HA (7000 Da)	
Molar ratio		1,6	1	Molar ratio
Weight ratio	1	2,2	1,3	Weight ratio
	Fe_3O_4@OA	DA-BSA	DA-HA (30000 Da)	
Molar ratio		1,6	1	Molar ratio
Weight ratio	1	2,2	1,3	Weight ratio

Through the same synthesis procedure, they were also produced **Fe_3O_4@DA** (fig 2.9) and **Fe_3O_4@DA-BSA** for other biological tests.

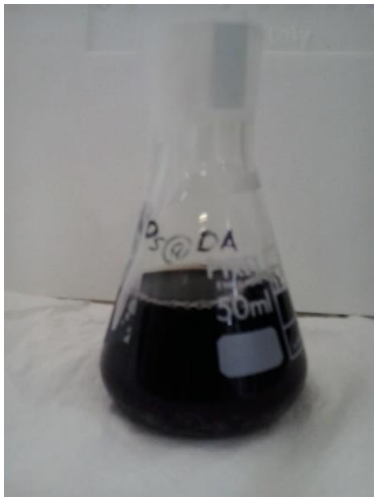

Fe_3O_4@DA

The dopamine doped nanoparticles of iron oxide, in contrast to the oily product from which they are obtained, remain suspended in the aqueous, dark and uniform solution, as can be seen from the image on the left.

This behavior in aqueous solution demonstrates that the exchange reaction of the oleic with dopamine has been correctly performed, and the nanoparticles solution is stable.

Figure 2.9 – Fe_3O_4@DA photo

Briefly scheme of the synthesis pathways from oleic acid coated nanoparticle

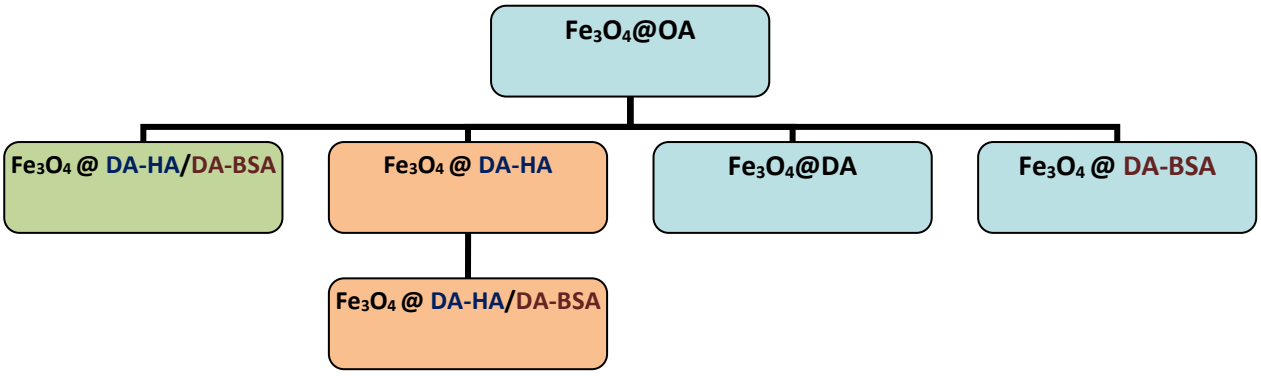

Legend:

"One pot" synthesis

"Two steps" synthesis

Purification and concentration of the products

Centrifugal filters could be used to to concentrate and purify the product by contaminants of the reagents. It is the best way in order to avoid concentrating the products through the concentration under reduced pressure or through heating that could damage the nanoparticles and denature the protein. Centrifugal filters with a 50000 Dalton molecular weight cut-off was found the correct choice in order to eliminate the residual impurities that derive from the entire synthesis process.

A small aliquot of the concentrated solution was lyophilized to determine by weighting the concentration of the obtained solution. The target concentration of the product for biological test was about 12 mg / ml.

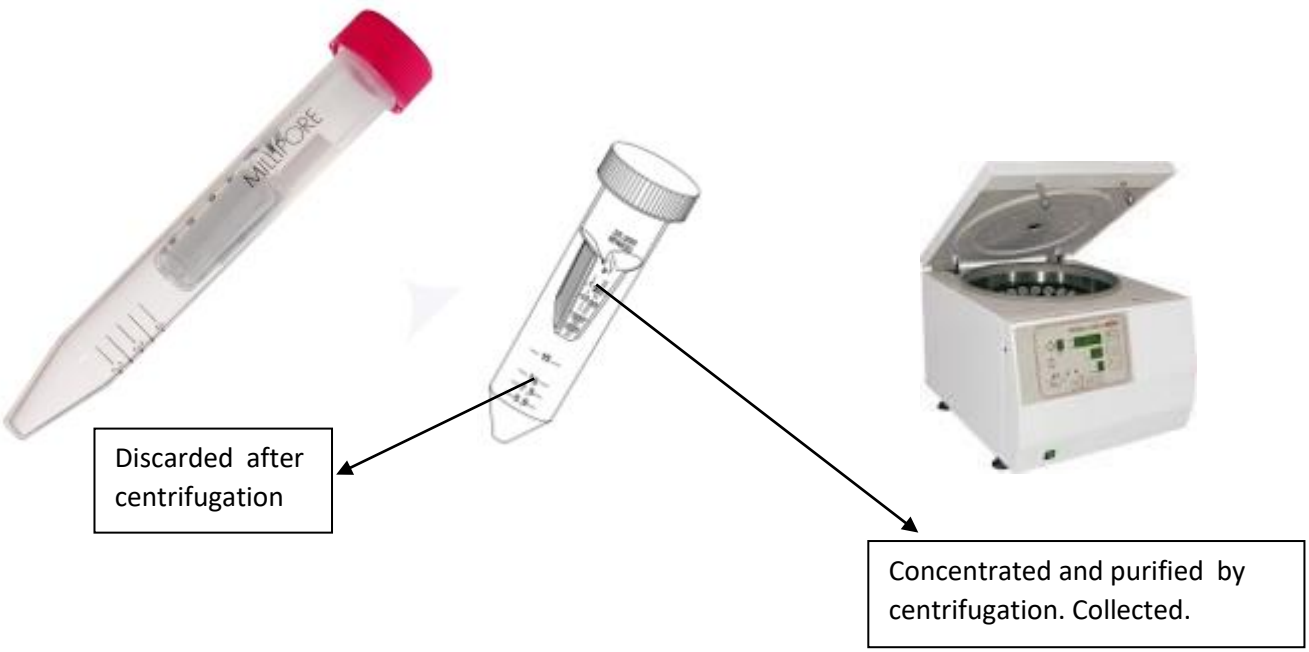

Fig 2.10 – purification arrays

2.2. CHEMICAL CHARACTERIZATION

Coated nanoparticles were characterized by IR spectroscopy. The ATR spectra of Fe_3O_4@DA-BSA/DA-HA - show bands related with the polysaccharide chain (HA): around 1000 cm^{-1} (C-O bond) and around 3300 cm^{-1} (large band of O-H bonds of the hydroxylic group) not present in the IR spectrum of Fe_3O_4@DA-BSA. Moreover at 1700 cm^{-1} it is present the band of the C=O of the amide group, between the protein or hyaluronic acid and dopamine.

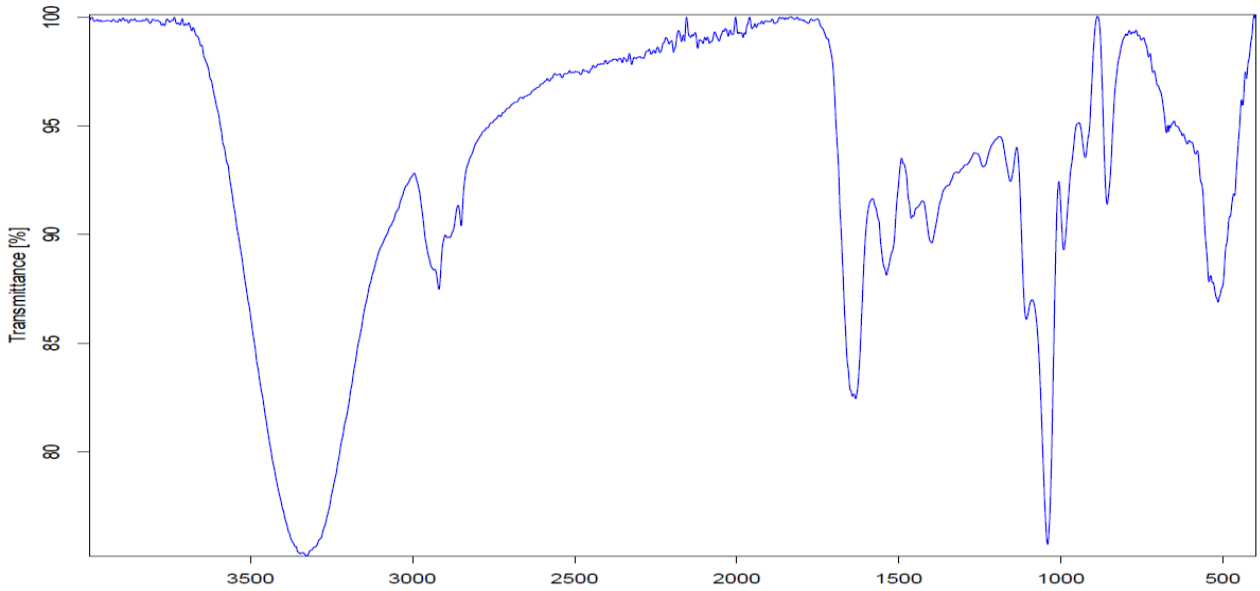

Figure 2.11 – ATR FT-IR spectrum of Fe_3O_4@DA-BSA/DA-HA

Morphological and size characterizations were done in order to study in detail the characteristics of nanoparticles: these compounds must be small in size, moreover they should ideally have a single size distribution.

Transmission electron microscopy images show a dark colour inorganic core, whereas the shell around the nanoparticles is more light.

Surprisingly the starting product, coated with sodium oleate (Fe_3O_4@OA), and its derivative, coated with hyaluronic acid (Fe_3O_4@DA-HA), appear to have a larger size inorganic core, than the core of the final product, the one with the heterogeneous shell (Fe_3O_4@DA-HA/DA-BSA). Size analysis by DLS confirms that the step in which the protein is added to the nanoparticle shell, allow to disaggregate the inorganic core of the starting NP and to obtain nanoparticles with smaller sizes of the inorganic core, suitable for biomedical purposes. In fact, the diameter of the nanoparticles, analyzed by number and volume, varies from dimension values that are far larger than 10 nm in size below this limit (see fig. 2.12; 2.13; 2.14). Figure 2.13 shows the final product, which differs from the others because it consists of big nanoparticles aggregates having a much small core.

Concluding, one pot synthesis product, prepared by the replacement of the oleate group with both the biomacromolecules in a single reaction, seems worse than the already described product: DLS analysis shows dimensions little bigger and TEM image show inorganic core aggregations while other iron oxide materials are not covered by the macromolecular shell: some nucleus seems naked (fig 2.14).

TEM analysis

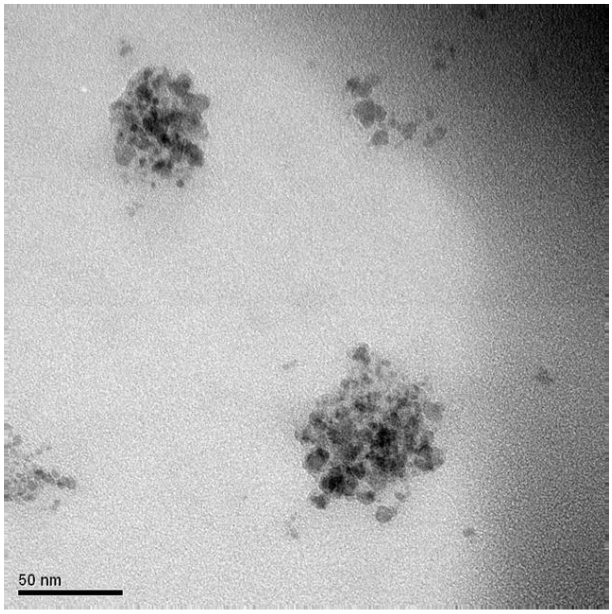

DLS analysis

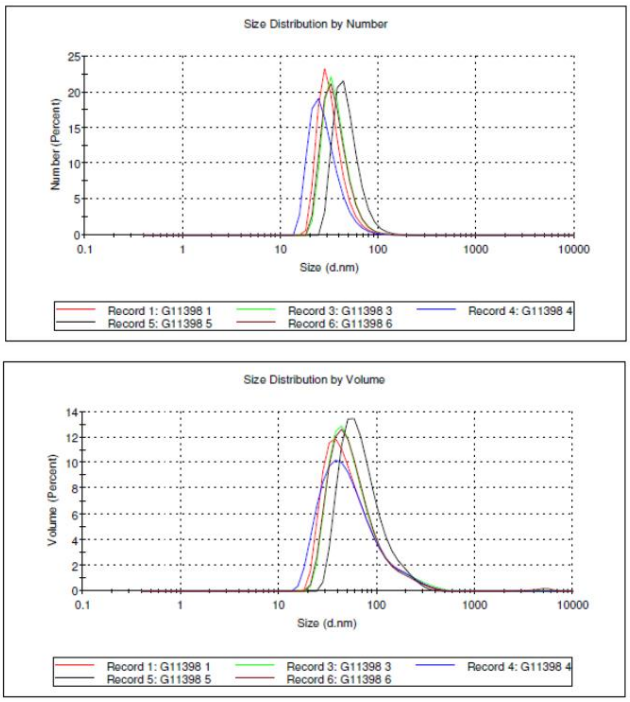

Figure 2.12 – TEM and DLS analysis: morphological and dimensional aspects of Fe_3O_4@DA-HA

TEM analysis

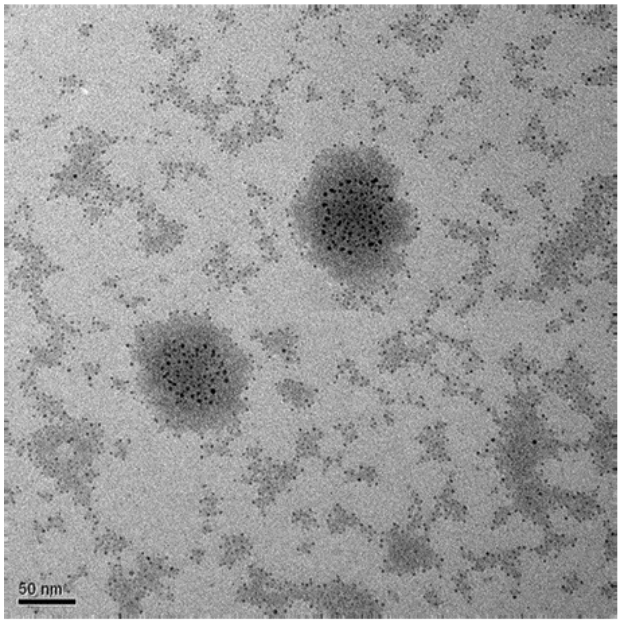

DLS analysis

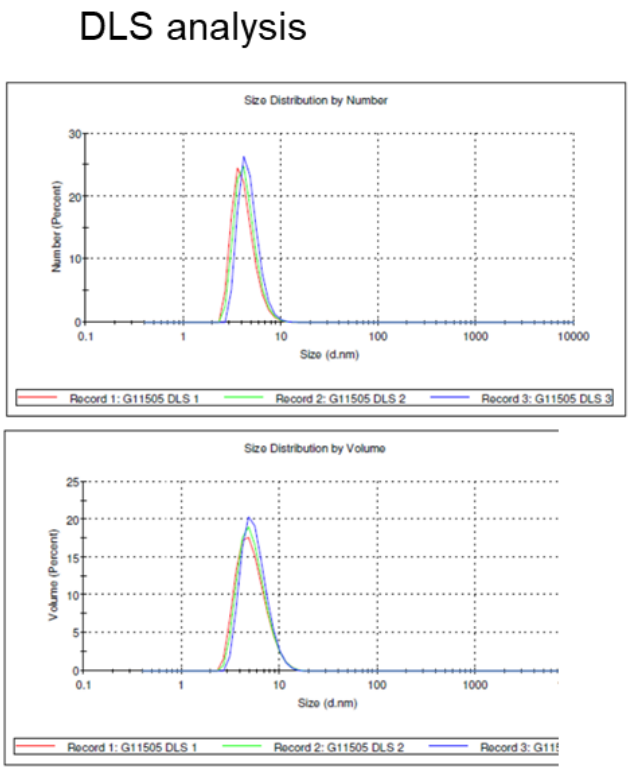

Figure 2.13 – TEM and DLS analysis: morphological and dimensional aspects of Fe_3O_4@DA-HA/DA-BSA

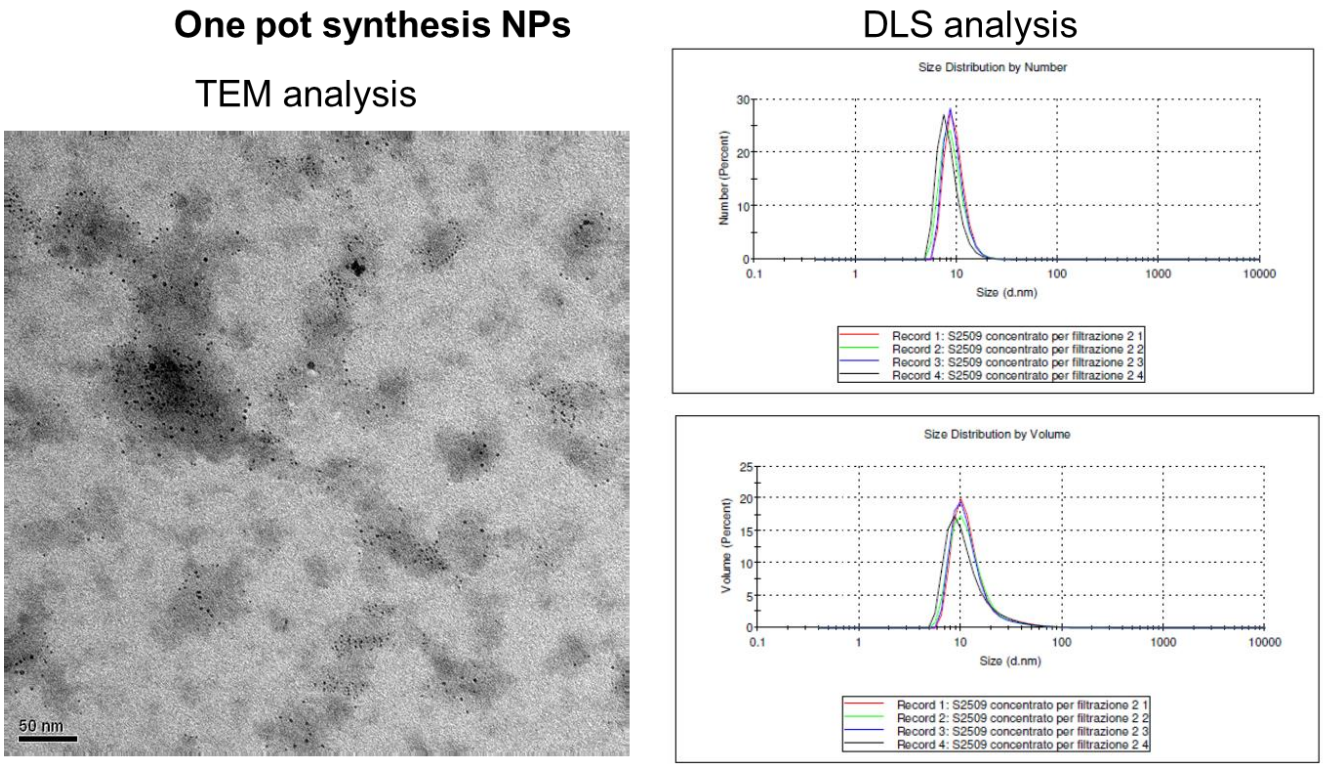

Figure 2.14 – TEM and DLS analysis: morphological and dimensional aspects of Fe_3O_4@DA-HA/DA-BSA synthesized by a "one pot step"

The analysis of Z-potential show a tendency of the coating to shield the positive charge of the nanoparticles coated with linker dopamine hydrochloride (Fe_3O_4@DA). Whereas the average value of the positive charge of the final compound (Fe_3O_4@DA-HA/DA-BSA) is 19 mV and it doesn't meet the good criteria in order to consider the nanoparticles as stable product: the magnitude of the zeta potential is predictive of the colloidal stability. Nanoparticles with Zeta Potential values greater than +25 mV or less than -25 mV typically have high degrees of stability. Dispersions with a low zeta potential value will eventually aggregate due to Van Der Waal inter-particle attractions.

2.3. BIOLOGICAL RESULTS

Preliminary MRI scanning on solution containing the different type of nanoparticles were performed in the Technion laboratory. The figure 2.15 shows images of solution of coated nanoparticles and reference solution of HA in buffer. The darkest sample correspond to sample 1 (without HA), the addition of free HA (sample 2) give a decrease of the dark grey of the MRI image. it is assumed that presence of free HA in the sample annulled the dark effect of the SPION. Sample 3 contain SPION+HA, the sign was less black compared to sample 1 even though the concentration of Fe_3O_4 in sample 3 is half of that in sample 1. Sample 4 is buffer for control.

Based on these results it was expected that nanoparticles loaded with BSA and HA showed a dark gray color in tumor tissue once they concentrated.

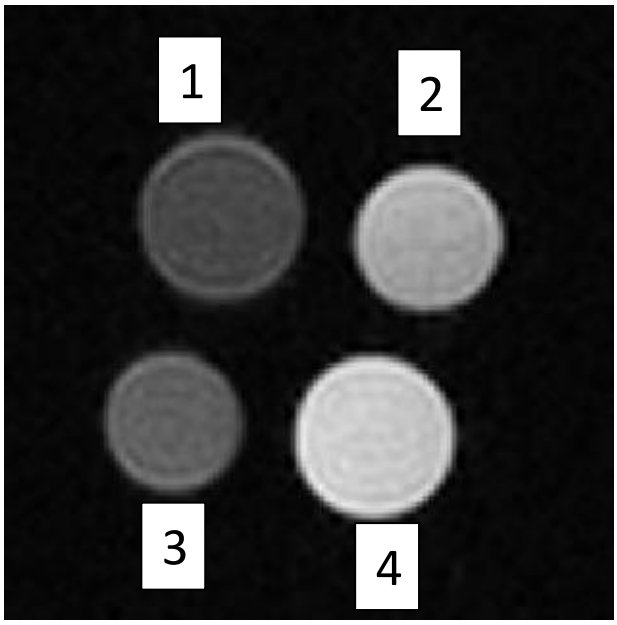

Figure 2.15 – it was useful to do in vitro test with four tubes: (1) sample of SPION without HA; (2) sample of SPION without HA with excess of free HA; (3) SPION sample as we used for the in vivo study; (4) buffer

With one of the SPION solution prepared was done also an in vivo experiment. To Mice were injected with cancer cells suspensions in the flank of the mice's upper leg, the tumor size was monitored three times a week and measured with a caliper. When the tumor reached an average volume of 40-50 mm3 SPIONS was injected (100 µl). At least one hour after the injection mice were taken for MRI imaging. It was expected that after injection of the SPION solution darkening of the tumor will observed. In practice only a minor darkening was observed (indicated by Mean grey level) (fig 2.16). This result is encouraging a further optimization of the product.

Pre Iniection

Post Iniection of 100 µl SPION solution

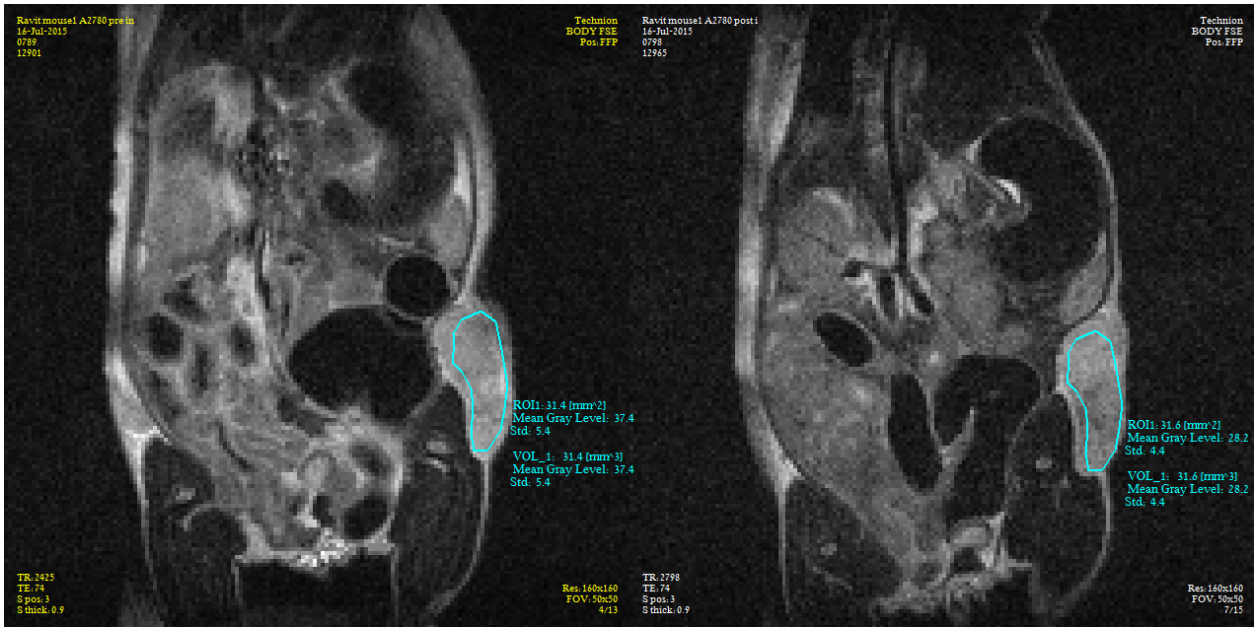

Time: 0 hr

Time: 4 hr

Fig 2.16 – in vivo test result on the mouse cancer tissue, before and four hours after the injection.

Bibliography

[1] Levy Davide, Roberto Giustetto, and Andreas Hoser. "Structure of magnetite (Fe_3O_4) above the Curie temperature: a cation ordering study." *Physics and Chemistry of Minerals* 39.2 (2012): 169-176.

[2] Nikiforov, V. N., A. N. Ignatenko, and V. Yu Irkhin. "Size and surface effects on the magnetism of magnetite and maghemite nanoparticles." *Journal of Experimental and Theoretical Physics* 124.2 (2017): 304-310.

[3] Korpany, Katalin V., et al. "Stable water-soluble iron oxide nanoparticles using Tiron." *Materials Chemistry and Physics* 138.1 (2013): 29-37.

[4] Liu, Xianqiao, et al. "Preparation and characterization of hydrophobic superparamagnetic magnetite gel." *Journal of Magnetism and Magnetic Materials* 306.2 (2006): 248-253.

[5] Maity, Dipak, et al. "Studies of magnetite nanoparticles synthesized by thermal decomposition of iron (III) acetylacetonate in tri (ethylene glycol)." *Journal of Magnetism and magnetic Materials* 321.19 (2009): 3093-3098.

[6] Lee, Yuhan, et al. "Bioinspired surface immobilization of hyaluronic acid on monodisperse magnetite nanocrystals for targeted cancer imaging." *Advanced Materials* 20.21 (2008): 4154-4157.

3 CONCLUSION AND PERSPECTIVES

The aim of this study was to design and develop a new theranostic nanosystem, named Fe_3O_4·DA-BSA/DA-HA, compatible with the human tissue and suitable for loading antitumor drugs. This work is a preliminary research to setup the synthesis procedure, to be use as starting point for further development and optimizations. The two-step synthesis proved to be better than the one-pot synthesis, since, as demonstrated by the NMR and DLS analysis, the nanoparticles appear more homogeneous, smaller in size, and all the iron oxide nuclei are adequately covered by the biological matrix. A possible explanation of the difficulty of obtaining a suitably covered shell and products of the same size could be related to a competition between protein and carbohydrate in binding to the inorganic core: the protein could be faster in binding and hyaluronic acid would remain in solution; or biomacromolecular aggregates could be formed and dopamine would remain embedded in a “tangle”, preventing the linking to the iron oxide core.

The novelty of this approach regards the structure of the product: it is a nanoparticle with a heterogeneous shell, the coexistence of a protein and a carbohydrate could express a very effective synergy in terms of biological activity. The first in vitro and in vivo tests reveal a small bioactivity, which encourages the research in this area by modifying the ratio between protein and carbohydrate: a slight increase in the amount of hyaluronic acid may be critical to concentrating most nanoparticles in tumor tissue, as this macromolecule can bind to the CD44 receptor over-expressed in the diseased tissue.

Lastly, once the product synthesis is optimized, the nanoparticle may be doped with paclitaxel or other drugs and the in vivo bioactivity can be tested.

4. MATERIALS AND METHODS

4.1 – SYNTHESIS

4.1.1 – PREPARATION OF MAGNETIC COLLOID

The chemical reaction of Fe_3O_4 precipitation is given by

$$Fe^{2+} + 2Fe^{3+} + 8OH^- \rightarrow Fe_3O_4 + 4H_2O$$

A complete precipitation of Fe_3O_4 is expected in the pH range 7.5-14 while maintaining a molar ratio of Fe^{2+}/Fe^{3+} = 1:2 under a non-oxidizing environment. Under oxidizing conditions, Fe_3O_4 may be oxidized as given by the following equations:

$$Fe_3O_4 + 0.25\ O_2 + 4.5\ H_2O \rightarrow 3\ Fe(OH)_3$$

$$Fe_3O_4 + 0.25\ O_2 \rightarrow 1.5\ Fe_2O_3$$

Aqueous dispersion of magnetic nanoparticles was prepared by the addition of an aqueous mixture of ferric and ferrous salts to a strong alkaline solution, such as ammonia. Oxigen is eliminated from the solution by using N_2 gas flow through the reaction medium in a closed system during the synthesis operation. [1] The magnetite gel was prepared by the following procedure: 3,44 g $FeCl_2.4H_2O$ and 9,40 g $FeCl_3.6H_2O$ in 160 ml deionized water under nitrogen gas with vigorous stirring at 80°C for 30 minutes. Then the mixture of 4 ml of NH_3 (25%), 4 ml oleic acid, and 4 ml acetone was slowly added to the solution at room temperature and the black bare magnetic gel was precipitated. Colour of the solution turned to black. Time of stirring lasted 30 minutes and then the solution was heated again for 30 minutes in order to coat the magnetite [1, 2 *with slight modifications*] The magnetite was isolated by magnetic decantation, then dissolved in hexane and re-precipitated with ethanol in order to remove the excess of oleic acid [3]

4.1.2 – PREPARATION OF DA-BSA DERIVATIVE

Scheme of the reaction

The aim of this step is to link dopamine to BSA through an amide bond. The reaction flask is thermostated at 8 ° C and shield from light to prevent the denaturation of the protein. 250 mg of BSA were dissolved in approximately 20 ml of PBS solution. 530 mg EDCI (605 µl) were added, under stirring, and, after ten minutes, 500 mg of dopamine hydrochloride were added to the solution. The reaction lasted 20 hours.

4.1.3 – PREPARATION OF DA-HA DERIVATIVE

Scheme of the reaction

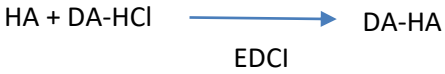

DA-HA derivative was prepared using conventional EDCI in pH 5.5 solution to avoid irreversible oxidation of dopamine. [4] Once dissolved 200 mg sodium hyaluronate in a flask containing 10 ml of PBS solution (pH=7.45) in order to disaggregate the polymer chains, pH was adjusted to 5.0-5.5 with HCl 1.0 M, and 95 mg dopamine hydrochloride and 31 mg (35 µl) EDCI were added into the flask. pH of the solution increased until 8.0 and immediately HCl 0,5 M was added to the solution in order to keep the pH values between 5.0 and 6.0 during 2-3 hours (reaction time). After 3 hours pH didn't increase anymore and the reaction was considered finished. All derivatives were purified by dialysis (pore size: 3500 Dalton).

Proton chemical shift observed: ^{1}H HA-DA (ppm) Glucosamine: A 1a 5.6, A1b 4.75, A1 4.56, A2 3.83, A3 3.71, A4 3.51, A5 3.46, A6 3.75, A6' 3.90, Me 2.02 Glucuronic acid : G1 4.45, G2 3.33, G4 3.71 G5 3.71 Dopamine CH_2 (9) 2.98-2.97 CH_2-Nr (10) 3.27 -3.23 CH (4) 6.85- 7.10

4.1.4 – PREPARATION OF Fe_3O_4@DA-HA/DA-BSA (ONE POT SYNTHESIS)

Once prepared the BSA-DA and HA-DA derivatives, the exchange reaction was performed in one step. 110 mg Fe_3O_4@OA were dissolved in 5 ml of chloroform. 650 mg of CTAB in a 30 ml of PBS solution was added to the nanoparticles solution. Such salt acts as a phase transfer agent, thus allowing to suspend Fe_3O_4@OA in water. Chloroform was difficult to remove because the organic salt generate a foam during the step of evaporation using a rotavapor and the product could be lost. Fe_3O_4@OA was added dropwise, under vigorous stirring to the aqueous solution of BSA-DA (240 mg) and DA-HA (130 mg) to perform the ligand exchange reaction. The product was soluble in PBS and the solid CTAB and the oil had to be discarded through centrifugation. The final product: Fe_3O_4@DA-HA/DA-BSA was a dark transparent solution.

4.1.5 – PREPARATION OF Fe_3O_4@DA-HA/DA-BSA (STEP BY STEP SYNTHESIS)

First step:

DA-HA derivative exchange reaction was performed in a first step buffer: 60 mg Fe_3O_4@OA were dissolved in 5 ml of chloroform. 650 mg of CTAB in a 30 ml of PBS solution was added to the nanoparticles solution. Such salt acts as a phase transfer agent, thus allowing to suspend Fe_3O_4@OA in water. In this way Fe_3O_4@OA was added dropwise, under vigorous stirring to the aqueous solution of DA-HA (80 mg) to perform the ligand exchange reaction. The product was soluble in PBS, the solid CTAB and the oil had to be discarded through centrifugation. This product was stored in the refrigerator in an dark glass container in order to precipitate the traces of CTAB later removed by further centrifugation. After the total removal of CTAB chloroform could be easily removed under vacuum. In this way it couldn't influence the solubility of BSA in the successive synthesis step.

Second step:

The second step was performed dripping the product of the first step (Fe_3O_4@DA-HA) into the flask containing a PBS solution of about 50 mg of DA-BSA. Fe_3O_4@DA-HA /DA-BSA was an orange and transparent solution. The final products were purified and concentrated using several centrifugal filter units (Amicon Ultra - 4 devices) at a rotational centrifugal force that is 2,822xg for 8-9 min. The final concentration is about 12,5 mg/ml (products lyophilized and weighed).

4.2 - DLS ANALYSIS

Dynamic Light Scattering analysis were done in order to study the size of the nanoparticles. Size per number, volume, and intensity were recorded by the Zetasizer instrument (Malvern). A 2 ml aliquot of a sample of nanoparticles was centrifuged and part of supernatant was analysed after sonication. The solvent used for the analysis was PBS solution for all samples except that for Fe_3O_4@OA, which is not soluble in water solution and so it was dissolved in hexane. The concentration of the samples varies between a 0,2 mg/ml - 5,5 mg/ml range. The temperature of the analysis was 25°C for all the scans. Glass cuvettes were used for every sample. The angle of scattering measurements was fixed at 173°. Each sample was read at least three time.

4.3 - Z-POTENTIAL MEASUREMENT

Zeta potential measurements were done in order to study the stability of the nanoparticles in solution. A Zetasizer Nano instrument (Malvern) was used. The samples were prepared following this procedure:

Concentration of the products until 12,5 mg/ml (especially BSA coated nanoparticles can't be easily analysed, because the concentration of the solution is too low for this technique) ;

Centrifugation of a small (1 ml) aliquot;

Sonication of the supernatant (aqueous solution);

Special polystyrene latex cuvettes equipped with electrodes were used;

Temperature of electrophoretic mobility measure was 25°C;

At least three reading replications were done for each sample.

Note: a new cuvette was used for each Z-pot measurement

4.4 – IN VITRO AND IN VIVO MAGNETIC RESONANCE IMAGING

MRI was investigated by the Israeli group of Prof. Yoav Livney, at the Faculty of Biotechnology and Food Engineering of Technion.

SPIONs were scanned using a 9.4 T preclinical MRI scanner (Bruker, Bremen, Germany). Echo Time (TE) and Repetition Time (TR): TR/TE = 3000/60.

The group is still continuing to study the products shipped by the group of Prof. Vismara.

4.5. MALDI–TOF MEASUREMENTS

Measurements of BSA samples and their corresponding dopamine derivatives were performed using an UV-MALDI–TOF Autoflex mass spectrometer (Bruker, Bremen, Germany) equipped with an ultraviolet laser (λ = 232 nm) operating in linear and positive ion mode in the mass range from 10 to 150 kDa. Each spectrum was recorded by averaging about 300 shots after appropriate mass range calibration performed with commercial standard proteins mixture (trypsinogen, protein A, albumin-bovine). The matrix solution, used either for analytes or standard proteins solution, was freshly prepared as a saturated solution of sinapinic acid (SA) in water 0.1% TFA:acetonitrile 2:1 (v/v). The analyte solutions were prepared at a concentration of 5–7 mg/mL in water (corresponding to about 100 pmol/µL of BSA protein) and mixed with the matrix solution in a 1:1 (v/v) ratio; then, 1 µL of this matrix/analyte mixture was loaded on the stainless steel probe and left to dry at room temperature.

Bibliography

[1] Kim, Do Kyung, et al. "Protective coating of superparamagnetic iron oxide nanoparticles." *Chemistry of Materials* 15.8 (2003): 1617-1627.

[2] Liu, Xianqiao, et al. "Preparation and characterization of hydrophobic superparamagnetic magnetite gel." Journal of Magnetism and Magnetic Materials 306.2 (2006): 248-253.

[3] Korpany, Katalin V., et al. "Stable water-soluble iron oxide nanoparticles using Tiron. "*Materials Chemistry and Physics* 138.1 (2013): 29-37.

[4] Lee, Yuhan, et al. "Bioinspired surface immobilization of hyaluronic acid on monodisperse magnetite nanocrystals for targeted cancer imaging." Advanced Materials 20.21 (2008): 4154-4157.

ACKNOWLEDGMENTS

Special thanks to prof. Giuseppe Falini and his group for their important contribution to the TEM, XRD, and TGA analyses conducted at the University of Bologna; to prof. Roberto Simonutti and dott. Michele Mauri of the Bicocca University, for the solid-state ^{1}H MQ NMR experiments that are carried out on a Bruker Minispec mq20 system, and for their future support.